DEVELOPMENT OF ASSAYS FOR THERAPEUTIC SCREENING IN MYOTONIC DYSTROPHY

Inyang Udofia Udosen, B.Sc., MRes.

Thesis submitted to the University of Nottingham

for the degree of Doctor of Philosophy,

September 2011

ABSTRACT

Myotonic dystrophy (DM) is an autosomal dominant inherited multisystemic neuromuscular disease. The molecular mechanism for DM is mediated by toxic RNAs containing expanded repeat units. DM1 is caused by a CTG repeat expansion in 3'-UTR of the *DMPK* gene while DM2 is caused by CCTG repeat in intron1 of the *ZNF9* gene. The molecular features of DM are formation of RNA foci, co-localisation of MBNL proteins with ribonuclear foci, splicing defects of a subset of pre-mRNAs with elevation of CUGBP1 in DM1.

In order to develop therapy for DM, assays were designed based on the molecular characteristics of the disease to screen compounds. Two primary assays were based on disruption of nuclear foci and on correction of misregulated splicing involving intron2 *CLCN1*.

The first part of this report deals with the development of a nuclear foci assay and splicing construct assay. Both assays were optimised in HTS and utilized in screens for molecules that clear nuclear foci from DM cells and correct misregulated splicing in intron2 of *CLCN1* respectively. High throughput screens of kinase and phosphatase inhibitor libraries using the nuclear foci assay and *CLCN1* splicing construct assay yielded two positive hits: protein kinase C inhibitors designated in the compound library as D8 (hypericin) and D9 (Ro-31-8220).

The second part of this thesis deals with the confirmation of compound hits obtained from the primary screen. I examined two aspects: mutant *DMPK* transcript entrapment in nucleus and splicing defects associated with the disease. A *BpmI* restriction assay was used to test the effect of compounds on mutant *DMPK* transcripts showed that both D8 and D9 were unable to release the mutant transcript into the cytoplasm. D8 demonstrated efficacy in reversing spliceopathy in alternative splicing assays of *IR*, *SERCA1 MBNL1* and *MBNL2* while D9 did not have this effect except on *MBNL1* which showed a very minor efficacy.

ACKNOWLEDGEMENT

I want to thank my supervisor, David Brook, for his help and support throughout the duration of this research project. In addition, I'll like to acknowledge Chris Hayes, the collaborator from the School of Chemistry, for his helpful comments and suggestions.

Many thanks to Javier Granados and Thelma, for teaching me the laboratory techniques. In addition, I'm grateful to Ami Ketley for her help in setting up the software which I used in running the screening project.

I also want to acknowledge and thank Tim Self for his help with confocal microscopy and Josephine Gilbert for her help in using the plate reader for high content imaging.

For their assistance and kind help, I also want to thank Francois, Tushar, Sukrat, Stella, Sarah, Kerry and Julie.

I'm grateful to my wife, Ndifreke, for her support and useful comment in writing this report.

Finally, I want to thank Muscular Dystrophy Campaign and Myotonic Dystrophy Support Group for their financial contribution to this project and my sponsor, AKUTECH, for nominating me for her research studentship.

DECLARATION

I confirm that this is my own work and the use of all materials from other sources have been properly and fully acknowledged.

Inyang Udofia Udosen

TABLE OF CONTENTS

CHAPTER ONE: INTRODUCTION

1.1 History and Occurence of DM....1

1.2 Classification and features of DM....2

1.3 Unstable Repeat Expansion Disorders (UREDs)....5

1.3.1 Genetic Basis of DM....8

1.3.2 Genetic Instability of Repeat Expansions in DM....9

1.4 Molecular Models for Pathogenesis of DM....10

1.4.1 DMPK Haploinsufficiency....10

1.4.2 Chromatin Structure Alteration Model....11

1.4.3 RNA dominant gain-of-function Mechanism....13

1.5 Alternative Splicing Regulation....17

1.5.1 Cis-acting Elements....18

1.5.2 Trans-acting Splicing Factors....19

1.5.2.1 Splicing Factor Regulation in DM....22

1.5.2.1.1 Muscleblind-like (MBNL)....22

1.5.2.1.2 CUG-BP1....24

1.5.2.1.3 Heterogenous nuclear ribonucleoproteins (hnRNPs)....27

1.5.2.1.4 Other Splicing Factors....28

1.5.3 Misregulation of Alternative Splicing in DM....28

1.5.3.1 *CLCN-1*....32

1.5.3.2 *IR*....33

1.5.3.3 *RYR* and *SERCA*....34

1.5.3.4 Cardiac troponin (*cTNT*)....35

1.5.3.5 Fast Skeletal troponin (*TNNT3*).....36

1.5.3.6 Myotubularin-related protein1 (*MTRM1*).....36

1.5.3.7 Muscleblind-like (*MBNL*).....37

1.5.3.8 *Tau*.....38

1.5.3.9 Other Splicing abnormalities.....39

1.5.4 Mechanism of Misregulated Splicing.....40

1.6 Possible Targets for Therapeutic Intervention in DM.....45

1.6.1 Disruption of RNA-MBNL interactions.....45

1.6.2 Inhibition or Destruction of Mutant RNA.....47

1.6.3 Correction of Spliceopathy.....48

1.6.4 Increased activity of MBNL.....50

1.6.5 Inhibition of CUG-BP1 activity.....50

1.7 Advances in Screening Assays Development for DM.....51

1.7.1 High Throughput Screening (HTS).....53

1.8 Aim of Study.....53

CHAPTER TWO: MATERIALS AND METHODS

2.1 Microbiological Methods.....58

2.1.1 Media.....58

2.1.2 Antibiotics.....58

2.1.3 Microbiological plates.....59

2.1.4 Glycerol Stocks.....59

2.2 Tissue Culture Methods.....59

2.2.1 Solutions, Antibiotics and Media.....59

2.2.2 Cell Cultures.....60

2.2.3 Tissue Culture Passage....60
2.2.4 Selection of Clones and Fibroblast Differentiation....61
2.2.5 Cryopreservation of Cells....61
2.2.6 Defrosting and Growing Cells from Liquid Nitrogen....62
2.2.7 Fixation of Cells....62
2.2.7.1 Immunofluorescence....63
2.2.7.2 Fluorescence *in situ* Hybridisation (RNA-FISH)....63
2.2.8 Compound Treatment of DM Cells....64
2.3 Molecular Biology Protocols....64
2.3.1 PCR Methods....64
2.3.1.1 Reverse Transcription PCR....66
2.3.1.2 DNA Sequencing....68
2.3.1.3 Fragment Length Analysis....69
2.3.1.4 DNA Mutational Analysis of DNA fragments....69
2.3.2 Gel Electrophoresis....70
2.3.2.1 DNA molecular weight marker....71
2.3.2.2 Quantification of DNA and RNA....71
2.3.2.3 Restriction Digestion of DNA....71
2.3.2.4 DNA Recovery and Purification....72
2.3.3.5 DNA Ligation....72
2.3.3 Plasmid DNA Purification....73
2.3.4 Fibroblast/Cell DNA Purification....74
2.3.5 Cell RNA purification....75
2.3.5.1 Fractionated RNA Purification....75
2.3.5.2 DNA Removal from RNA....77

2.3.6 Protein Extraction from cultured cells....77
2.3.6.1 Protein Quantification....77
2.3.6.2 Western Blot....78
2.4 Transgene Generation and DNA Transfer....79
2.4.1 Splicing gene constructs....80
2.4.2 Transformation....81
2.4.3 Transfection....82
2.5 Microscopy....83
2.5.1 Widefield Microscopy....83
2.5.2 Confocal Microscopy....83
2.5.3 High Throughput Imaging....84
2.6 Electronic Databases....84

CHAPTER THREE: DEVELOPMENT OF PRIMARY ASSAYS

3.1 Introduction....85
3.2 Nuclear Foci Assay....85
3.3 Use of GFP-MBNL1 to Generate Clones for RNA-MBNL1 interactions in foci....88
3.3.1 Construction of truncated GFP-MBNL....90
3.4 Splicing Construct Assays....93
3.4.1 *CLCN-1* Splicing Construct Assay....95
3.4.2 *SERCA2* Splicing Construct Assay....96
3.4.3 Proof of Concept....96
3.5 Generation of Stable lines from Controls and DM fibroblast with transgenes....97

3.6 Summary.....101

CHAPTER FOUR: VALIDATION OF PRIMARY ASSAYS AND COMPOUND SCREENING

4.1 Introduction.....102

4.2 Validation of Splicing construct Assay.....102

4.2.1 Differentiation of DM1 clones containing *CLCN1* splicing construct alters its splicing.....103

4.2.2 *CLCN1* splicing in DM1 fibroblasts clone is altered by MBNL downregualtion but not in wild type clone.....105

4.3MBNL downregulation reduces Nuclear foci in DM1 cells.....110

4.4 Compound Screening.....111

4.4.1 Compound Library for Screening.....111

4.4.2 Protein Kinase C Inhibitors.....113

4.5 PKC Inhibitors D8 and D9 clear nuclear foci from DM cells.....114

4.6 Correction of misregulated splicing in *CLCN1* reporter construct by PKC inhibitors D8 and D9 in DM1 myoblasts.....116

4.7 Summary.....121

CHAPTER FIVE: DEVELOPMENT OF SECONDARY ASSAYS AND TESTING OF PUTATIVE HITS

5.1 Introduction.....123

5.2 Secondary Assays.....123

5.2.1 Mutant *DMPK* analysis.....123

5.2.1.1 DNA Mutational analysis of *DMPK* exon10 for *BpmI* polymorphism....124
5.2.1.2 *BpmI* Restriction analysis....128
5.2.2 Alternative Splicing assays....129
5.2.2.1 Insulin Receptor Splicing assay....129
5.2.2.2 Sarcoplasmic/endoplasmic Reticulum Ca^{2+}-ATPase1 Splicing assay (*SERCA1*)....132
5.2.2.3 Muscleblind-like Splicing assay....134
5.2.2.3.1 Muscleblind-like 1 Splicing assay....135
5.2.2.3.2 Muscleblind-like 2 Splicing assay....136
5.3 Validation of Compounds....138
5.3.1.1 Mutant DMPK transcripts were not released into cytoplasm by *MBNL* downregualtion....139
5.3.1.2 PKC inhibitors do not release mutant *DMPK* transcripts into cytoplasm....140
5.3.2 D8 partially rescues *IR* splicing defect in DM1 myoblasts but not in DM2 fibroblasts....147
5.3.3 PKC inhibitors do not improve *SERCA1* splicing defect in DM2 fibroblasts....151
5.3.3.1 D8 treatment increases *SERCA1* splicing in DM1 myoblasts....153
5.3.4 D8 increases *MBNL1* splicing in DM1 myoblasts but not in DM2 fibroblasts....155
5.3.5 PKC inhibitors are ineffective in reversing *MBNL2* exon 7 splicing in DM2 fibroblasts while D8 demonstrates marginal rescue in DM1

myoblasts.....160

5.4 Summary.....163

CHAPTER SIX: DISCUSSION

6.1 Translocation of Nuclear *DMPK* Transcript.....165

6.2 Spliceopathy as a Potential Target for DM Therapy.....168

6.3 Cell-based model systems for HTS Drug Screens in DM.....171

6.4 Limitations of Study.....172

6.5 Recommendations.....173

6.6 Conclusion.....174

REFERENCES.....176

APPENDIX A.....190

APPENDIX B.....191

APPENDIX C.....192

FIGURES

Figure 1.1 Contraction of fist by a myotonic patient demonstrating difficulty in relaxing muscles of the hand after a grip.....3

Figure 1.2 Patient with adult onset DM1 displaying features of facial muscle weakness and atrophy.....4

Figure 1.3 Schematic representation of *DMPK* and its flanking genes showing its proximity to CTG repeats as proposed in this model.....12

Figure 1.4 RNA-dominant gain-of-function model for DM aetiology.....13

Figure 1.5 Exonic organisation of MTMR1 gene indicating the various isoforms.....37

Figure 1.6 Proposed mechanism for splicing misregulation by MBNL1 and CUG-BP1 leading to DM phenotype.....41

Figure 1.7 Developmental regulation of alternative splicing by MBNL1 and CUG-BP1.....44

Figure 1.8 Chemical Structure of Pentamidine.....46

Figure 1.9 Schematic representation of molecular events leading to DM.....54

Figure 1.10 Schematic model of splicing concept.....55

Figure 1.11 Schematic diagram of *BpmI* restriction assay.....57

Figure 2.1 Transgene constructs pGR-CLCN1 and pGR-SERCA2 on pEGFP-C1 plasmids used for transformation.....81

Figure 3.1 Schematic diagram showing average numbers of ribonuclear inclusion and foci distribution between wild type and DM cells.....86

Figure 3.2 RNA-FISH screens for foci in DM cell.....87

Figure 3.3 MBNL1 deletion in the pGFP-MBNL constructs showing deleted domains.....90

Figure 3.4 Schematic representation for generation of truncated versions GFP-MBNL.....92

Figure 3.5 Schematic diagram showing alternative splicing of intron 2 of *CLCN1* and intron 19 of *SERCA2* in DM patients and unaffected persons.....94

Figure 3.6 Mouse muscle C2C12 cells transfected with splicing constructs express both green and red fluorescence.....97

Figure 3.7 PCR amplification of cell clone DNA resolved on an agarose gel to confirm the presence of splicing construct pGR-CLCN1.....98

Figure 3.8 Confirmation of the presence of pGR-SERCA2 on a representative gel for isolated clones.....99

Figure 3.9 Fluorescent images of the cell clones transfected with transgene construct pGR-CLCN1 showing splicing of the construct.....100

Figure 4.1 Intron 2 of *CLCN1* splicing transgene is spliced out in DM1 fibroblasts as shown by the expression of both GFP and DsRed in these cells.....104

Figure 4.2 MBNL1 and 2 double knockdown alters *CLCN1* splicing in DM1 fibroblasts.....106

Figure 4.3 MBNL1 downregulation in wild type clone of *CLCN1* trangenes.....107

Figure 4.4 MBNL1 was reduced in MBNL doubleknockdown in DM1 clonal cells.....108

Figure 4.5 Downregulation of MBNL1 in wild type clonal cells.....108

Figure 4.6 MBNL2 protein levels were decreased in MBNL doubleknockdown of DM1 clonal cells.....109

Figure 4.7 MBNl2 protein levels were reduced in MBNL doubleknockdown sample in wild type clones.....109

Figure 4.8 siRNA MBNL1 and 2 doubleknockdown reduces the number of nuclear foci.....111

Figure 4.9 Compound screening analysis of DM cells.....115

Figure 4.10 Chemical structures of PKC inhibitors D8 and D9.....115

Figure 4.11 D8 and D9 treatment reverses DM-like splicing patterns of intron 2 retention of CLCN1 splicing in DM1 myoblasts.....117

Figure 4.12 HTS scans on plate reader of DM1 myoblast containing *CLCN1* splicing construct.....118

Figure 4.13 HTS scans of untreated wild type fibroblasts.....119

Figure 4.14 HTS imaging of DM1 fibroblast with *CLCN1* splicing transgene untreated with compounds.....120

Figure 4.15 D9 treatments of wild type fibroblasts containing the *CLCN1* construct.....121

Figure 4.16 DM1 fibroblast containing *CLCN1* splicing construct did not show any alteration in its splicing on treatment with D8 and D9.....121

Figure 5.1 The location of primers on flanking introns of DMPK exon 10...124

Figure 5.2 Elution profiles of mutational analysis of *BpmI polymorphism* of *DMPK* in wild type, DM1 and DM2 fibroblasts.....125

Figure 5.3 Mutational analysis of nuclear and cytoplasmic cDNAs of DM1 fibroblasts showing the presence of mutant *DMPK* transcripts in the nucleus.....126

Figure 5.4 *DMPK* mutational analysis of nuclear and cytoplasmic cDNAs from PKC and DMSO treated DM cells.....127

Figure 5.5 *Bpm I* restriction of RT-PCR amplicons from total RNA extracts of DM1 fibroblast.....128

Figure 5.6 *BpmI* polymorphism analysis of nuclear and cytoplasmic fractions from DM1 and wild type.....129

Figure 5.7 Alternative splicing scheme for *IR* involving exon 11 splicing analysis.....130

Figure 5.8 *IR* splicing screens of wild type, DM1 and DM2 fibroblasts.....131

Figure 5.9 *IR* splice isoforms in DM1 and wild type myoblasts.....132

Figure 5.10 Scheme for *SERCA1* alternative splicing analysis involving exon 22.....133

Figure 5.11 *SERCA1* splice isoforms in wild type and DM fibroblasts.....133

Figure 5.12 *SERCA1* splice isoforms in wild type and DM1 myoblasts.....134

Figure 5.13 Wild type and DM fibroblasts showing similar proportions of *MBNL1* exon7 isoforms.....135

Figure 5.14 *MBNL1* splice isoforms in wild type and DM1 myoblasts.....136

Figure 5.15 DM fibroblasts a showing decreased proportion of the +exon 7 isoform.....137

Figure 5.16 The DM1 cell line exhibited increased MBNL2 + exon 7 splice isoforms.....138

Figure 5.17 *MBNL* downregulation does not release mutant *DMPK* transcripts into cytoplasm.....140

Figure 5.18 PKC inhibitor treatment of DM1 cells did not release the mutant transcript from the nucleus into the cytoplasm.....141

Figure 5.19a Cytoplasmic *DMPK* showing non-release of the mutant *DMPK* transcript.....141

Figure 5.19b PKC inhibitor D9 treatment shows a reduction of the mutant transcript in the nucleus.....142

Figure 5.20 Analysis of the mutant *DMPK* and normal allele by Genescan.....142

Figure 5.21 Statistical analysis of the effect of various treatments on nuclear *DMPK* in DM1 fibroblasts.....143

Figure 5.22 Analysis of nuclear *DMPK* following treatment of myoblasts....144

Figure 5.23 The non-release of mutant *DMPK* transcript into the cytoplasm of DM1 myoblasts following treatments.....145

Figure 5.24 Statistical analysis of effect D8 and D9 treatments in comparison with controls.....146

Figure 5.25 D8 shows slight reversal of *IR* splicing defect in DM2 fibroblast.....147

Figure 5.26 PKC inhibitors have no effect on improving the proportion of *IR* splice isoform B following treatment in DM2 fibroblast.....148

Figure 5.27 Analysis of *IR* splice isoforms in DM2 fibroblasts showing that PKC inhibitors D8 and D9 treatments did not have significant effects.....149

Figure 5.28 D8 treatment produces a slight increase in the IR-B isoform in DM1 myoblasts.....150

Figure 5.29 D8 treatment showed a significant effect on the proportion of the IR-B isoforms in DM1 myoblasts.....151

Figure 5.30 D8 treatment does not alter the ratio of *SERCA1* splice isoforms in DM2 fibroblasts.....152

Figure 5.31 Analysis of SERCA1a isoforms showing no significant effect of PKC inhibitor treatments.....153

Figure 5.32 D9 treatment shows absence of SERCA1a isoforms while D8 treated DM1 myoblasts demonstrate an increase in SERCA1a isoform.....154
Figure 5.33 Statistical analysis shows that D8 treatment improves *SERCA1* splicing in DM1 myoblasts.....155
Figure 5.34 *MBNL1* splicing in PKC inhibitor treated DM2 fibroblasts and controls.....156
Figure 5.35 PKC inhibitors were ineffective in reversing missplicing of *MBNL1* +exon7 in comparison with controls.....157
Figure 5.36 PKC inhibitor D8 treatment effects reversion of *MBNL1* exon 7 splicing.....158
Figure 5.37 D8 treatment produces a very significant effect on *MBNL1* exon 7 splicing in DM1 myoblasts.....159
Figure 5.38 Analysis of *MBNL2* exon 7 splice isoform in DM2 fibroblasts are not affected by D8 treatment.....160
Figure 5.39 D8 treatment shows no significance in DM2 fibroblasts.....161
Figure 5.40 D8 treatment produced a decreased +exon 7 isoform of *MBNL2*.....162
Figure 5.4 D8 showing a significant effect on exon 7 splicing in DM1 myoblasts.....163
Figure 6.1 Model for compound screenings used in this study.....172

TABLES

Table 1.1 List of non-coding triplet repeat expansion diseases.....6

Table 1.2 List of triplet repeat expansion diseases involving those in the coding regions.....7

Table 1.3 List of genes associated with DM with its alternative splice site sequences and its silencers.....18

Table 1.4 Auxiliary elements that regulate alternative splicing of genes associated with DM.....19

Table 1.5 A subset of splicing regulatory factors and their respective binding sites on targets genes.....21

Table 1.6 List of misregulated alternative splicing events in myotonic dystrophy.....31

Table 3.1 Proportion of DM1 fibroblasts expressing GFP-MBNL1 and SNAP-tagged MBNL1 protein at different time points.....90

Table 3.2 Truncated constructs.....91

Table 3.3 The proportion of DM1 fibroblast expressing truncated versions of GFP-MBNL1 after 24 hours.....93

Table 3.4 Truncated versions of GFP-MBNL2 in transiently transfected wild type (WT) and DM2 fibroblasts.....93

Table 3.5 Clonal cells generated by G418 selection from wild type and DM cells using transgene constructs.....100

Table 4.1 List of protein kinase inhibitors library and their respective names.....112

Table 4.2 Phosphatase inhibitor library and its nomenclature.....113

CHAPTER ONE: INTRODUCTION

1.1 History and Occurence

Myotonic dystrophy was first identified in 1909 by Steinert. The disease was mainly defined by delay in muscle relaxation after contraction, commonly referred to as myotonia, with weakness and degeneration of muscles. Other phenotypes associated with the disease include cataracts, cardiac disease, digestive problems, excessive sleeping, premature balding and insulin resistance (Harper 2001).

Myotonic dystrophy (DM) is the most common form of muscular dystrophy in adults and is inherited as an autosomal dominant neuromuscular disease. The condition is a multisystemic disease with complex aetiology that also affects the heart (Harper 2001). There are two forms of DM namely: myotonic dystrophy type 1 (DM1) and myotonic dystrophy type 2 (DM2). DM results from two transcribed and unrelated mutations.

DM occurs in around one in every 8000 adult persons in the population. DM type 1 accounts for 98% of DM patients (Brook et. al. 1992; Mahadevan et. al. 1992). The molecular mechanism for the pathogenesis of DM was first identified in 1992 as mutation resulting in expanded CTG triplet repeat units in the 3'-UTR of the dystrophia myotonica protein kinase (*DMPK*) gene which is present on Chromosome 19 (Brook et al, 1992; Fu et al, 1992; Mahadevan et al, 1992). In 1995, a gene neighbouring *DMPK* called *SIX5*, which was previously referred to as DM locus-associated homeodomain protein

(*DMAHP*), was reported to be affected by DM1 mutation (Boucher et al, 1995).

The other form of DM which is referred to as DM2 is less common and shares similar disease phenotype as well as molecular phenotype (Harper 2001). DM2 was first identified in 1994 as similar to DM1 but without the CTG expansion mutation (Ricker et al, 1994; Thornton et al, 1994). Many symptoms of DM1 were also associated with DM2 including, myotonia and slight muscle weakness in proximal muscles, in contrast to distal muscles found in DM1. Hence the new syndrome was described as proximal myotonic myopathy or PROMM (Ricker et al, 1994) and was subsequently referred to as proximal myotonic dystrophy (Udd et al, 1997). Those referred to as having PROMM, proximal myotonic dystrophy and DM2 were associated with the same locus (Ranum et al, 1998; Liquori et al, 2001). Ranum et al (1998) mapped DM2 locus to a 10 centiMorgan region on chromosome 3. Subsequent mapping of DM2 was found on chromosome 3q21.3 (Ricker et al, 1999).

The DM2 mutation was reported to be an unstable CCTG repeat expansion in intron1 of the zinc finger protein 9 gene (*ZNF9*), formerly referred to as *CNBP* (Liquori et al 2001).

1.2 Classification and features of DM

DM is classified into 2 major forms based on clinical features and manifestations namely: DM1 and DM2. Both forms of DM are multisystemic with similar effects on organ systems. However, there are differences in symptoms between DM1 and DM2 and they include age of onset, absence of

congenital forms in DM2, mode of muscle weakness, and very little association of the nervous system with DM2 (Machuca-Tzili et al, 2005).

DM1 can be classified into three forms based on the age of onset, degree of its severity and clinical features: congenital, classical and minimal DM.

The congenital form of DM1 occurs at birth and in a severe manner. Its symptoms manifest as neonatal hypotonia, facial displegia, joint contractures, frequent fatal respiratory failure, feeding difficulties and delay in development. There is a high risk of dying from congenital DM1 during the neonatal period and those that survive show non-progressive psychomotor retardation and go on to develop features of adult-type classical form of DM1 (Harper 2001).

The classical form of the disease is the most common type and exhibits symptoms between the ages of 20 to 40 years in life manifesting with slow progression over time. The major feature of this disease form is myotonia with delayed relaxation of patients' muscles after contraction due to repetitive discharges of action potential; progressive muscular weakness (dystrophy) and wasting (Harper 2001).

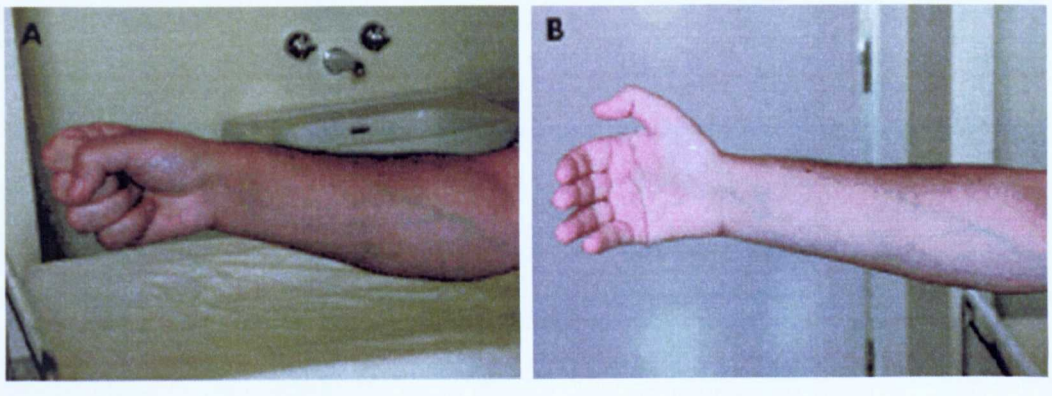

Figure 1.1: Contraction of fist (A) by a myotonic patient demonstrating difficulty in relaxing muscles of the hand (B) after a grip (from Pelargonio et al, 2002)

The minimal forms of the disease, which start later in life, over the age of 50, and shows very mild degree of muscle weakness and myotonia or cataracts (Harper 2001).

Figure 1.2: Patient with adult onset DM1 displaying features of facial muscle weakness and atrophy (from Machuca-Tzili et al, 2005)

Furthermore, the disease causes central nervous system disorders with cognitive impairment, mental retardation and attentive disorders and sometimes affects the heart leading to conduction system abnormalities, supraventricular and ventricular arrhythmias and to a lesser extent myocardial dysfunction as well as ischaemic heart disease (Pelargonio et al, 2002). Hypogammaglobulinaemia has also been associated with both forms of the disease (Day and Ranum 2005).

1.3 Unstable Repeat Expansion Disorders (UREDs)

Short repeat units normally stable in mitosis and meiosis, as well as through generations, could become unstable and undergo expansions beyond a threshold repeat number resulting in hereditary disorder. This occurence of triplet repeat expanded units was proposed as the genetic basis for DM1 and this concept was used to identify tetranucleotide repeat units in DM2. Since 1991, up to 30 unstable repeat expansion disorders have been identified (Machuca-Tzili et al, 2005).

UREDs are classified into two major forms namely: those whose expanded units are in untranslated region of the gene (table 1.1) and those with mutations in coding (table 1.2) region (Machuca-Tzili et al, 2005). For disorders whose expanded repeats occur in noncoding untranslated region, the mutations are proposed to disrupt transcription, RNA processing and translation. In the second group whose mutations occur in coding region, it has been proposed to involve CAG or GCG codons resulting in abnormally long polyglutamine or polyalanine tract which results in a mutated protein with undesired properties such as neutral toxicity (Machuca-Tzili et al, 2005).

Disorder	Mode of Inheritance	Repeat Unit	Normal	Pathogenic
DM1	Autosomal Dominant	(CTG)n	5-37	50-above 3000
FRDA Friedreich's ataxia	Autosomal Recessive	(GAA)n	6-32	200-1700
SCA8 Spinocerebellar ataxia 8	Autosomal Dominant	(CTG)n	16-92	100-127
PPP2R2B Spinocerebeller ataxia 12	Autosomal Dominant	(CAG)n	7-45	55-78
FMR1 Fragile XA	X-linked	(CGG)n	6-52	230-2000
FMR2 Fragile XE	X-linked	(CGG)n	4-39	200-900
FAM 11A Fragile XF	X-linked	(CGG)n	7-40	306-1008
CBL2 Jacobsen syndrome	Sporadic	(CCG)n	11	100-1000

Table 1.1: List of non-coding triplet repeat expansion diseases (adapted from Machuca-Tzili et al, 2005)

Disorder	Mode of Inheritance	Repeat Unit	Normal	Pathogenic
Huntington disease (HD)	Autosomal Dominant	(CAG)n	10-34	40-121
Spinobulbar muscular dystrophy	X-linked	(CAG)n	9-36	38-62
ATX1 Spinocerebellar ataxia 1	Autosomal Dominant	(CAG)n	6-39	40-82
ATX2 Spinocerebellar ataxia 2	Autosomal Dominant	(CAG)n	13-33	32-3000
ATX3 Spinocerebellar ataxia 3	Autosomal Dominant	(CAG)n	13-44	55-84
CACNA1A Spinocerebellar ataxia 6	Autosomal Dominant	(CAG)n	4-18	20-29
SCA7 Spinocerebellar ataxia 7	Autosomal Dominant	(CAG)n	4-35	37-306
TBP Spinocerebellar ataxia 17	Autosomal Dominant	(CAG)n	25-42	47-63
Dentatorubral-pallidoluysian atrophy	Autosomal Dominant	(CAG)n	3-35	49-88
Infantile spasm syndrome	X-linked	(GCG)n	10-16	17-23
Cleidocranial dysplasia	Autosomal Dominant	(GCG)n	11,17	27
Epicantus inversus syndrome type II	Autosomal Dominant	(GCG)n	14	>14
Hand-foot-genital syndrome	Autosomal Dominant	(GCG)n	18	24,26
Synpolydactyly	Autosomal Dominant	(GCG)n	15	22-29
PABP2	Autosomal Dominant	(GCG)n	6-7	8-13
Holoprosencephaly	Autosomal Dominant	(GCG)n	15	25

Table 1.2: List of triplet repeat expansion diseases involving those in the coding regions (adapted from Machuca-Tzili et al, 2005)

1.3.1 The Genetic Basis of DM

The underlying genetic basis for both types of myotonic dystrophy is the occurrence of repeat expansions in untranslated region of unrelated genes occurring at different loci.

DM1 is caused by mutations leading to microsatellite repeat expansions of CTG in the non-coding 3' untranslated region of *DMPK* gene (Brook et al, 1992). Unaffected individuals have variable numbers of repeats which ranges from 5 to 38 repeats while patients have CTG repeats of 50 up to 3000 (Brook et al, 1992 & Harper 2001). The length of microsatellite repeat expansion correlates with severity of disease with the largest repeats associated with severe congenital form of DM. The disease also shows an increase in repeat expansion with age (Brook et al, 1992) as well as generational expansion between parents and children (Hunter et al, 1992). The CTG repeat expansions are unstable in mitotic divisions and this instability leads to mosaicism in somatic as well as germ-line tissues (Harley et al, 1992; Jansen et al, 1994; Wong et al, 1995).

The second form of myotonic dystrophy (DM2) is caused by CCTG repeat expansion in intron 1 of the *ZNF9* gene (Liquori et al, 2001). Repeat tetranucleotide expansions in DM2 ranges from 75-11000 units (Harper 2001).

In DM1, CTG repeat expansions has been proposed to affect the expression of the *DMPK* gene, leading to loss or decrease in its expression. This decreased expression has been suggested to be due to defective processing of *DMPK* pre-mRNA. Functional studies in support of this idea were carried out by Reddy and co-workers (1996) in which they demonstrated that the loss of *DMPK* expression could result in muscle disease in homozygous *Dmpk* knockout

mouse which showed signs of late degree of myopathy. The loss of *DMPK* expression did not manifest other associated symptoms such as myotonia and cataracts that are seen in human patients.

In addition and to my knowledge, there is no functional study of CCTG repeat units on mouse model for DM2.

1.3.2 Genetic Instability of Repeat Expansions in DM

Repeat expansions of CTG exhibit a high degree of somatic mosaicism as well as differences between generations in DM1 patients (Martorell et al, 1995; Martorell et al, 1998).

Somatic and germ-line tissue mosaicism involving CTG repeat variation has been reported (Jansen et al, 1994). In the above study, it was suggested that these unstable CTG repeat variability resulted from early embryonic mitosis during somatic and germ-line tissue formation leading to intergenerational changes in repeat expansion lengths among DM patients.

The larger CTG repeat expansion lengths are associated with cases of severe congenital DM (Tsilfidis et al, 1992). It was also observed that there was association between cardiac involvement and CTG repeat length in DM patients (Melacini et al, 1995).

Evidence in support of this concept was demonstrated in a DM transgenic mouse carrying expanded repeat by Seznec et al (2000), which exhibited intergenerational repeat instability as well as somatic repeat instability which was dependent on size and age.

Evidence from these studies point to the role of increased size of expanded repeat lengths as a contributing factor to disease severity and progression.

1.4 Molecular Models for Pathogenesis of DM

The molecular mechanism for DM has been proposed to involve three models which include *DMPK* haploinsufficiency, chromatin structure and RNA gain-of-function models.

1.4.1 DMPK Haploinsufficiency

In this model, the CTG repeat expansions in the 3'-UTR of the *DMPK* gene affects its transcription or cause transcripts containing expanded CTG repeats to be retained in the nucleus (Davis et al, 1997). This leads to reduced levels of DMPK protein.

Studies have reported decreased levels of DMPK protein from DM1 allele (Fu et al, 1993; Furling et al, 2001; Novelli et al, 1993). However, the reduced expression of DMPK has been reported to play a minor role in pathogenesis of DM1 (Fu et al, 1993).

Studies involving transgenic mice testing the viability of haploinsufficiency have shown that this model of disease mechanism does not account for DM1 pathology. A study by Reddy et al (1996) on *Dmpk* knock-out mice removing the first seven exons and replacing them with a neomycin cassette showed that homozygous mice displayed minimal myopathy, muscle degeneration and reduced skeletal muscle force while its heterozygous counterpart did not show any DM symptoms. This was followed by another study showing *Dmpk* dosage alterations in mice results in cardiac conduction abnormality (atrioventricular block) which was more pronounced in homozygous than in heterozygous mice (Berul et al, 1999; Berul et al, 2000).

Jansen et al (1996) developed *Dmpk* knock-out mice that resembled the one used by Reddy et al (1996) in which a hygromycin cassette was used in place of neomycin cassette. The mice only showed mild myopathy and altered calcium levels (Benders et al, 1997; Jansen et al, 1996).

The evidence from these mice models suggest that *DMPK* haploinsufficiency cannot explain most aspects of DM1 pathogenesis as the mice did not display unique features such as myotonia and cataracts.

1.4.2 Chromatin Structure Alteration Model

Studies on chromatin structure of DNA with CTG repeats have suggested that expansion mutations modify the chromatin structure and alter expression of *DMPK* and neighbouring genes (Jansen et al, 1996; Klesert et al, 1997; Michalowski et al, 1999; Otten and Tapscott, 1995; Thornton et al, 1997).

Wang and Griffith (1994) demonstrated formation of hyperstable and abnormally stronger nucleosomes by expanded CTG repeats. It has been suggested that CTG repeats result in the formation of more condensed chromatin structures and consequently loss of *DNase1* sensitive site. Since *DNase1* sensitivity indicates relaxed chromatin structure making it accessible for transcription factors and RNA polymerase, the presence of CTG repeats may block these processes to hinder transcription of *DMPK* and its neighbouring genes (Otten and Tapscott 1995).

The CTG repeat-induced changes in chromatin structure affect expression of neighbouring genes *SIX5* and *DMWD* (dystrophia myotonic-containing WD repeat motif) (Frisch et al, 2001). Other genes mapped around *DMPK* include *GIPR*, *20-D7* and *symplekin* (Alwazzan et al, 1998).

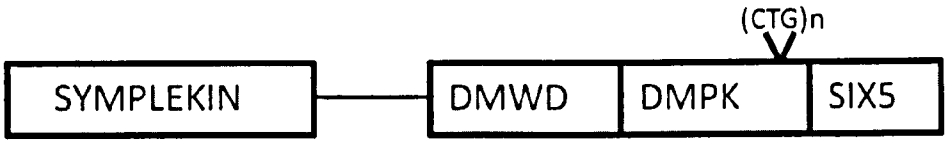

Figure1.3: Schematic representation of *DMPK* and its flanking genes showing its proximity to CTG repeats as proposed in this model

SIX5 (formerly *DMAHP*) is located immediately downstream of *DMPK* and the repeat expansion forms part of the promoter region of *SIX5* (figure 1.3). *SIX5* encodes the DM locus-associated homeodomain protein, homologous to Drosophila sine oculis homeobox 5, which is involved in eye development (Winchester et al, 1999).

It has been reported that there is a reduction in *SIX5* expression in DM1 patients in comparison with controls which leads to its involvement in cataract formation in these patients (Alwazzan et al, 1999; Klessert et al, 1997; Thornton et al, 1997; Winchester et al, 1999). An animal study involving knock-out of *six5* in mice by replacement of its first exon by β-galactosidase reporter showed development of cataracts (Jansen et al, 1996; Klessert et al, 2000).

DMWD formerly known as *59* is located immediately upstream of *DMPK*. It has been reported to be mainly expressed in adult mouse testis and brain and it has been suggested that it may be associated with the mental retardation and testicular symptoms observed in DM1 (Jansen et al, 1996). However, this model does not account for the main phenotypes associated with both DM1 and DM2 patients.

1.4.3 RNA dominant gain-of-function Mechanism

The hypothesis for this model first arose from studies that *DMPK* RNA with expanded repeat units were trapped in the nucleus to form foci in patients' cells (Taneja et al, 1995; Davis et al, 1997; Hamshere et al, 1997). The study by Taneja et al (1995) used CAG oligonucleotide probes to detect *DMPK* transcripts with expanded repeats which gave bright foci in the nuclei of DM patients' cells which were not detected in the fibroblasts of unaffected persons. It was suggested that the concentration of mutant *DMPK* transcripts containing repeat expanded units in the nucleus represented abnormal RNA processing which could be indicative of the disease phenotype (figure 1.4).

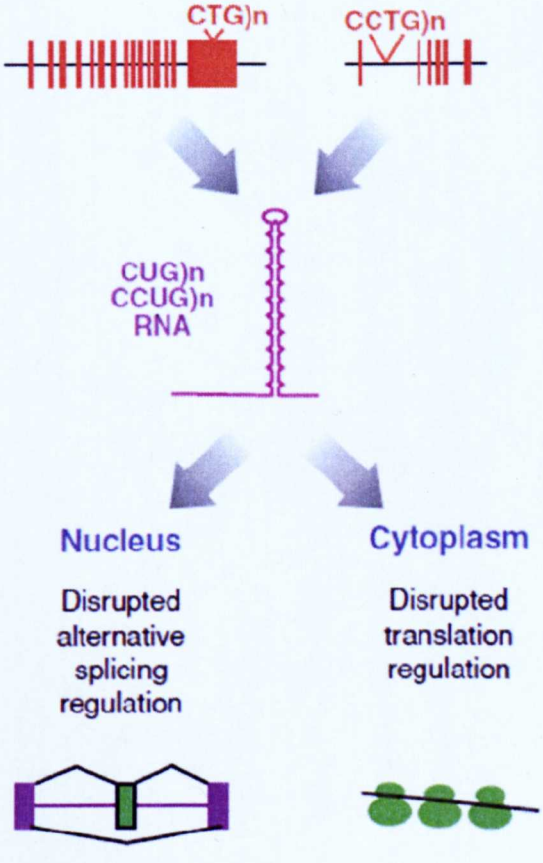

Figure1.4: RNA-dominant gain-of-function model for DM aetiology (taken from Ranum and Cooper, 2006) showing negative effects of expanded repeat RNA on alteration of cellular functions

Other evidence in support of the observation by Taneja et al (1995) comes from the finding that mutant *DMPK* transcripts were found exclusively in the nucleus and not in the cytoplasm of DM cells (Davis et al, 1997) with a critical repeat threshold number of between 80 to 400CTGs (Hamshere et al, 1997).

Nuclear foci found in DM cells have been proposed to be formed due to interactions between expanded CUG transcripts (for DM1) and expanded CCUG repeat transcripts (for DM2) with certain RNA binding proteins (Miller et al, 2000; Fardaei et al, 2001).

It has been suggested that single stranded CTG repeats fold to form unusual structures such as duplex hairpins (Wells 1996). A study has shown that RNA containing expanded repeats within pathogenic lengths fold to form hairpin structures which in turn interact with RNA binding proteins (Michalowski et al, 1999). The interactions of the hairpin with RNA binding proteins prevent these proteins from performing their normal cellular functions, causing them to accumulate in the hairpins to form foci (Miller et al, 2000).

One of the RNA binding proteins proposed to interact with expanded repeat transcripts in foci is muscleblind-like proteins (MBNL). The MBNL has been shown to colocalise with expanded CUG or CCUG repeats in nuclear foci (Fardaei et al, 2001; Fardaei et al 2002; Miller et al, 2000). The most abundant isoform of MBNL proteins (MBNL1) has been reported to be the major determinant of nuclear foci formation in DM (Dansithong et al, 2005).

In a study to assess effect of expression of CTG repeats, a mouse myoblast C2C12 cell line was used to demonstrate that CUG expansion alone formed foci but only CUG expansion in DMPK 3'-UTR was able to inhibit myoblast

differentiation via reduced MyoD levels (Amack et al, 1999; Amack &Mahadevan, 2001). These studies were important as it provided a proof for the contribution of expanded repeat RNA to DM-like features.

Several lines of evidence now support the RNA gain-of-function hypothesis as the primary event in DM pathogenesis (Mankodi et al, 2000; Mahadevan et al, 2006; Seznec et al, 2001). Mouse models have been used to test the RNA dominant negative function hypothesis in many studies (Mankodi et al, 2000; Seznec et al, 2001; Mankodi et al, 2002; Mahadevan et al, 2006; Orengo et al, 2008).

In one study, transgenic mice were generated expressing human skeletal muscle alpha actin containing 250 CTG repeats in a mouse background designated as HSA^{LR} and these were observed to replicate DM features of myotonia and myopathy while mice containing 5 CTG repeats did not have DM phenotype (Mankodi et al, 2000). Another study by Mahadevan and colleagues (2006) used an inducible mouse model under control of tetracycline inducible system to demonstrate that RNA toxicity and cardiac conduction defects seen in DM could be reversible. In this study, mice with $(CTG)_5$ *DMPK* 3'-UTR and mutant $(CTG)_{200}$ *DMPK* 3'-UTR when induced with doxycycline, both developed DM-like features such as cardiac conduction abnormalities and abnormal RNA splicing. In addition, there was appearance of foci in $(CTG)_{200}$ *DMPK* 3'-UTR mice but not in $(CTG)_5$ *DMPK* 3'-UTR. This mouse model suggests that it has limitations for studying effect of CTG repeats because of the presence of both splicing and cardiac conduction abnormalities in $(CTG)_5$ *DMPK* 3'-UTR mice which does not correlate to that seen in unaffected persons carrying 5CTG repeats.

Furthermore, Orengo et al (2008) used an inducible transgenic mice containing *DMPK* 3'-UTR with 960 CTG repeats under tamoxifen induction to show severe skeletal muscle degeneration, a feature of DM not seen in other mouse models. In addition, the study showed splicing misregulation that was responsive to only CUGBP1 as opposed to those demonstrated by Mahadevan et al (2006) and Mankodi et al (2002). Because this model did not demonstrate misregulation of MBNL1 responsive splicing events, it does not lend itself as a good model for DM study.

Finally, Seznec et al (2001) developed two mice models for DM study with one containing 300 CTG repeat (DM300) and the other having 20 CTG repeats (DM20) both in its natural DMPK context obtained from DM1 patient and unaffected person. The DM300 mice displayed myotonia, presence of nuclear foci, abnormal skeletal muscle histology and altered Tau protein isoforms consistent with that seen in DM1 patients which was absent in DM20 line. The DM phenotypes obtained from this mouse model were consistent with that reported in Mankodi et al (2000). Further studies involving HSA^{LR} mouse has been used to demonstrate *Clcn1* missplicing (Mankodi et al, 2002), splicing abnormalities *of Mbnl1*, *Serca1*, *Zasp,Cypher* and *m-Titin* (Lin et al, 2006) as well as in studying reversal of both missplicing and myotonia by Kanadia et al (2006). The DM300 line has been reported to be utilized in therapeutic screens (Mulders et al, 2009). Both HSA^{LR} and DM300 provide a good and reliable model for use in studying DM as well as in therapeutic screening due to their ability to recapitulate DM associated symptoms.

1.5 Alternative Splicing Regulation

Alternative splicing is the mechanism that controls gene expression and protein diversification through multiple RNA isoforms from a single pre-mRNA. It is determined by additional factors such as cell cycle phase, developmental stage, cell type, organ or tissue. In disorders such as DM, the alternative splicing process is altered leading to alterations in relative proportion of isoform obtained.

Alternative splicing influences cell fate decisions like apoptosis in mammals as well as sexual differentiation in Drosophila and its misregulation has been reported in human disease. Of the estimated 30,000 protein-coding genes in human, most code for alternatively spliced transcripts and this accounts for the difference between the number of human genes and human proteome complexity (Lander et al, 2001).

In humans, most of the protein coding genes are separated by introns and the production of functional mRNAs is determined by the accuracy of pre-mRNA splicing in which introns are spliced out and exons joined together. The excision of introns involves two transesterification reactions which occur in a macromolecular complex (spliceosome) that consist of more than 100 proteins and about five RNA species- U1, U2, U4, U5, U6 among others (Nilsen, 2003). Many regulatory elements direct and regulate the process of alternative splicing. They are normally referred to as splicing factors.

1.5.1 Cis-acting Elements

Alternative splicing depends on the assembly of the basal splicing machinery in spliceosome complexes within consensus sequences present in every 5' and 3' splice site boundary between introns and exons. The spliceosome functions to identify and select splice sites, and also catalyse the sequential transesterification reactions to remove introns and join exons together. The effectiveness of the spliceosome to act on an exon depends on the strength of the splice site which relates to its complementarity to consensus splice site sequences, exon size, and availability of auxiliary cis elements. Exons that have undergone alternative splicing are often small and possess weak 5' and 3' sites, and their auxiliary elements serve to improve splice site recognition as well as mediating selection of splice sites involved in specified cells (McCullough and Berget, 1997).

Gene	Exon	Effect	Sequence	Location	*Trans*-acting factor	Ref.
Cardiac troponin T	5	exon skipping in adult cardiac muscle	cgcugcggc	intronic (18-26nt upstream)	MBNL	Ho et al. 2004
Insulin Receptor	11	Exon skipping in non-muscle tissues	uuacucggacac auguggccuccaa gugucagagccag uggu	Intronic (52-95nt upstream)	CUG-BP	Savkur et al. 2001
Microtubule associated protein tau	3	Varying degree of exon skipping in adult CNS	Uuag	Exonic	Nova1, SWAP, KSRP	Arikan et al. 2002
Microtubule associated protein tau	10	Same	ucaaaggauaauau caaa	Exonic	unknown	D'Souza & Schellenberg, 2000
Microtubule associated protein tau	10	Same	ucacacgu	Intronic (11-18nt Downstream	unkown	D'Souza & Schellenberg, 2002

Table 1.3: List of genes associated with DM with its alternative splice site sequences and its silencers which are *trans*-acting factors (adapted from Pozzoli & Sironi 2005)

Auxiliary elements involved in controlling the use of alternative splice sites have the following characteristics: they are small in size, have variable sequence, are individually weak, and occur in multiple copies. The auxiliary elements are mostly single-stranded with secondary structure reported to be involved in the activity of a few elements (Blanchette and Chabot, 1997). Auxilliary elements could be present in exons or introns and when they are intronic, they can be present upstream, downstream or flank both sides of the regulated exon.

Gene	Splicing specificity	Element involved	Sequence	Location of element	Ref.
CLCN-1 intron2	Intron retention in DM	Enhancer	UGUUUGUUUG UUUGUUUGUU GUUUGUUUGU UUGU	Upstream of exon3	Charlet-B et al. 2002
DMPK exon 16	Specific for developmental stage, removed in DM	Enhancer	(CUG)n	upstream	Tiscornia & Mahadevan 2000
Tau exon 10	Misregulated in DM	Enhancer	CCCAUGCG	downstream	D'Souza & Schellenberg, 2002

Table 1.4: Auxiliary elements that regulate alternative splicing of genes associated with DM (adapted from Ladd & Cooper, 2002)

Finally, auxiliary elements are involved in enhancing or repressing splice-site selection. Based on their location and effect, they are referred to as exonic splicing enhancers or silencers or intronic splicing enhancers or silencers.

1.5.2 Trans-acting Splicing Factors

Several exonic splicing enhancers are known to interact with serine/arginine (SR) proteins, which is a family of essential splicing factors, to allow inclusion of alternative exons having weak splice sites in their pre-mRNA by promoting splicing of nearby introns (Wu and Maniatis, 1993; Zhu et al, 2001). The

activity of SR proteins on alternative splicing is countered by constitutive splicing factor heterogenous nuclear ribonuclear protein A1. The alternative splicing of a few RNAs can be regulated in cell populations by altering the ratios of constitutive splicing factors since overexpressing SR proteins or hnRNP A1 has been shown to have a similar effect on the splicing of alternatively spliced pre-mRNAs in vitro or in transient transfection assays (Zhu et al, 2001).

The hnRNPs are reported to be necessary for the many aspects of mRNA biogenesis and metabolism. They are a group of RNA-binding proteins involved in alternative splicing. Members of A/B type of hnRNPs are the most abundant and are reported to be involved in splice site selection. Activation of distal 5' splice sites has been suggested to be due to negative effect of hnRNP A1 on alternative splicing functions of splicing factors SF2/ASF or SC35. However, hnRNP A2 and B1 have been reported to have greater splice switching activities than hnRNP A1 (Mayeda et al, 1994).

Other trans-acting splicing factor are the CELF (CUG-BP and ETR3-like factors) proteins also referred to as Bruno-like proteins which have a binding preference for uridine/purine repeat elements (Good et al, 2000; Ladd et al, 2001 and Takahashi et al, 2000). CELF proteins are important because of their role in misregulation of alternative splicing of many mRNAs in myotonic dystrophy.

Splicing factor	Protein Regions	Binding sites	Target genes
ASF/SF2	RNA recognition motif; arginine-serine repeats-containing domain	RGAAGAAC	HipK3, CaMKIIδ
SC35	RNA recognition motif; arginine-serine repeats-containing domain	UGCUGUU	AChE
SRp55	RNA recognition motif; arginine-serine repeats-containing domain	GGCAGCACCUG	cTnT, CD44
hnRNP A1	RNA recognition motif; arginine-glycine-glycine repeats	UAGGGA/U	HipK3,SMN,c-H-ras
hnRNP A2/B1	RNA recognition motif; arginine-glycine-glycine repeats	(UUAGGG)n	HIV Tat, IKBKAP
hnRNP H	RNA recognition motif; arginine-glycine-glycine repeats; glycine-tyrosine-arginine rich domain	GGGA, G-rich	PLP, c-SRC, Bcl-x
PTB	RNA recognition motif	UCUU, CUCUCU	nPTB, c-SRC, Fas, cTNT, CGAP, NMDA, CLBC, hnRNP A1
Cugbp	RNA recognition motif	U/G-rich	cTNT, IR
Cugbp2	RNA recognition motif	U/G-rich	cTnT, Tau, Cox-2
Celf4	RNA recognition motif	U/G-rich	Mtmr1, cTnT
Mbnl1	CCCH zinc finger domain	YGCU(U/G)Y	cTnT, IR, Clcn1,Tnnt3
Rbm4	RNA recognition motif; CCHC zinc finger domain	C/U-rich	MAPT, α-tropomyosin, Tau

Table 1.5: A subset of splicing regulatory factors and their respective binding sites on target genes (adapted from Gabut et al, 2008)

Many exons can be regulated by factors with antagonistic effect. These antagonistic activities could be effected trans-acting factors that can act alternatively as repressors and activators on different target RNAs. This explains the interaction of CUG-BP and MBNL proteins in the regulation of cardiac troponin T (Philips et al, 1998) and insulin receptor pre-mRNAs

(Savkur et al, 2001). The alteration in the relative ratios of these protein factors has been suggested to lead to defect in splicing patterns in DM (Philips et al, 1998; Savkur et al, 2001; Kalsotra et al, 2008).

1.5.2.1 Splicing Factor Regulation in DM

Many proteins have been implicated in splicing misregulation in DM. They include muscleblind-like protein, CUG-binding protein 1, heterogenous nuclear ribonucleoprotein among others which will be discussed in the following sections.

1.5.2.1.1 Muscleblind-like (MBNL)

This expanded repeat RNA-binding protein and splicing factor was first identified in Drosophila melanogaster for its role in photoreceptor development and terminal muscle differentiation (Artero et al, 1998; Begemann et al, 1997). In humans, MBNL are homologs to those of Drosophila and are of three types: MBNL1, MBNL2 and MBNL3. These MBNL proteins are encoded by different genes. *MBNL1*, *MBNL2* and *MBNL3* genes have been mapped to chromosome 3, 13 and X respectively (Fardaei et al, 2002). Each of the muscleblind-like proteins exist in different splice isoforms with MBNL1 having nine isoforms, MBNL2 has three alternative splice isoforms while MBNL3 has six splice isoforms (Fardaei et al, 2002;Kino et al, 2004; Pascual et al, 2006). MBNL1 was discovered for its affinity for binding to CUG repeats (Miller et al, 2000). Subsequently, MBNL2 and 3 were found to colocalise with RNA foci in DM1 and DM2 cells (Fardaei et al, 2001; Mankodi et al, 2001; Miller et al, 2000).

The three muscleblind-like proteins are present in brain, heart, placenta, lung, liver, kidney, pancreas and skeletal muscle. MBNL1 and 2 are mostly expressed in heart and skeletal muscle while MBNL3 is mainly expressed in placenta (Fardaei et al, 2002).

MBNL1, the most abundant muscleblind-like protein, has been implicated in pathogenesis of DM due to its sequestration by RNA expanded repeats (Miller et al, 2000). This proposal was validated by Kanadia et al (2003) using a mouse knock-out for mbnl1 isoform ($mbnl1^{\Delta 3/\Delta 3}$) which replicated DM-like features such as myotonia, cataracts and misregulation of splicing. A follow up study by Kanadia et al (2006) involving adeno-associated virus (AAV)-mediated mbnl1 overexpression in HSA^{LR} mice showed that it reversed myotonia in skeletal muscle as well as rescueing associated misregulated splicing in this mouse model.

These data suggest that MBNL1 downregulation is the major cause of DM. If this is the case, by what mechanism does it influence the manifestation of DM phenotype? The answer to this could lie in the function of MBNL1 as a regulator of alternative splicing.

One of the major molecular features of DM is misregulation of alternative splicing. It has been reported that MBNL1 depletion leads to misregulation of splicing in many genes and in some cases it resulted in DM phenotypes (Ranum and Cooper, 2006). MBNL1 sequestration has been implicated in misregulated splicing of *CLCN1*, *cTNT* and *IR* leading to myotonia, cardiac conduction defects and insulin resistance seen in DM patients (Charlet et al, 2002b; Dansithong et al, 2005; Ho et al, 2004; Lin et al, 2006).

The role for MBNL1 in alternative splicing misregulation in DM was demonstrated by Ho et al (2004) which showed that siRNA downregulation of MBNL1 in HeLa cells altered both *cTNT* and *IR* splicing. In addition, MBNL1 overexpression in DM1 cultured myoblast was necessary to reverse *IR* splicing defect (Dansithong et al, 2005). Consequently, AAV-mediated overexpression of mbnl1 in HSA^{LR} skeletal muscle restored *CLCN1* splicing and rescued myotonia (Kanadia et al, 2006). Indeed, MBNL1 is predominantly localised in the nucleus where it switches from the cytoplasm during normal skeletal muscle development (Lin et al, 2006), thus it has been suggested that MBNL1 sequestration by repeat expanded RNA disrupts a subset of spliceforms to produce isoform ratios more typical of the embryo leading to multisystemic symptoms in DM1.

Eventhough the MBNL1 sequestration model for misregulated splicing and DM pathogenesis has been confirmed in many studies, it does not completely explain the mechanism for DM pathogenesis. One aspect of DM that is not accounted for by loss of MBNL1 function is the lack of muscle wasting in $mbnl1^{\Delta 3/\Delta 3}$ mice. In addition, MBNL1 was observed to be sequestered by both CAG and CUG formed foci but only CUG repeats were able to disrupt splicing of *cTNT* and *IR* (Ho et al, 2005b). This suggests that other factors besides MBNL1 could contribute to these splicing defects.

1.5.2.1.2 CUG-BP1

The CUG binding protein (CUG-BP) was first identified for its ability to bind to CUG repeat in a gel-shift assay (Timchenko et al, 1996a). CUG-BP1 belongs to the CELF (CUG-BP and ETR3-like factor) family, a splicing

regulation group of RNA proteins (Timchenko et al, 1996a; Timchenko et al, 1996b; Ladd et al, 2001) whose members are implicated in regulating translation and in cell-specific splicing of transcripts during normal development and disease (Ladd et al, 2001).

Further studies on the interaction of CUG-BP1 with expanded CUG repeats have shown conflicting results to that reported by Timchenko et al (1996a). CUG-BP1 does not bind to the whole length of the hairpin of double-stranded CUG repeats in *DMPK* RNA but only at its base when observed under electron microscopy (Michalowski et al, 1999) and shows non-colocalisation with expanded repeat RNA foci in DM1 and DM2 (Fardaei et al, 2001). CUG-BP has been demonstrated to be phosphorylated by protein kinase C (PKC) in DM1 to form the active isomers- CUG-BP1 and CUG-BP2 (Kuyumcu-Martinez et al, 2007; Savkur et al, 2001) which are involved in regulation of alternative splicing.

CUG-BP1 protein levels are not elevated in wild type and DM2 skeletal muscles nor are they elevated in HSA^{LR} mice skeletal muscle (Lin et al, 2006). However, they are increased in DM1 muscle cultures (Savkur et al, 2001). The decrease in CUG-BP1 in DM1 mouse model (HSA^{LR}) as opposed to its levels in DM1 muscles could be due to expression of expanded CTG in its natural context of *DMPK* 3'-UTR which might have signal for inducing its increase (Amack et al, 1999; Amack and Mahadevan, 2001; Orengo et al, 2008). The level of CUG-BP1 has been shown to increase in cultured fibroblasts and myoblasts of DM1 patients (Charlet et al, 2002b; Philips et al, 1998; Roberts et al, 1997; Savkur et al, 2001). To validate the point mentioned above, Lin et al

(2006) had reported downregulation of CUG-BP1 in wild type skeletal muscles of mice within three weeks of its post-natal life.

CUG-BP1 is involved in regulation of alternative splicing and its elevation in DM1 patients' results in misregulation or defects in splicing (Charlet et al, 2002a; Charlet et al, 2002b; Philips et al, 1998; Savkur et al, 2002). Its overexpression in wild type (normal) cells has been shown to promote embryonic splice isoform expression in *CLCN-1* (Charlet et al, 2002b; Faustino and Cooper, 2003), *IR* and *cTNT* (Philips et al, 1998; Savkur et al, 2001) in DM1 patients.

Further studies on the effect of CUG-BP1 in alternative splicing in mouse models make a case for its role in spliceopathy leading to DM-like symptoms (Ho et al, 2005a; Mahadevan et al, 2006; Orengo et al, 2008). For example in a study by Orengo et al (2008), it was observed that elevated levels of CUG-BP1 was associated with misregulation of splicing in *CLCN-1* exon7a, *SERCA1* exon 22 and *CYPHER* exon11 in an inducible mouse model expressing 960 CTG repeat expanded units in a *DMPK* 3'-UTR background. Other splicing abnormalities specifically related to CUG-BP1 regulation such as *Ank2*, *Capzb* and *Fxr1* were also found in this model. DM-like splicing defects were also reported in the heart and skeletal muscle by Ho et al (2005a) in mice overexpressing CUG-BP1 under control of mouse creatine kinase promoter. These mice also replicated DM patterns of splicing for *TNNT2* exon5, *MTMR1* fetal exon as well as *CLCN1* exon7a. This was further confirmed in another study by Mahadevan et al (2006) using an inducible mouse model overexpressing both CTG_{200} and CTG_5 in *DMPK* 3'-UTR context. Both mice showed DM-like molecular symptoms which for CTG_5

DMPK 3'-UTR was unusual and the cause for this effect is not clear. From these studies by Orengo et al (2008) and Mahadevan et al (2006), it could be suggested that *DMPK* 3'-UTR might have signals for triggering CUG-BP1 elevation which in turn led to DM splicing patterns.

CUG-BP1 has been suggested to bind to U/G motifs of introns close to splice sites of *CLCN-1*, *IR* and *cTNT* pre-mRNAs (Charlet et al, 2002b; Philips et al, 1998; Savkur et al, 2001). In the nuclei of DM cells, CUG-BP1 is an antagonistic regulator to MBNL1 (Karlsotra et al, 2008) thus splicing abnormalities might not be exclusively induced by CUG-BP1 alone.

1.5.2.1.3 Heterogenous nuclear ribonucleoproteins (hnRNPs)

The hnRNPs are a large group of RNA-binding proteins occurring mainly in the nucleus with a subset of them involved in shuttling between nucleus and cytoplasm (Nakielny and Dreyfuss, 1999). The hnRNP A/B are the most abundant of this group of splicing proteins and are involved in regulating splice site selection (Mayeda et al, 1994). This group consist of isoforms A1/A1B, A2/B1, B2 and A3 which have similar RNA binding specificities (Mayeda et al, 1994). It has been reported that hnRNPA1 associates with U2 and U4 snRNPs during spliceosomal assembly (Buvoli et al, 1992).

Another type of hnRNP protein designated as hnRNP H has been suggested to act as splicing repressor or activator in different contexts (Chen et al, 1999; Chou et al, 1999). In addition, hnRNP H has been implicated in inhibiting nuclear transport of expanded repeat RNA by associating with it as well as interaction with branch point sequence (Kim et al, 2005). To assess its role in

alternative splicing, Paul et al (2006) demonstrated that hnRNP H overexpression inhibits *IR* exon11 retention in normal myoblasts. In addition, the study showed that hnRNP H acts in synergy with CUG-BP1 to misregulate *IR* exon 11 splicing. Furthermore, the study by Paul et al (2006) observed that hnRNP H whose levels are elevated in DM are recruited by MBNL1 and MBNL2 to form foci.

Another study by Fardaei et al (2001) reported that hnRNP C, another member of this family of protein, does not colocalise with CUG expanded repeats to form foci. Eventhough this group of proteins are known to be involved in regulation of alternative splicing, evidence for its role in DM pathology is limited and has not yet been well established.

1.5.2.1.4 Other splicing Factors

Many RNA-binding proteins and splicing factors have been demonstrated to alter splicing in DM. The Polypyrimidine Tract Binding (PTB) protein and PTB associated splicing factor (PSF) are known antagonists to CELF proteins in splice site selection (Tiscornia and Mahadevan, 2000) which makes a case for its role in splicing regulation in DM.

Warf et al (2009a) showed that U2 auxilliary factor (U2AF65) was inhibited by MBNL1 for splicing of exon5 in *cTNT* pre-mRNA via competition for the binding of U2AF65 at the 3' end of intron 4.

1.5.3 Misregulation of Alternative Splicing

About 30% of alternative splicing has been reported to introduce premature termination codons into mRNA resulting in nonsense-mediated decay (Lewis

et al. 2003). Alternatively spliced mRNA expression can be determined by cell type and developmental stage. Cell specific alternative splicing in most systems involves the effects of antagonistic factors that could influence different pathways.

In DM, misregulation of alternative splicing occurs in some splicing events that are normally regulated developmentally and in the disease, they fail to express the adult isoform mRNA in adult tissues. The developmental regulation of transcripts could be absolute (involving exon 22 of *SERCA1*, exon 7 of *MBNL1*, exon 11 of *ZASP*, exon5 of *cTNT*) or partial (in *ITGB1* exon17, *CAPZB* exon8). Instead the foetal mRNA and protein is expressed which cannot function in adult tissues resulting DM phenotype.

Misregulated splicing in DM differs from aberrant splicing observed in other genetic diseases because aberrant splicing results from mutations within exons or splice site to create cryptic splice sites and expression of non-natural mRNAs (Faustino and Cooper, 2003).

Myotonia and insulin resistance which are major symptoms in DM, are associated with splicing misregulation of muscle-specific chloride channel (*CLCN-1*) and insulin receptor (*IR*) respectively. Myotonia has been implicated in reduced expression of CLCN-1 in both patients and HSA^{LR} mouse model (Charlet et al, 2002b; Mankodi et al. 2002). Patients with DM show manifest reduction in expression of CLCN-1 protein below 10% of normal levels necessary to cause myotonia. This reduced CLCN-1 protein expression is due to misregulated alternative splicing of the *CLCN-1* gene (Charlet et al, 2002b; Mankodi et al, 2002)

Loss of functional CLCN-1 protein in DM patients is due to the failure of the gene to switch from embryonic splicing pattern, involving the inclusion of one or both of two alternative exons, which alters the *CLCN-1* mRNA open reading frame (Charlet et al. 2002b; Mankodi et al, 2002).The *CLCN-1* mRNA containing these misplaced exons could be degraded by non-sense mediated decay.

DM patients also manifest an abnormal form of insulin resistance. This insulin resistance is associated with inability to express *IR* splice variant (IR-B) that normally occurs in adult skeletal muscle. Instead, DM patients express the nonmuscle *IR* isoform (IR-A) which has a lower signalling ability than those expressed in adult skeletal muscle and the expression of this isoform in DM skeletal muscle cultures has been implicated in the decreased responsiveness to insulin compared to control cultures from unaffected individuals (Savkur et al, 2001).

Other studies have suggested the involvement of a missplicing event in myotonic dystrophy that involves Z-band alternatively spliced PDZ-domain protein (Machuca-Tzili et al, 2006 ;Lin et al, 2006), *CYPHER* (Lin et al. 2006), and in dystrophin (Nakamori et al, 2007).

Other misregulated splicing events observed in DM include those involving cardiac troponin T (Philips et al, 1998), *tau* (Sergeant et al. 2001), myotubularin-related protein 1 (Buj-Bello et al, 2002), fast skeletal troponin T (Kanadia et al, 2003), N-methyl-D-aspartate receptor (Jiang et al, 2004), amyloid precursor protein (Jiang et al, 2004), *SERCA1* and *SERCA2* (Kimura et al. 2005) .

Gene	Exon/Intron	DM f eature	References
Amyloid precursor protein	Exon 7	Exon exclusion	Jiang et al, 2004
Cardiac troponin T	Exon5	Exon inclusion	Philips et al, 1998
Chloride channel	Intron 2	Intron inclusion	Charlet et al, 2002b
Chloride channel	Exon 7a	Exon inclusion	Charlet et al, 2002b Mankodi et al, 2002
Dystrophin	Exon71 or 78	Exon exclusion	Nakamori et al, 2007
Fast skeletal troponin T	Fetal exon	Exon inclusion	Kanadia et al, 2003
Insulin Receptor	Exon 11	Exon exclusion	Savkur et al, 2001
Muscleblind-like 1	Exon 7	Exon inclusion	Lin et al, 2006
Muscleblind-like 2	Exon 7	Exon incusion	Lin et al, 2006
M-titin	Exon 5	Exon inclusion	Lin et al, 2006
Myotubularin-related protein	Exons 2.1 and 2.2	Exon exclusion	Buj-Bello et al, 2002 Ho et al, 2005a
N-methyl-D-aspartate receptor	Exon 5	Exon inclusion	Jiang et al, 2004
Ryanodine receptor	Exon 70 (AS I)	Exon exclusion	Kimura et al, 2005
Sarcoplasmic/endoplasmic reticulum Ca^{2+} ATPase 1	Exon 22	Exon exclusion	Kimura et al, 2005
Sarcoplasmic/endoplasmic reticulum Ca^{2+} ATPase 2	Intron 19	Intron retention	Kimura et al, 2005
Tau	Exon 2, 3 and 10	Exon exclusion	Sergeant et al, 2001 Jiang et al, 2004
Tau	Exon 6	Exon exclusion	Leroy et al, 2006
Z-band alternatively spliced protein	Exon 6a	Exon inclusion	Machuca-Tzili et al, 2006
Z-band alternatively spliced protein	Exon 11	Exon inclusion	Lin et al, 2006

Table 1.6: List of misregualted alternative splicing events in myotonic dystrophy (adapted from Ranum and Cooper, 2006)

Misregulated splicing of these groups of pre-mRNAs involves either intron retention, exon exclusion or inclusion of exons containing stop codons. This results in reduced expression of functionally irrelevant protein or truncated proteins in myotonic dystrophy patients. The misregulated splicing events in DM are discussed in detail below.

1.5.3.1 *CLCN-1*

The muscle-specific chloride channel (*CLCN-1*) is responsible for regulating the flow of Cl^- ions across the cell membrane in the sarcolemma of skeletal muscle (Aromataris & Rychkov, 2006). Misregulation of *CLCN-1* is associated with myotonia, a major symptom of DM. Myotonia in both patients and mouse models (HSA^{LR}) is linked to reduced CLCN-1 protein expression (Charlet et al, 2002b; Mankodi et al, 2002). Indeed, loss of CLCN-1 in patients is caused by inability to switch its splice isoforms from embryonic to adult pattern (Mankodi et al, 2002).

The misregulated splicing of *CLCN-1* involves intron 2 retention which contains a premature stop codon or inclusion of two novel exons located between exon 6 and 7 (Charlet et al, 2002b).

DM patient samples have intron 2 retained in *CLCN-1* mRNA as well as retention of the novel exons. This leads to truncated mRNA which is subsequently removed by nonsense mediated decay (NMD) leading to loss of CLCN-1 protein (Charlet et al, 2002b; Mankodi et al, 2002). Since *CLCN-1* is developmentally regulated, its embryonic spliceforms retain intron 2 and two novel exons (6a/7a) which are absent in adult splice isoforms. Lueck et al (2007) demonstrated in mice that *clcn-1* goes through a splicing transition

within the first three weeks of postnatal life. During the transition process from foetal to adult, *Clcn-1* splicing switches to isoforms having intact reading frames and an increase in *Clcn-1* mRNA as well as its function. In contrast to a DM mouse model (HSA^{LR}) used in the same study, it was shown that the splicing transistion was absent with reduction in Clcn-1 function and myotonic discharges (Lueck et al, 2007).

The finding in a DM mouse model by Lueck et al (2007) had also been confirmed in a previous study by Mankodi et al (2002) using DM mouse with similar background.

1.5.3.2 Insulin Receptor (*IR*)

The *IR* is a tetramer consisting of two α- and two β- subunits. Its alpha subunit interacts with insulin which causes intracellular units to be autophosphorylated. *IR* RNA exhibits two alternative splice isoforms as a result of inclusion or exclusion of a 36 nucleotide long exon 11 of α-subunits to give isoforms designated as IR-A and IR-B. IR-A lack exon 11 while IR-B retain it (Seino et al, 1989). Furthermore, *IR* splice isoforms expression is tissue-specific. The IR-A splice isoform which predominates in non-muscle tissue has twice the affinity for insulin, decreased signalling capacity and twice lower activity for tyrosine kinase while the IR-B splice isoform is mainly expressed in tissues carrying out glucose homeostasis such as adipose tissue, liver and skeletal muscle (Kellerer et al,1992; McClain 1991;Mosthaf et al, 1990; Vogt et al, 1991).

It has been suggested that DM patients are associated with insulin resistance (diabetes type 1) as a result of splicing abnormalities in *IR*. DM1 muscle cultures have been observed to have predominance of IR-A, the non-muscle splice isoform with lower signalling capacity (Savkur et al, 2001; Savkur et al, 2004). The IR-A isoform which lacks exon 11 necessary for its biochemical activity was demonstrated to be due to MBNL1 and MBNL2 depletion and/or elevated level of CUG-BP1 in DM1 myoblasts (Dansithong et al, 2005; Ho et al, 2004; Paul et al, 2006). In addition, DM2 patient muscle displays similar *IR* splicing abnormality found in DM1 (Savkur et al, 2004).

1.5.3.3 *RYR* and *SERCA*

The sarcoplasmic reticulum (SR) proteins Ryanodine receptor (*RyR1*) and Sarcoplasmic/endoplasmic reticulum Ca^{2+}-ATPase (*SERCA*) are responsible for regulating calcium homeostasis in skeletal muscle (Kimura et al, 2005). The *RyR* is encoded by three genes: *RyR1*, *RyR2* and *RyR3*. *RyR1* is abundant in skeletal muscle; *RyR2* is mainly expressed in heart muscle while *RyR3* occurs in limited levels in immature skeletal muscles (Meissner et al, 1994; Giannini et al, 1995; Sutko & Airey, 1996). *RyR1* splice variants are regulated in a developmental and tissue-specific manner (Futatsugi et al, 1995).

In DM1 muscle cultures, *RyR1* splicing is altered resulting in the splice isoform that lacks exon70 referred to as AS1(-) in contrast to AS1(+) having exon70 that predominates in normal cultures (Kimura et al, 2005).

The other SR protein *SERCA* is also encoded by three genes: *SERCA1*, *SERCA2* and *SERCA3*. Its spliced transcripts are regulated in a developmental and tissue specific way to give isoforms differing in C-terminal regions.

SERCA1 has two alternatively spliced isoforms: SERCA1a which is the adult splice isoform and SERCA1b which is the embryonic isoform are expressed in fast-twitch (type2) skeletal muscle. SERCA2a occurs in slow-twitch (type1) skeletal muscle and cardiac muscles while SERCA2b is found in all tissues. SERCA3 is found mainly in non-muscle tissues (Burk et al, 1989; Lytton et al, 1992).

DM1 skeletal muscle cultures were observed to have a significant proportion of embryonic isoform lacking exon22 (SERCA1b) in relation to controls (Kimura et al, 2005). This splicing abnormality was further confirmed in HSA^{LR} mice and *SERCA1* was also found to be developmentally regulated in mice (Kimura et al, 2005; Lin et al, 2006).

In addition, it was also found that the *SERCA2d* isoform containing full length intron19 occured at a lower level in DM1 cells (Kimura et al, 2005).

1.5.3.4 Cardiac Troponin T (*cTNT*)

Cardiac troponin T (*cTNT*) is expressed mostly in cardiac muscles and its splicing event in DM was first discovered in 1998. It had been shown that *cTNT* was subject to developmental regulation. The embryonic splice isoform includes exon 5 which is excluded in the adult isoform. In DM, there is a shift towards the embryonic isoform having exon 5 (Philips et al, 1998; Savkur et al, 2001) and it has been demonstrated that overexpression of CUG-BP1 in normal skeletal muscles induces a shift toward DM-like isoform for *cTNT* (Philips et al, 1998).

To further confirm this, CUG-BP1 overexpressing mice reproduce DM-like splicing pattern for *cTNT* by increased exon 5 inclusion (Ho et al, 2005a).

In addition, it has been suggested that *cTNT* splicing defects could be responsible for cardiac abnormalities seen in DM patients (Philips et al, 1998).

In another context, MBNL produces adult splicing patterns by excluding exon 5 through binding to introns upstream of alternatively spliced exons in *cTNT* (Ho et al, 2004). Recently, Warf et al (2009) demonstrated that MBNL1 controls *cTNT* exon5 splicing by competing with U2AF65 for binding to 3' end of intron4.

1.5.3.5 Fast Skeletal Troponin T (*TNNT3*)

The alternative splicing of this gene was found to include a fetal exon in DM patients which was lacking in unaffected persons' muscle cultures (Kanadia et al, 2003).

Furthermore, this was confirmed in a muscleblind-like knock-out mouse model ($mbnl^{\Delta 3/\Delta 3}$) which showed DM-like splicing patterns for *TNNT3* expressing fetal the exon isoform (Kanadia et al, 2003).

1.5.3.6 Myotubularin-related protein1 (*MTMR1*)

MTMR1 belongs to the phosphatase family of proteins suggested to be involved in the myogenesis of differentiating myoblasts. It undergoes developmental regulation with alternative splicing of two fetal isoforms (A and B) that switches to an adult isoform C in adult skeletal muscle and cardiac muscles during development (Buj-Bello et al, 2002).

It has been observed in differentiating congenital DM1 muscle cells that there has been a reduced level of isoform C with the presence of a novel abnormal isoform G (Buj-Bello et al, 2002). In confirmation of this, Ho et al (2005) showed *MTMR1* splicing abnormality similar to that expressed in DM patients displaying predominance of A and B isoforms in a transgenic mice overexepressing CUG-BP1. The splicing abnormality in these isoforms A and B involves exon 2.1 which is present in isoform B but lacking in isoform A as well as exon 2.2 (figure 1.5) which is only present in isoform C (Ho et al, 2005).

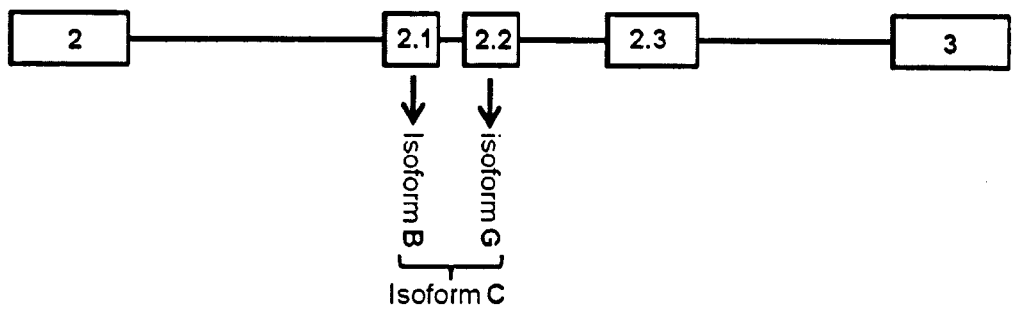

Figure 1.5: Exonic organisation of MTMR1 gene indicating the various isoforms of its transcripts formed by exons lying between exon 2 and 3 (adapted from Ho et al, 2005).

1.5.3.7 Muscleblind-like (*MBNL*)

This group of proteins is involved in the splicing of pre-mRNAs of many genes and its function is altered in DM. Alternative splicing of *MBNL1* occurs at exon 3,5,7 and 9 to give nine splice isoforms. It has been shown to undergo post-natal splicing transition to give MBNL1 isoforms having different cellular activities (Lin et al, 2006).

In DM, *MBNL1* is to be defectively spliced at exon 7 resulting in the inclusion of this exon in DM patients and its absence in controls (Botta et al, 2008; Cardani et al, 2009; Lin et al, 2006). Similarly, *MBNL2* shows identical splicing misregulation in exon 7 in DM (Lin et al, 2006).

Further confirmation was demonstrated in a DM mouse model HSA^{LR} reproducing *mbnl1* splicing defects similar to DM patients (Lin et al, 2006). In addition, *MBNL1* was shown to undergo a post-natal splicing switch in wild type mice (Lin et al, 2006). The predominance of *MBNL1* splice isoforms containing exon 7 in DM may account for its localisation in the nucleus (Botta et al, 2008; Cardani et al, 2009; Lin et al, 2006).

1.5.3.8 *Tau*

Tau is expressed mainly in the brain and neurons. It is a microtubule associated protein involved in microtubule network modulation. *Tau* also interacts with tubulin during cytoskeleton formation (Buee et al, 2000). Alternative splicing of *tau* pre-mRNA exon 2, 3 and 10 generates six splice isoforms in adult human brain. These exons are developmentally regulated and foetal isoforms lack all the three exons (Andreadis et al, 1992).

In DM, there is predominant expression of foetal isoform of *tau* in which one or many of exons 2,3,6 and 10 are absent (Jiang et al, 2004; Leroy et al, 2006; Sergeant et al, 2001). Defects in exon 6 splicing has also been reported for DM (Leroy et al, 2006).

To validate the role of *tau* in DM, transgenic DM mouse model expressing CTG repeats in *DMPK* 3'-UTR context displayed abnormal tau protein expression consistent with observation in DM1 patients (Seznec et al, 2001).

1.5.3.9 Other Splicing abnormalities

N-methyl-D-aspartate receptor (*NMDAR1*) exon 5 inclusion in DM1 patients is the most prominent effect of spliceopathy observed in the patient's brain (Jiang et al, 2004). Also occurring in the brain is the splicing defect in amyloid precursor protein (*APP*) involving exon 7 exclusion in DM1 patients (Jiang et al, 2004). Lin et al (2006) observed increased inclusion of M-line exon 5 in *M-Titin* in comparison with controls. In addition, they also discovered that exon 11 inclusion of Z-band alternatively spliced protein (*ZASP*) in DM patients. Another splicing variant of *ZASP* involving a novel exon 6a absent in normal controls was observed in DM muscles (Machuca-Tzili et al, 2006).

Dystrophin, a cytoskeletal structural protein involved in signalling in the sarcolemma, is abnormally spliced at exons 71 or 78 resulting in exclusion of these exons in DM1 patients (Nakamori et al, 2007).

Indeed, misregulated alternative splicing accounts for some of the major symptoms in DM such as myotonia, insulin resistance among others. Splicing defects in DM could provide clues and targets for therapeutic intervention because of its contribution to the disease condition.

1.5.4 Mechanism of Misregulated Splicing

CUG expanded repeat RNAs have a trans effect and modify the normal splicing forms of a group of pre-mRNAs. Mankodi and colleagues (2000) demonstrated an alteration in the splicing of *CLCN-1* pre-mRNA in HSA^{LR} transgenic mice which has a repeat expansion in a non-*DMPK* RNA background. Other evidence in support of CUG repeat containing mRNA inducing a splicing switch, comes from transient expression studies of CUG expanded repeat containing *DMPK* RNA in cell culture. Co-expression of mRNA containing CUG expanded repeats with splicing reporter minigene constructs of cardiac troponin T (*cTNT*) and *IR* causes DM splicing isoform for the alternative exons (Phillips et al, 1998; Savkur et al, 2001; Charlet et al, 2002b).

The mechanism by which CUG repeat RNA induces a trans-dominant effect is proposed to involve sequestration of one or more splicing regulators by RNA containing large repeats leading to nuclear depletion and consequent loss-of-function by these regulators. Evidence supporting this hypothesis comes from the binding to CUG repeats of two RNA-binding proteins involved in alternative splicing (Miller et al 2000; Timchenko et al, 1996b). One of them is CUG-BP1 which belongs to the CELF group of six genes that encode proteins regulating many post-transcriptional processes including translation initiation, alternative splicing, RNA editing and mRNA stability. The second family of CUG repeat RNA binding proteins is the muscleblind-like (MBNL) of which there are three members. MBNL proteins, as well as CUGBP, also control alternative splicing regulation by its binding to specific sites within pre-mRNA.

Several studies have reported a functional role for the loss of MBNL in the misregulation of splicing in DM. MBNL proteins were shown to bind to expanded CUG repeat RNA which folds to form a hairpin structure having G-C base pairs with bulged unpaired U residues (Napierala & Krzyzosiak, 1997). The binding of MBNL was found to be proportional to the length of CUG repeat (Miller et al. 2000) and is consistent with direct association of repeat expansion with disease severity. In addition, it has been suggested that MBNL proteins could bind directly to intronic elements to control *cTNT* and *IR* splicing that are misregulated in DM (Ho et al, 2004).

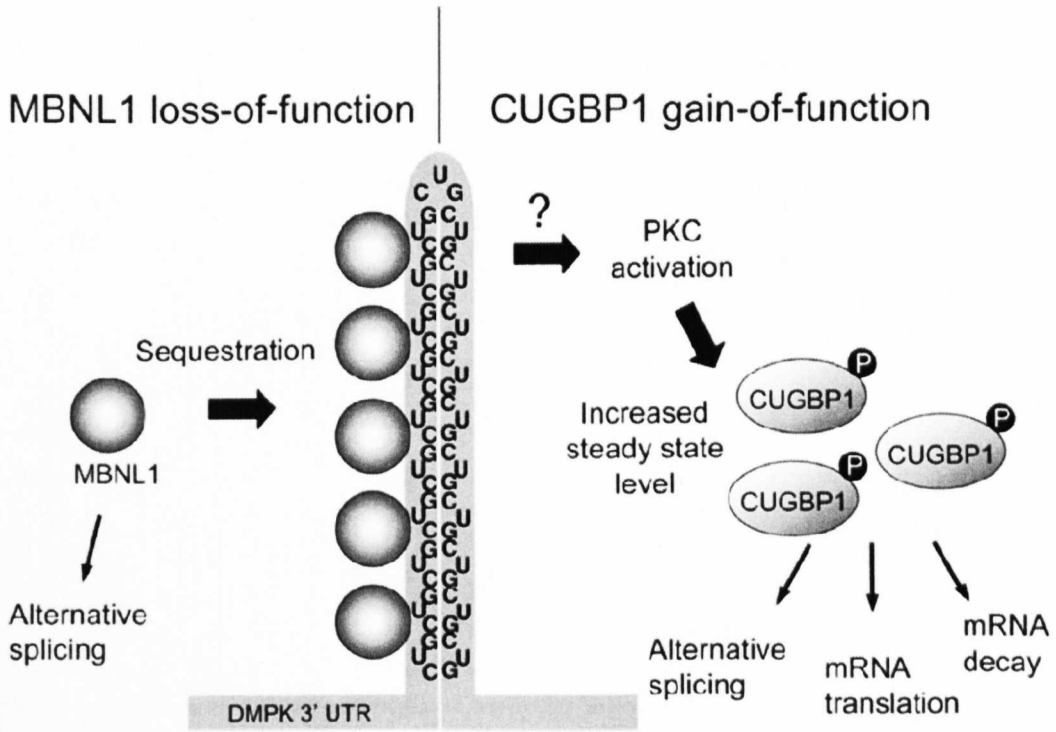

Figure1.6: Proposed mechanism for splicing misregulation by MBNL1 and CUG-BP1 leading to DM phenotype (taken from Lee and Cooper, 2009)

Evidences from several studies have also proposed a role for CUG-BP1 in abnormal splicing regulation of DM (Charlet et al, 2002a; Dansithong et al, 2005; Jiang et al, 2004). In one study, CUG-BP1 was identified by Timchenko and co-workers (1996a) to bind to CUG repeat RNA. However, CUG-BP1 binds to short single stranded CUG repeats and this binding does not correlate with the length of repeat RNA. CUG-BP1 and other CELF protein family members do not colocalize with CUG repeat foci (Fardaei et al, 2001).

In alternative splicing regulation, three of the abnormal splicing regulation events found in DM involving *cTNT*, *IR* and *CLCN-1* were observed to be regulated by CUG-BP1 (Charlet et al, 2002b; Phillips et al, 1998; Savkur et al, 2001). In addition, the splice isoforms observed in these three genes correlate with higher CUG-BP1 activity. Studies have reported the elevation of CUG-BP1 protein steady-state levels in DM tissues and cell cultures (Dansithong et al, 2005; Savkur et al, 2001). In addition, evidence supporting its role is the decrease of CUG-BP1 protein expression in mouse skeletal muscle and heart after birth (Ladd et al, 2005), which correlates with the normal developmental splicing pattern regulation in tissues altered in DM. Overexpression of CUG-BP1 in heart and skeletal muscle of transgenic mice led to the foetal splicing form of *cTNT*, *CLCN-1*, and myotubularin-related protein 1(Ho et al, 2005a).

MBNL and CUG-BP1 have been implicated in the regulation of *cTNT* and *IR* in DM. These two proteins act as antagonistic regulators of the *cTNT* and *IR* splicing so that the splice isoforms found in DM correlate with loss of MBNL and gain of CUG-BP1 effects. The proposal above points to loss of MBNL activity as the primary cause of splicing defects in DM while CUG-BP1 could be an antagonistic regulator.

However, another proposal speculates that loss of activity by MBNL is not the main event during the splicing defect observed in DM. This proposal comes from transient transfection studies involving expression of CUG repeat-containing RNA that leads to a splicing switch in trans with co-expression of *cTNT* and *IR* minigenes (Philips et al, 1998; Savkur et al, 2001). The splicing of minigenes was used as a reporter of trans effects of CUG repeat RNA. Mutations affecting CUG-BP1 binding sites make *cTNT* and *IR* minigenes resistant to trans effects of CUG repeat RNA, hence suggesting that binding of CUG-BP1 to *cTNT* and *IR* mRNAs is necessary for these co-expressed repeats to influence splicing (Philips et al, 1998; Savkur et al, 2001). Furthermore, mutation in *cTNT* minigene that is resistant to CUG-BP1 or CUG repeat RNA is responsive to MBNL1 siRNA-mediated decrease efficiently like in nonmutated mingene (Ho et al, 2005b). These observations show that co-expressed CUG repeat RNA does not reduce MBNL levels enough to change the splicing pattern seen in wild type minigenes. MBNL depletion alone does not account for the effect the CUG repeat RNAs could have on alternative splicing of the wild type *cTNT* minigene. Previous studies however, show a difference in phosphorylation status and nucleocytoplasmic distribution of CUG-BP1 (Roberts et al, 1997). These changes could affect nuclear protein steady state levels or RNA binding or splicing regulation.

RNA containing CUG repeats formed nuclear foci and were observed to colocalize with co-expressed GFP-MBNL1 (Ho et al, 2005a). Further studies involving fluorescence recovery after photobleaching demonstrated in cell culture that the affinity of GFP-MBNL1 for CUG and CAG repeat were similar (Ho et al, 2005a). These findings led to the view that colocalization of MBNL1

with RNA foci alone is not responsible for misregulated splicing in DM and that trans effects of CUG repeats on splicing are more than just sequestration of MBNL1 which may include other splicing factors.

Another study of the effects of RNA containing CUG repeats proposes that both MBNL and CELF proteins regulate and control a subgroup of alternative splicing events during developmental stages (Miller et al, 2000). In accordance with this hypothesis, is the loss of CELF protein expression at developmental stages in several tissues and the idea that MBNL and CELF proteins are antagonistic regulators of developmental stage splicing events both in normal cells and in DM (figure 1.7).

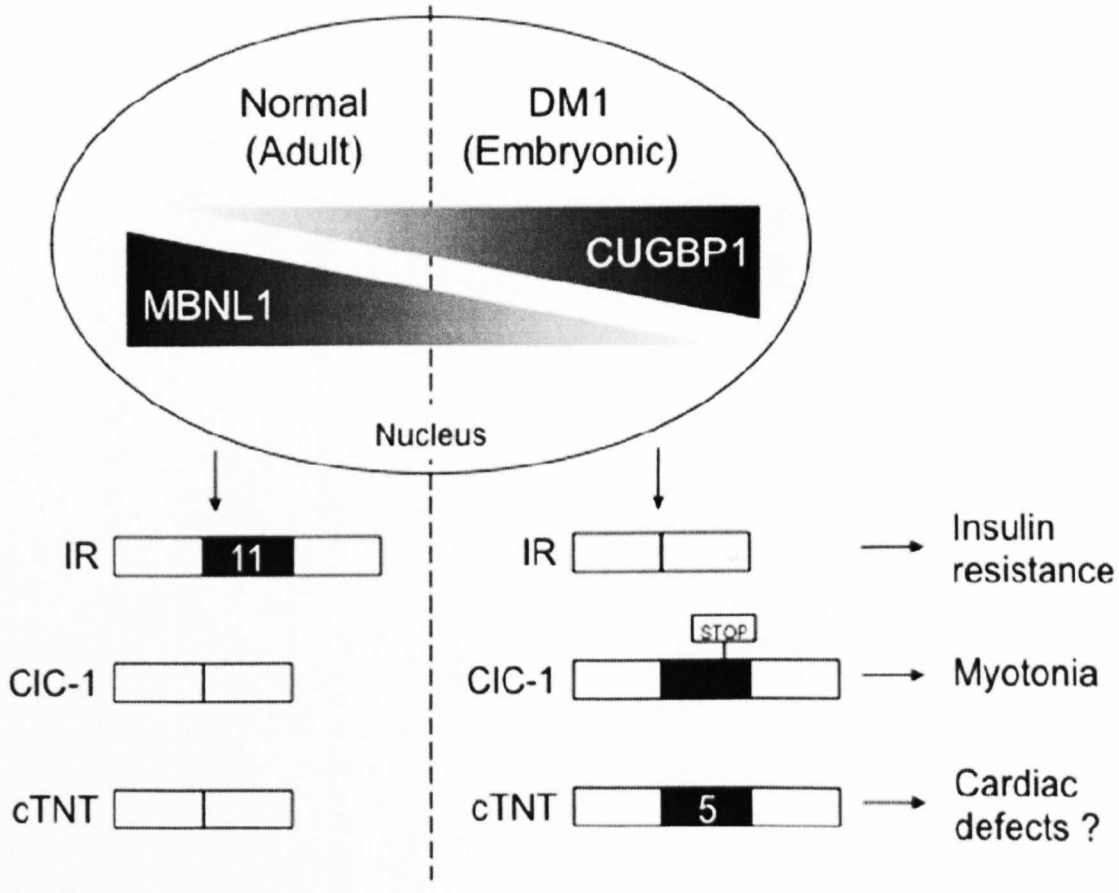

Figure 1.7: Developmental regulation of alternative splicing by MBNL1 and CUG-BP1 (taken from Lee and Cooper, 2009)

1.6 Possible Targets for Therapeutic Intervention in DM

With the underlying mechanisms for DM pathogenesis which appear to be mediated by toxic RNAs acquiring dominant negative function via sequestering the splicing factor MBNL, possible targets targets for therapeutic intervention would include: (1) disrupting interactions in foci between MBNL and RNA CUG repeats in DM1 or CCUG repeats in DM2; (2) destruction or removal of mutant RNA containing repeat expansions; (3) correction of misregulated splicing; (4) increased dosage of MBNL and (5) inhibition of CUGBP1.

1.6.1 Disruption of RNA-MBNL Interactions

The RNA mediated disorder in DM1 has been proposed to be caused by expanded CUG repeats RNA trapped in the nucleus which in turn interacts with MBNL to cause DM-like effects (Kanadia et al, 2003; Mahadevan et al, 2006). This event represents a viable target for therapeutic intervention in DM.

Several studies have carried out screens for inhibitory molecules that can block MBNL1 interactions with CUG or CCUG expanded repeats which could provide clues to modifying disease phenotype (Arambula et al, 2009; Gareiss et al, 2008; Lee et al, 2009a; Lee et al, 2009b; Mulders et al, 2009; Pushechnikov et al, 2009; Wheeler et al, 2009).

In a study by Arambula and co-workers (2009), the rational design of ligands that selectively bind to CUG repeats in RNA at high affinity was shown to displace MBNL1 from MBNL1-poly(CUG) complex. Antisense oligonucleotides (AON) such as 2-O-methyl-phosphorothioate-modified

(CAG)7 AON has been reported to reduce ribonuclear complexes in RNA foci (Mulders et al, 2009).

In another study, a morpholino antisense oligonucleotide CAG25 has been shown in a mouse model to bind to CUG expanded RNA and inhibit its interaction with MBNL1 resulting in reduction of nuclear foci as well as correction of misregulated alternative splicing of *Clcn1* to restore ion channel function (Wheeler et al, 2009).

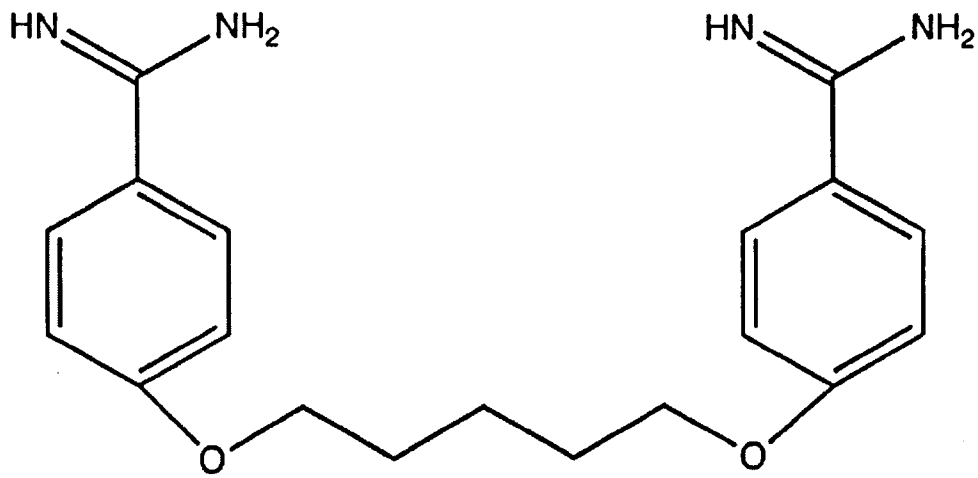

Figure 1.8: Chemical Structure of Pentamidine

In a most recent study by Warf and colleagues (2009b), gel-shift-assay for MBNL1-CUG repeat showed a molecule pentamidine inhibited RNA CUG-protein complex by competively displacing MBNL1. In addition, pentamidine was shown to partially rescue splicing defects of insulin receptor and cardiac troponin pre-mRNAs misregulated in DM.

Thus, MBNL1-CUG repeat interactions could provide a potential target for modifying downstream effects such as missplicing and associated disease phenotypes found in DM.

1.6.2 Inhibition or Destruction of Mutant RNA

The toxic effect of expanded CUG or CCUG repeat RNA in myotonic dystrophy disease phenotype makes it a potential functional target for therapy. Compounds that can specifically target mutant RNA leading to its destruction, removal or inhibition would be relevant to reversing disease phenotype. An inducible mouse model of DM having expanded CTG repeat has demonstrated that the disease phenotype is reversible (Mahadevan et al, 2006).

In another study, degradation of expanded CUG repeats was tested using retroviral mediated antisense gene therapy. The antisense RNA was shown to be effective in degrading mutant *DMPK* RNA leading to its reduction. In addition, myoblast function was restored and CUGBP1 levels were reduced in human DM1 myoblasts (Furling et al, 2003).

In another study, a hammerhead ribozyme was used to induce reduction of *DMPK* nuclear foci via site-specific cleavage of mutant RNA resulting in restoration of alternative splicing patterns of insulin receptor in DM1 myoblasts (Langlois et al, 2003).

Another approach to reducing expanded CUG repeat RNA would be to use short interfering RNA (siRNA) which has been reported to be effective in fibroblasts of DM1 (Krol et al, 2007).

These studies support the proposal that destruction of mutant RNA could be a beneficial strategy for therapy in DM1. These approaches could also be applied to DM2 cells to reduce expanded CCUG repeat RNA.

In DM2, the processing of the *ZNF9* mRNA from the normal and mutant alleles are similar because of removal of intron1 containing mutant RNA,

hence there is no degradation of *ZNF9* mRNA (Margolis et al, 2006). However, the excised CCUG expanded repeat RNA which is intronic form hairpins that trap MBNL1 in a mechanism similar to CUG repeat in DM1 and targeting CCUG expanded repeat for degradation would also be useful for therapy.

Another strategy for potential DM therapy would be inhibition of expanded repeat transcripts to prevent their interaction with muscleblind-like protein in order to make them available for cellular functions of regulating alternative splicing.

Several studies have been carried out to identify inhibitors that can bind to expanded CUG or expanded CCUG repeat RNA to prevent its interaction with muscleblind-like proteins (Arambula et al, 2009; Gareiss et al, 2008; Lee et al, 2009; Pushechnikov et al, 2009 and Warf et al, 2009).

In a study by Wheeler et al (2009), a 25-mer morpholino antisense oligonucleotides having CAG triplet repeats was designed to bind specifically to CUG repeat RNA with high affinity leading to the release of MBNL1 from nuclear foci and subsequent degradation of RNA.

Ribonuclear foci formation in DM could be utilized in therapeutic intervention of RNA-mediated disease. The development of cell-based assays based on nuclear foci will allow screening of compounds and molecules in high-throughput screens (HTS).

1.6.3 Correction of Spliceopathy

Studies have shown that defects in splicing of *CLCN-1* and *IR* lead to myotonia and insulin resistance respectively- found in DM patients (Charlet et

al, 2002b; Mankodi et al, 2002 and Savkur et al, 2001). The abnormality in splicing regulation of *CLCN-1* pre-mRNA involves inclusion of exon 7a containing a premature stop codon into the mature transcript. Another splicing misregulation in the same gene involves retention of intron 2 which contains a termination codon (Charlet et al, 2002b and Mankodi et al, 2002). Misregulation of splicing involving exon 7a and intron 2 leads to a truncated transcript which is removed by nonsense-mediated decay or truncated, functionally irrelevant CLCN-1 protein.

Abnormal splicing of the insulin receptor transcript results in exclusion of exon 11 to produce an isoform with lower signalling activity causing insulin resistance and diabetes in DM patients (Savkur et al, 2001).

Correction of splicing abnormalities has become a potential target for therapeutic intervention in DM. A proof-of-function study by Kanadia and co-workers (2006) showed reversal of RNA missplicing for *Clcn-1* exon 7a, *Cypher* exon 11, *Serca1* exon22 and fetal exon of *Tnnt3* in a DM mouse model overexpressing MBNL1.

Chemical agents such as morpholino antisense oligonucleotide (CAG25) have been shown in a transgenic mouse model HSA^{LR} to partially correct the defect in *Clcn-1* leading to the restoration of ion channel function (Wheeler et al, 2009). In a previous study, Wheeler and colleagues (2007) used a morpholino antisense oligonucleotide (AON) that targets 3' splice site of *Clcn-1* exon 7a to inhibit inclusion of this exon in a DM mouse model. This restored splicing regulation of *Clcn-1* mRNA leading to an increase in level of *Clcn-1* mRNA and protein.

Finally, pentamidine was shown to reverse splicing defects in insulin receptor and cardiac troponin in a HeLa cell model (Warf et al, 2009b). Chemical agents that have the benefit to correct splicing defect would be beneficial in the therapy of DM.

1.6.4 Increased Activity of MBNL1

In DM, loss of MBNL1 function leads to spliceopathy which has been demonstrated to be due to negative effects of toxic RNA with expanded repeats (Charlet et al, 2002b; Kanadia et al, 2003; Lin et al, 2006).

A study to test the role of MBNL1 in reversing spliceopathy and modifying disease phenotype was carried out in HSA^{LR} mouse model (Kanadia et al, 2006). In this study, the mouse was injected with adeno-associated virus (AAV) overexpressing MBNL1. The overexpression of MBNL1 protein was demonstrated to restore normal splicing patterns resulting in reversal of myotonia. This shows that the development of therapeutic agents based on overexpressing MBNL1 would be beneficial in treatment of DM.

1.6.5 Inhibition of CUG-BP1 activity

The RNA-mediated toxicity causes upregulation of CUGBP1 activity in DM via activation of Protein Kinase C (PKC) by expanded CUG repeats in DM1. The hyperphosphorylation of CUGBP1 results in its increased stability leading to its increased levels and spliceopathy in DM1 patients (Kuyumcu-Martinez et al, 2007; Orengo et al, 2008).

In a mouse model expressing 960 CUG repeats showing loss of MBNL1, myotonia and splicing abnormalities; CUGBP1 level was elevated as well as

splicing abnormalities regulated only by CUGBP1 were observed (Orengo et al, 2008).

Another study using a DM1 mouse model expressing cardiac-specific expanded CUG repeat RNA, the administration of PKC inhibitors improved cardiac conduction abnormalities (Wang et al, 2009). In addition, these inhibitors reduced phophorylation of CUGBP1 and decreased its protein levels (Kuyumcu-Martinez et al, 2007). Furthermore, there was reduction in splicing defects regulated specifically by CUGBP1 (Wang et al, 2009). The use of PKC inhibitors could provide another potential target for treatment of DM1.

1.7 Advances in Screening Assays Development for DM

Many DM therapeutic compound screens utilize RNA repeat units-MBNL1 interactions. In a study by Gareiss et al (2008), a fluorescently labelled RNA repeat having the sequence Cy3-CCG-$(CUG)_{10}$-CGG was monitored for interactions with a compound library in a technique referred to as resin-bound dynamic combinatorial chemistry (RBDCC). The RBDCC is a competitive assay that utilizes the affinity of resin-bound compounds to bind the fluorescently labelled RNA by competing with each other. The hit compounds in this assay were identified by removing fluorescent resin beads indicating that the compound in resin beads have bound to the fluorescent RNA.

These fluorescent beads were subsequently identified by mass spectral analysis. For this assay, a resin-bound dynamic combinatorial library (RBDCL) of 11325 molecules was made from 150 cysteine-containing building blocks and four positive hits were obtained. The authors did not report whether the compound hits obtained in this assay could reverse spliceopathy associated

with DM, nor whether the hits obtained in this assay are toxic when applied to DM patients' cell cultures.

Gel-shift assays have been utilized in identifying compounds that inhibit CUG expanded repeats interaction with MBNL1 (Warf et al, 2009; Wheeler et al, 2009). In a study by Wheeler et al (2009), a CAG25 antisense oligonucleotide was demonstrated to bind CUG repeat hairpins by blocking CUG repeat-MBNL1 complexes to form a stable CUG repeat-morpholino heteroduplex in a gel-shift assay. Subsequently, Warf et al (2009) used a similar technique to identify pentamidine as lead compound that disrupted MBNL1-CUG repeat interactions in a gel-shift assay. However, gel-shift assays may not be sufficient in screening therapy of DM as toxicity and side effects of compounds cannot be determined hence any compounds identified in this way may need further testing in cell cultures to assess their effects on cell viability as well as in rescuing of splicing defects and foci clearance in DM patients' cells.

Another screening assay for identification of compounds that bind to CUG repeats exploited isothermal titration calorimetry (ITC) to identify compounds that could bind to T-T and U-U mismatches in CTG or CUG repeats by forming hydrogen bonds (Arambula et al, 2009). This assay was also shown to disrupt complex structure formation between MBNL1 and poly(CUG). It is not possible to determine if assays of this nature can identify compounds with no toxic or side effects unless applied to DM cells.

A modular design of ligands that bind to RNA repeat with high affinity and specificity has been reported in a technique called Huisgen dipolar cycloaddition reaction (HDCR) (Lee et al, 2009a; Lee et al, 2009b; Pushecnikov et al, 2009; Disney et al, 2010). HDCR was used to direct ligands

on microarray surfaces and its interaction with RNA repeats units were analysed bioinformatically. Eventhough, molecules identified by this approach were found to be permeable in mouse muscle cells C2C12, the issue is whether their cellular uptake and localisation, especially with respect to repeat RNA in nucleus would be effective in DM cells.

1.7.1 High Throughput Screening (HTS)

Thus far only one assay based on intron 2 splicing of *CLCN1* in DM cells has been reported for its application in DM-related HTS which identified AKT V (also known as protein kinase B) inhibitor triciribine (O'Leary et al, 2010). However, this assay used in HTS was limited in its ability to determine the level of compound effect on correcting intron 2 splicing in a quantitative manner. In addition, the hit compound in this screen was not confirmed for its effect on foci reduction as well as rescue of splicing defects in DM.

HTS is especially important in the development of DM therapy as it facilitates screening on a large scale, libraries of compounds in a short time.

1.8 Aim of Study

The objective of this study is to design and develop cell-based assays that could be utilized for screening molecules and compounds for DM therapy. These assays have been designed based on molecular events that lead to DM with the red arrows representing potential target for therapeutic intervention (figure 1.9).

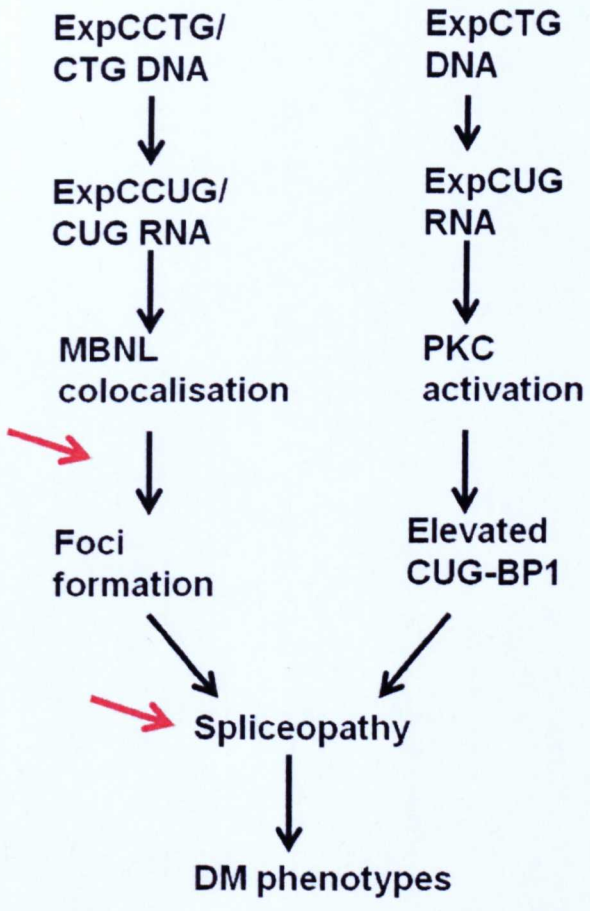

Figure1.9: Schematic representation of molecular events leading to DM. The red arrows indicate possible target for therapeutic screening

The assays developed fall into two major categories:

1) Primary assays that allow screening of large numbers of compounds on a large scale in High Throughput Screens (HTS). Two assays were developed for HTS namely: (a) Splicing construct assay and (b) Nuclear foci assay.

2) Secondary assays that permit validation of positive compound hits from primary screening assays for their effect on mutant RNA transcripts and spliceopathy. They include: (a) *BpmI* polymorphism assay (b) *IR* splicing assay (c) *SERCA1* splicing assay and (d) *MBNL* splicing assay

The splicing construct used in the primary assay was based on splicing of transgenes in wild type and DM cells. The splicing construct involves transgenes whose 5' and 3' ends were tagged with green fluorescent protein (GFP) and Dioscorea red fluorescent protein (DsRed) respectively contained in a plasmid vector (figure 2.1). The expression of GFP and DsRed proteins were used as qualitative and quantitative measure of the splicing process in which only of a GFP is expressed by cells if there is no splicing while both GFP and DsRed is expressed in cells that splicing occurs (figure 1.9). The production of only GFP by cells is due to the presence stop codon in intron 2 of pGR-CLCN1 or frameshift in open reading frame by intron 19 of pGR-SERCA2 whose retention leads to either truncated translation (pGR-CLCN1) or out of frame translation (pGR-SERCA2).

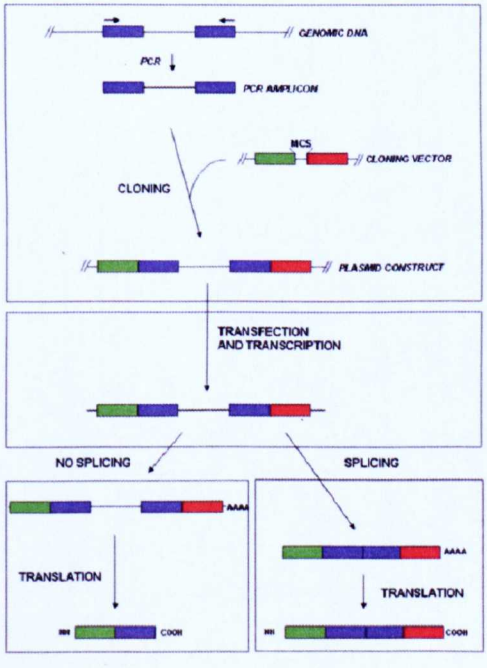

Figure 1.10: Schematic model of the splicing concept for transgene construct when splicing occurs leading to intron exclusion (bottom right) to produce both GFP and DsRed or no splicing (bottom left) resulting in intron inclusion to produce only GFP.

The aim is to transfect the transgenes into both C2C12 and DM cell lines and DsRed/GFP ratio was used as reference in determining the rate of alternative splicing in these cells. Cells with transgenes were selected to generate stable clones for subsequent application in screening assays.

Based on the splicing concept, normal cells would produce equal ratios of green and red fluorescent proteins which would indicate that intron is spliced out while DM cells would show ratios of zero showing intron retention. The transgene splicing under study are those involving intron 2 of skeletal muscle-specific chloride channel (*CLCN1*) and intron 19 of sarcoplasmic/endoplasmic reticulum Ca^{2+}-ATPase (*SERCA2*) whose flanking exons alongside with introns of interest were cloned into the vector.

The other primary assay based on interactions between RNA expanded repeats and muscleblind-like proteins to form nuclear foci. Nuclear foci would be used to screen for compounds that could disrupt RNA repeat-MBNL1 interactions in nuclear foci of DM cells. As a parallel assay to nuclear foci, GFP-tagged muscleblind-like (pGFP-MBNL) transfected into DM cells in order to study its colocalisation with RNA repeat units in nuclear foci and stable clones obtained from pGFP-MBNL would subsequently be used in compound screens to identify molecules that can disrupt this colocalisation.

In secondary assays, validation of hit compounds from primary assays were applied to assess their effect on mutant RNA transcript in *Bpm1* polymorphism assay involving *Bpm1* restriction analysis (figure 1.11); as well as assessing by RT-PCR its effectiveness in rescueing spliceopathy involving exon 11 of *IR*, exon 22 of *SERCA1* and exon 7 of *MBNL1* and *MBNL2*.

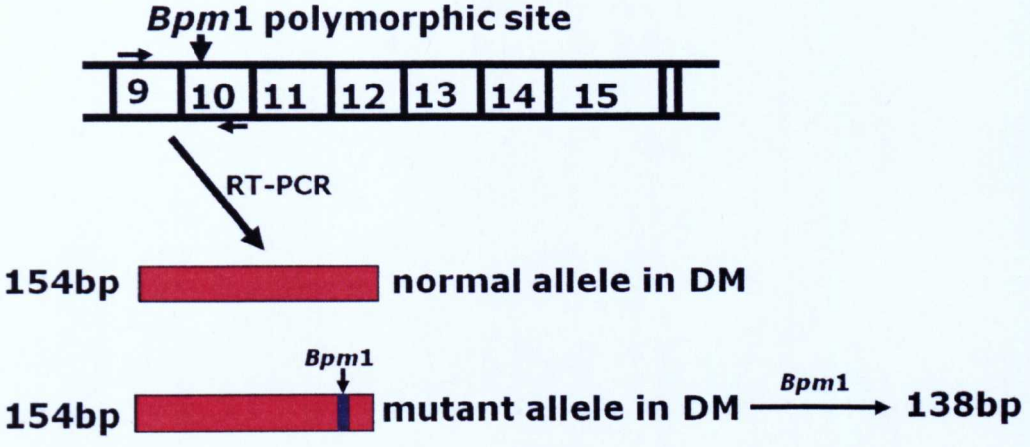

Figure 1.11: Schematic diagram of the *Bpm1* restriction assay for the presence of normal and mutant *DMPK* transcripts

CHAPTER TWO: MATERIALS AND METHODS

All experiments were carried out under standard conditions and at room temperature unless stated otherwise.

2.1 Microbiological Methods

All microbiological methods were carried out under aseptic conditions and were performed in accordance with molecular cloning protocols by Sambrook & Russell (2001).

2.1.1 Media

The medium used for microbiological work was Luria Broth, SOB and SOC media. LB consist of 10g/l Bacto-tryptone, 5g/l yeast extract, 10g/l,NaCl and 2mM NaOH(pH 7.0).The SOB medium was made up of 10g/l Bacto-tryptone, 5g/l Bacto-yeast extract, 0.548g/l NaCl, 0.186g/l KCl and 2mM NaOH (pH 7.0). The SOC medium was prepared from SOB media by mixing 40mls of SOB with 800µl of 20% glucose followed by addition of 200µl of 1M $MgCl_2$.

2.1.2 Antibiotics

Antibiotic used for selection was kanamycin which had previously been dissolved and diluted in water to a stock concentration of 25mg/ml. The stock antibiotics were stored at -20°C. The working concentration of the antibiotic was 25µg/ml in the selection procedure.

2.1.3 Microbiological Plates

Petri dishes of 90mm in diameter were used as selection plates into which kanamycin antibiotic was added to the LB medium to give a final concentration of 25μg/ml.

2.1.4 Glycerol Stocks

For long term storage, bacterial cultures were prepared by picking single colonies and immersed in test tubes containing 5mls of LB with kanamycin and were subsequently put in a shaking incubator at 200rpm for 8 hours. The bacterial cultures were then harvested by pelleting at 1000g for 10 minutes. The cultures were resuspended in 420μl LB medium and 80μl of 80% glycerol was added. Vortexing was applied to the mixture which was frozen in liquid nitrogen followed by storage at -70°C.

2.2 Tissue Culture Methods

These were carried out inside a laminar flow cabinet at room temperature. With the exception of C2C12 lines, all fibroblast lines used for tissue culture work had been previously telomerised to immortalise them.

2.2.1 Solutions, Antibiotics and Media

Solutions used for tissue culture study were Dulbeccos Modified Eagle's Medium (DMEM) from GIBCO containing 4,500mg/L glucose, L-glutamine and pyruvate; Foetal Bovine Serum (FBS) from GIBCO; Penicillin/Streptomycin from GIBCO containing 10,000 units of Penicillin G and 10,000μg/ml streptomycin sulphate in 0.85% saline; 50mg/ml Geneticin

(G418) from GIBCO; Dimethyl Sulphoxide (DMSO) from Sigma; phosphate buffer solution (DPBS) from GIBCO made up of $Cacl_2$, $MgCl_2$ and phosphate buffer saline; 1mg/ml doxycyclin from Clonetech; and 0.25% porcine Trypsin-EDTA solutions from Sigma.

2.2.2 Cell Cultures

Cell lines used in the study include mouse muscle cells (C2C12), DM2 fibroblast line, KAGOtelo; two wild type lines one of which contains inducible MyoD, NIRAtelo and SBteloMyoD; and a DM1 fibroblast cell line containing inducible MyoD, KBteloMyoD which can be differentiated into myoblasts in the presence of doxycyclin. All human fibroblasts used in this project had been previously telomerised.

2.2.3 Tissue Culture Passage

C2C12 cell lines and fibroblasts were visualized under the microscope to determine their degree of confluency. Cells of 80-100% confluency were split by passage. This involves removing the old media using serological pipettes and washing the cells with 10ml PBS. This was followed by the addition of 2.0ml of 0.25% Trypsin-EDTA to the flask containing the cells and the flask was subsequently incubated at 37°C and 5% CO_2 for 5-10 minutes to dislodge the monolayer of cells from the bottom of the flask as well as separate cells from each other. The flask was visualized under the microscope for dissociation of the cell monolayer and 8 ml of fresh complete medium was added to the flask. The cells were then split and transferred to two or three other sterile $75cm^3$ flask based on the original confluency. These procedures

were performed in a Walker laminar flow safety cabinet under aseptic conditions.

2.2.4 Selection of Clones and Fibroblast Differentiation

Clones of human fibroblasts and C2C12 lines were selected after the cells were transfected with transgene constructs. Selection of clones was carried out in G418 under 200μg/ml for fibroblast and 600μg/ml for C2C12 cells.

DM1 fibroblasts used in this project had been previously infected with Lentivirus containing a MyoD inducible vector and in the presence of doxycyclin were induced to differentiate into myoblasts by addition of doxycyclin to a concentration of 2μg/ml for 6-8 days.

2.2.5 Cryopreservation of Cells

The cryoprotectant used for preserving C2C12 lines and human fibroblasts was dimethyl sulphoxide (DMSO) at the concentration of 10%. Confluent cells were drained of medium and washed with PBS. This was followed by addition of trypsin to the cells and incubation at 37°C for 5 minutes for the cells to dissociate from each other. The cells were subsequently resuspended in 10ml of complete media and the mix was transferred to a falcon tube and pelleted by centrifugation at 1500 rpm for 3 minutes with the supernatant removed by decantation. This was followed by resuspension of pellets in 1.5ml of 10% DMSO in complete media and transferred into cryotubes for storage at -80°C. The cells were subsequently transferred into liquid nitrogen after 24 hours.

2.2.6 Defrosting and Growing Cells from Liquid Nitrogen

Cells lines frozen in liquid nitrogen vials were removed from the liquid nitrogen storage tank and given a quick thaw by immediate incubation in a water bath at 37°C for 5 minutes. The vial of cells was immediately removed from the water bath and 1ml of pre-warmed complete media was added. The solution was subsequently transferred into a universal tube containing 10ml of complete media in order to reduce toxicity of the DMSO used in frozen cells. This was followed by centrifugation of cells at 1000rpm for a minute and the supernatant was removed. The cell pellets were resuspended in 10ml of complete media so as to remove DMSO thereby reducing damage to cells. The entire 10ml cell suspension was placed into a T-75 flask containing a further 10ml of complete media and incubated at 37°C/5% CO_2 overnight for growth.

2.2.7 Fixation of Cells

Cells were fixed prior to imaging in fluorescent and immunofluorescent screens as well as in fluorescent in situ hybridisation staining (FISH). In both fluorescent and immunofluorescent scans, cells were washed thrice with PBS followed by methanol:acetone fixation for 5 minutes. Alternative fixation was performed with 4% paraformaldehyde for FISH. Cells were subsequently washed three times with PBS before FISH or mounted for fluorescent screening. In fluorescent imaging, after washing with PBS, mount media consisting of 50% glycerol in PBS was added to the cells on coverslips for visualization under the fluorescence microscope.

2.2.7.1 Immunofluorescence

Fibroblasts were seeded into 96-well plates and allowed to grow overnight to 80% confluency. The cells were then washed thrice with PBS. Fixation of the cells was performed using ice cold methanol:acetone (50:50) for 5 minutes. Cells were subsequently washed thrice with PBS and blocked for non-specific reaction with 10% BSA in PBS for an hour at 37°C followed by three washes in PBS. The cells were incubated with 30-40µl of the primary MBNL1 antibody diluted four times in PBS at 37°C for an hour. This was followed by washing with PBS three times and the cells were subjected to incubation for an hour with 40µl fluorescent secondary antibody, Alexa 488 goat anti-mouse IgG, which had been diluted four hundred times in 1% horse serum, 1% FBS and 0.1% BSA in PBS. This was followed by washes with PBS and the addition of Hoechst dye and left for five minutes to stain the cells. The cells were subsequently washed with PBS and stored in 4°C fridge for subsequent scanning on the plate reader.

2.2.7.2 RNA Fluorescence *in situ* Hybridisation (RNA-FISH)

RNA-FISH analysis was performed on wild type and DM1 fibroblasts to identify RNA transcripts with expanded repeat units that appear as foci. Cells were prepared for RNA-FISH analysis by washing with PBS followed by fixation with 4% PFA for 10 minutes. The cells were then washed thrice in PBS and subsequently permeabilised in 80% ethanol. This was followed by three washes with PBS prior to denaturation. The cells were treated for 10 minutes with denaturation solution consisting of 40% formamide and 20x SSC

in sterilised distilled water and subsequently washed in PBS. The cells were then hybridised with Cy3 labelled oligonucleotide probe [$(CAG)_{10}$ for DM1 and $(CCAG)_{10}$ for DM2] in hybridisation solution consisting 10% dextran sulphate, 0.2% BSA, 40% formamide, 20X SSC, 2mM Vanadyl Adenosine Complex and 1mg/ml salmon sperm DNA. The Cy3 labelled oligonucleotide was used at a concentration of 0.07ng/μl. The cells were then incubated overnight at 37°C and washed thrice with 5mM $MgCl_2$ in PBS. This was followed by staining with Hoechst dye for five minutes prior to storage at 4°C for subsequent scanning on the plate reader.

2.2.8 Compound Treatment of DM cells

Cells were treated with compounds in both 96-well plates and T-75 flasks. For high throughput screens, initial concentrations of 100μM, 48μM, 8 μM and 1.6 μM were used. This was later adjusted by optimisation in the 96-well plates depending on the effect of compound used. For secondary testing, compound treatment was performed in T-75 flasks. These treatments were carried out in conjunction with Professor David Brook and Professor Chris Hayes.

2.3 Molecular Biology Protocols

These techniques which include amplification, resolution and restriction of DNA among others were carried out under specified conditions.

2.3.1 PCR methods

The PCR analysis was performed in a final volume of 20μl and consists of 1.0μl of DNA (50ng/μl for cell DNA or 5ng/μl for plasmid DNA), 2.0μl of 10x

PCR buffer [made up of 750mM Tris-HCl pH 8.0, 200mM $(NH_4)_2SO_4$, 0.1%(v/v) Tween 20] , 1.2µl of 15mM $MgCl_2$, 0.8 µl of 20mM dNTPs, 1.0µl each of 10pmol forward and reverse primers, 13.7 µl of distilled water and 0.3 µl of 5U/ µl of ABgene red hot Taq polymerase or 0.02U/µl Phusion polymerase.

The primers used for PCR analysis were 19-26 nucleotides long having GC content between 40-60%. The primers used to amplify *CLCN1* in pGR-CLCN1 were sinCLCNf and DsRedORFr; SERCA2f and DsRedORFr were used for *SERCA2* in pGR-SERCA2; while pEGFP-C1F and DsRedORFr amplified PGR-vector (primer sequences in the appendix).

For CLCN1 PCR, the following conditions were used: Denaturation at 95°C for 5 minutes followed by 20 cycles (for plasmid DNA) or 30 cycles (for genomic DNA) of 95°C for 1 minute; 55°C annealing of primers for 1 minute and extension at 72°C for 2 minutes. Final extension was carried out at 72°C for 10 minutes.

For SERCA2 amplification, the following conditions were applied: Denaturation at 95°C for 5 minutes followed by 20 cycles (plasmid DNA) or 30 cycles (genomic DNA) of 95°C for 1 minute; annealing of primers at 58.7°C for 1 minute; and 72°C extension for 50 seconds. Final extension was carried out at the same temperature for 10 minutes.

The PGR-vector PCR involved the following conditions: Denaturation at 95°C for 5 minutes followed by 20 cycles (plasmid DNA) of 95°C for 1 minute; 59°C annealing for 1 minute and 72°C extension for 2 minutes with final extension carried out at 72°C for 10 minutes.

For colony PCR, plasmid DNA from extracted miniprep samples for each colony were subjected to PCR conditions mentioned above.

For GFP-MBNL1 and GFP-MBNL2 deletions, PCR was carried out at 33 cycles consisting of denaturation at 98^0C for 30 seconds, repeating cycles of 98^0C for 5 seconds; and extension at 72^0C for 5 minutes. Final extension was performed at 72^0C for 5 minutes and it was cooled immediately to 4^0C.

The primers and their respective sequences used for PCR are listed in appendices.

2.3.1.1 Reverse Transcription PCR

RNA samples for cDNA synthesis were treated with *DNase1* prior to reverse transcription using New England Biolab protocols (for those involving *IR* splicing). 1.0-2.0μg of RNA was added to an eppendorf tube containing 4.0μl of dNTP, 2.0μl of random hexamers with DEPC H_2O were added to give a volume of 16μl. The mixture was subsequently heated for 5 minutes to remove secondary structures, centrifuged and cooled on ice. This was followed by addition of 2.0μl 10x NEB reverse transcriptase buffer (consisting of 500nM Tris-HCl, 750mM KCl, 30mM $MgCl_2$ and 100nM dithiothreitol), 1.0μl of RNase inhibitor and 1.0μl of 200U/μl reverse transcriptase before it was left in the water bath for an hour at 42°C. The samples were subsequently heated at 90°C for 10 minutes to inactivate the enzyme prior to its use in PCR.

For insulin receptor splicing analysis, amplification was carried out using $1/20^{th}$ of the synthesized cDNA with forward primer (IRfor) and reverse primer (IRrev). Thirty cycles of PCR was performed, consisting of denaturation at

95°C for 5 minutes, followed by repeating cycles of 95°C for 30 seconds; annealing at 60°C for 30 seconds; and extension at 72°C for 30 seconds. This was followed by a final extension of 72°C for 5 minutes. RT-PCR products were resolved by electrophoresis on 3% agarose gels with bands scanned under UV light. For quantification of insulin receptor isoforms, a fluorescently-labelled primer (IRfor) was used as the forward primer and PCR products was analysed on Genescan following 26 cycles of amplification.

For *SERCA1* splicing analysis, 1/20th of cDNA was amplified with Serca1for and Serca1rev primers at thirty four cycles consisting of denaturation at 95^{0}C for 5 minutes, repeating cycles of 95^{0}C for 30 seconds; annealing at 60^{0}C for 1 minute and extension at 72^{0}C for 1 minute. This was followed by a final extension at 72^{0}C for 5 minutes. Quantification of *SERCA1* splice isoforms was carried out at 27-28 cycles using fluorescently-labelled Serca1rev.

For *MBNL1* splicing, 1/20th of cDNA was amplified with MBNL1for and MBNL1rev primers at 30 cycles consisting of denaturation at 95^{0}C for 5 minutes, repeating cycles of 95 ^{0}C for 30 seconds; annealing at 62^{0}C for 30 seconds; and extension at 72 ^{0}C for 45 seconds. Final extension was performed at 72^{0}C for 5 minutes. Quantification of *MBNL1* splice isoforms were performed at 22-24 cycles using fluorescently- labelled MBNLfor primer.

For *MBNL2* splicing, 1/20th of cDNA was amplified with MBNL2for and MBNL2rev primers at 30 cycles consisting of denaturation at 95^{0}C for 5 minutes followed by repeating cycles of 95^{0}C for 30 seconds; annealing at 60^{0}C for 30 seconds; and extension at 72^{0}C for 45 seconds. This was followed by final extension of 72^{0}C for 5 minutes. The quantification of *MBNL2* splice isoforms was carried out at 22-24 cycles using MBNL2for fluorescent primer.

For *BpmI* analysis of DMPK, 1/20th of the synthesized cDNA was used for PCR amplification using N11 as forward primer with 133 as reverse primer. Amplification was performed by modifying protocols used in Hamshere et al (1997). Conditions included denaturation at 95°C for 5 minutes, with repeating cycles of 95°C for 30 seconds; annealing at 58°C for 1 minute; and extension at 72°C for 1 minute. This was followed by a final extension of 5 minutes at 72°C. The PCR product was subsequently subjected to 98°C for 1 minute followed by rapid cooling at 4°C for 10 minutes to promote formation of homoduplexes for overnight *BpmI* restriction digestion. The final products were resolved on 3% agarose gels. In order to quantify relative levels of expression of normal and mutant DMPK alleles, a fluorescently-labelled primer N11 was used to amplify DMPK between 22-26 cycles and the resulting products were restricted overnight with *BpmI* prior to analysis on Genescan.

2.3.1.2 DNA sequencing

Miniprep samples of pGR-*CLCN1*, pGR-*SERCA2*, pGR-vector and pGFP-*MBNL1 & 2* were diluted to give a final concentration of 50ng/µl. PCR products were diluted to give a concentration of 10ng/µl.The primers used for sequencing were subjected to 1:10 dilution to give a concentration of 10pmol/µl.

Primers used to sequence pGR-*CLCN1* were sinCLCN1f, sinCLCN1r, DsRedMonoF and pEGFP-C1R. For pGR-SERCA2 sequencing, SERCA2f and pEGFP-C1R were used while pEGFP-C1F and pEGFP-C1R were used to sequence PGR-vector and GFP-*MBNL 1&2*.

For PCR products, the primers IRfor and IRrev were used to sequence insulin receptor splice isoforms; and N11 and 133 were used for the *DMPK* gene.

All sequencing reactions were carried out by Geneservice and also ABI prism 377 automated sequencer at the University of Nottingham.

2.3.1.3 Fragment Length Analysis

PCR products from reverse transcription-PCR were analysed on ABI prism 3130 genetic sequencer to quantify the levels of expression of splice isoforms of insulin receptor, *SERCA1*, *MBNL1* and *MBNL2* as well as in *DMPK* for *BpmI* analysis of normal and mutant transcripts in both nuclear and cytoplasmic extracts. The resulting peaks from the sequencer were analysed using Genescan peak scanner software in which areas of the respective peaks were used to calculate the relative proportions of isoforms and transcripts.

2.3.1.4 Mutational Analysis of DNA fragments

DNA mutational analysis was carried out on a Transgenomic Wave DNA fragment analysis system, a form of high pressure liquid chromatography (HPLC), which consists of a detector, an oven for heating to specific temperature, and an autosample compartment for loading samples into the machine by 96-well plate. The wave machine has separation columns fitted which are constantly infused by a mixture of Tri-ethylammonium and acetonitrile. Alteration of the proportions of tri-ethylammonium and acetonitrile determines the separation of DNA from PCR products.

Tri-ethylammonium provides a hydrophobic coat for the DNA molecule. The charged nitrogen in tri-ethylammonium bonds with the negatively charged phosphate backbone of DNA so as to bind it to the column and separate it from unused dNTPs, primers, $MgCl_2$ and Taq polymerase. DNA fragments are released from the column by reducing the relative proportions of tri-ethylammonium and the DNA is analysed by the detector for the presence or absence of mutations. Furthermore, smaller molecules and those with secondary structures are released more readily from the column. DNA fragments without mutation form homoduplexes while those having the mutation form heteroduplexes. The homoduplexes are read on the detector as the long standard peak while heteroduplexes are detected as shorter peaks that appear beside the long peaks. Mutational analysis was used to identify a polymorphism in *DMPK* that is associated with DM.

2.3.2 Gel Electrophoresis

Gels of different concentration were used to separate DNA fragments of different size ranges. For DNA of 1kbp and above, a 1% gel was used. Fragments above 300bp were separated using 2% agarose and, 3% agarose was used to separate DNA sizes of less than 300bp. The 1% agarose gel was made by dissolving 0.5g of agarose in 50ml of 1x TAE (which is composed of 40mM Tris-Acetate, 10mM EDTA) and heating in microwave oven followed by the addition of ethidium bromide dye to a final concentration of 1.0µg/µl. On cooling, the gel was poured into its rack and allowed to solidify for subsequent transfer to gel tank. 2µl of the gel loading buffer containing 30% glycerol,

0.025% bromophenol blue and 0.025% xylene cyanol was added to DNA and the mixture was loaded into agarose gels followed by running under electric current. The gels were then visualized under UV fluorescence for identification of bands.

2.3.2.1 DNA molecular weight marker

Determination of DNA fragment sizes were carried out using both 100bp and 1kb ladder (from Invitrogen) on agarose gels.

2.3.2.2 Quantification of DNA and RNA

DNA samples were quantified either on a nanodrop spectrophotometer or on agarose gel using a quantitative λ*Hind*III ladder, while RNA was quantified on a nanodrop.

2.3.2.3 Restriction Digestion of DNA

Restriction digest of DNA was carried out using enzymes and reagents obtained from New England Biolabs in accordance with manufacturer's instructions. The components of the restriction mixture consisted of 1μg of DNA, 10U/μl of restriction enzyme, 10x restriction buffer (buffer 3 consisting of 100mM NaCl, 50mM Tris-HCl, 10mM $MgCl_2$, and 1mM dithiothreitol while buffer 4 is made up of 50mM potassium acetate, 20mM Tris-acetate, 10mM Magnessium acetate and 1mM dithiothreitol), 1μg bovine serum albumin and distilled water. The mixture was incubated in a water bath for 1-2

hours at the optimal temperature and specifically overnight for *BpmI* restriction digest. This was followed by separation to its respective sizes using agarose gel electrophoresis.

2.3.2.4 DNA Recovery and Purification

The extraction and purification of separated DNA fragments from agarose gels was carried out using the QIAquick gel extraction kit from QIAGEN in accordance with manufacturer's protocols. Gel bands visualized on a UV transilluminator were excised using a scalpel. The sample was then weighed and 3 volumes of buffer added and incubated at 50°C to dissolve. Isopropanol was added to the mix and transferred to spin column inside a collection tube and centrifuged for a minute for DNA to bind to the column. DNA was then eluted with water.

2.3.2.5 DNA Ligation

After amplification and visualisation on 1% agarose gel, restriction fragments were extracted and plasmid DNA (pGFP-MBNL) was self-ligated in 20µl mixture consisting 1.0 µl of 400U/µl T4 ligase, 2.0 µl of 10x ligase buffer composed of 500mM Tris-HCl, 100mM $MgCl_2$, 100mM dithiothreitol and 10mM ATP (both from New England biolabs) and 17.0 µl of plasmid DNA and left at room temperature for 4 hours.

2.3.3 Plasmid DNA Purification

Plasmid DNA was purified using QIAGEN plasmid DNA purification kit protocol following overnight incubation of bacterial cultures. Pellets of bacterial cells were harvested by centrifugation followed by resuspension in 10ml of buffer P1 composed of 50mM Tris.Cl, pH 8.0, 10mM EDTA and 100μg/ml RNase A. The cells were subjected to lysis for 5 minutes in 250μl of buffer P2 [comprising 200mM NaOH, 1% (w/v) SDS] and subsequently neutralized by 10ml of chilled buffer P3 (which consists of 3.0M potassium acetate at pH of 5.5) to precipitate proteins as well as cell debris followed by incubation at room temperature for 10 minutes. The lysate was filtered using a QIAGEN filter cartridge into a 50ml tube. The filtered lysate was applied to the QIAGEN column previously equilibrated with buffer QBT [composed of 750mM NaCl, 50mM MOPS at pH of 7.0, 15% (v/v) isopropanol and 0.15% (v/v) Triton X-100] and washed twice with buffer QC made up of 1.0M NaCl, 50mM MOPS with pH of 7.0 and 15% (v/v) isopropanol. DNA was eluted with elution buffer QN [composed of 1.6M NaCl, 50mM MOPS at pH of 7.0 and 15% (v/v) isopropanol] and precipitated in 100% isopropanol followed by centrifugation. DNA pellets were subsequently washed with 70% ethanol and centrifuged to concentrate the pellets. The supernatants were discarded and the pellets were air-dried at room temperature prior to redissolution in 300μl of distilled water. The concentration and purity was measured on the nanodrop.

2.3.4 Fibroblast/Cell DNA Extraction

DNA extraction from C2C12 and fibroblasts cell lines was carried out using a Puregene-Gentra DNA purification kit in line with protocols specified by the manufacturer with modifications. In summary, about 1,000,000 cells per flask were trypsinized and transferred into an eppendorf tube with complete medium. The cells were pelleted with centrifugation at 16,000xg for 5 seconds and the supernatant removed leaving the cells and 2-3 µl of residual medium in the tube. The cells were resuspended by vortexing and 300µl of cell lysis solution (pH 4.0) composed of Tris[hydroxymethyl] aminomethane, ethylenediaminetetraacetic acid and sodium dodecyl sulfate was added to lyse the cells. 1.5µl of RNase solution was added to the cell lysate and incubated at 37°C for an hour to remove RNA. This was followed by addition of 100µl of protein precipitation solution (pH 2.7) to the cell lysate to precipitate proteins with vortexing at high speed to obtain a uniform mixture. The mixture was then centrifuged at 16,000xg for 5 minutes to pellet precipitated proteins. The supernatant containing DNA was transferred into a fresh eppendorf tube with 300µl of 100% isopropanol and inverted to mix prior to centrifugation at 16,000g for 5 minutes. The supernatant was discarded and 300µl of 70% ethanol was added to wash the DNA pellet. The sample was centrifuged for 3 minutes and ethanol was decanted and the tubes were air-dried for 20-30 minutes at room temperature. DNA pellets were dissolved by adding 50µl of dH_2O and heated in a 65°C water bath for an hour. DNA concentration was subsequently quantified on the nanodrop before use for DNA analysis.

2.3.5 Cell RNA Purification

Cell and fibroblast lines for total RNA extraction were carried out in accordance with Purescript-Gentra purification protocols. Flasks of cells were trypsinized and about 1,000,000 cells were pelleted at 16,000g for 5 seconds. Supernatant was discarded and 10μl of residual media was left in the tube along with the cell pellets. This was followed by addition of 20μl of DEPC H_2O to inhibit RNase and 300μl of cell lysis solution (consisting of citric acid, ethylenediaminetetraacetic acid and sodium dodecyl sulphate) was added to lyse cells. 100μl of protein-DNA precipitation solution (made up of citric acid and sodium chloride) was added and the mixture was inverted 10 times to mix before incubation on ice for five minutes. It was subsequently centrifuged for 5 minutes at 16,000g to pellet proteins and DNA and the supernatant containing RNA was transferred into a fresh eppendorf tube containing 300μl of 100% isopropanol. The mixture was inverted 50 times to mix and subsequently centrifuged to pellet RNA. The supernatant was discarded and RNA pellet was washed with 75% ethanol and centrifuged. The supernatant was discarded and RNA pellet was air-dried for 20-30 minutes. The pellets were dissolved by adding 50μl of DEPC H_2O and left on ice for 30 minutes. The amount of RNA was quantified on the nanodrop and used for reverse transcription. The remainder was stored in -80°C for further use.

2.3.5.1 Fractionated RNA Purification

Fractions of nuclear and cytoplasmic RNA were obtained from tissue culture cells by modifying protocols used in Hamshere et al (1997). Cells were washed

in ice-cold PBS followed by addition of 1ml of 0.65% Nonidet P-40 previously prepared by mixing 10% (v/v) Nonidet P-40 in 1.5mM $MgCl_2$, 0.15M NaCl and 0.01M Tris.HCL with pH of 8.0 all in DEPC H_2O. Addition of Nonidet P-40 to cells in the flask for 1-2 minutes disrupts the cell membrane to liberate cytoplasmic contents but the nuclear membrane is intact and appears grainy under an inverted microscope. The solution in the flask was drained into a fresh eppendorf tube for cytoplasmic extracts. A further 2mls of Nonidet P-40 was added to dislodge the nuclei and the contents of the flask were drained into a tube and nuclear extracts pelleted by centrifugation. The supernatant was discarded. 400µl of DEPC H_2O was added to nuclear pellet to resuspend it, followed by addition of 100µl of 0.5M Tris-HCl , 0.05M EDTA and 2.5% (v/v) sodium dodecyl sulphate (SDS) to nuclear extracts. For cytoplasmic extracts, 250µl of 0.5M Tris-HCl, 0.05M EDTA and 2.5% (v/v) SDS was added. Both nuclear and cytoplasmic RNA extracts were purified by two phenol/chloroform extractions. The RNA was subsequently precipitated in equal volumes of isopropanol containing 0.3M sodium acetate (pH 5.3) by centrifugation. RNA pellets were washed in 75% ethanol, centrifuged and the supernatants discarded. The pelleted RNA was air-dried at room temperature for 15-20 minutes and dissolved in 40µl of DEPC H_2O, prior to quantification on a nanodrop. The sample was electrophoresed on an agarose gel to confirm its quality. Cytoplasmic RNA samples found to contain genomic DNA on agarose gel analysis were treated with *DNase1*.

2.3.5.2 DNA Removal from RNA

Both total RNA and some samples of cytoplasmic RNA containing genomic DNA were treated with *DNase1* in accordance with Promega protocols. 1.0µl of 10x *DNase1* Buffer [composed of 400mM Tris-HCl (pH 8.0), 100mM $MgSO_4$ and 10mM $CaCl_2$) and 1.0µl of enzyme (1U/µl for every 1µg RNA) was added to RNA samples and incubated at 37°C followed by addition of 1.0µl of stop solution [consisting of 20mM EGTA (pH 8.0)] to inhibit *DNase1* reaction. The mixture was subsequently heated in 65°C water bath for 10 minutes to destroy *DNase1* prior to its use in reverse transcription.

2.3.6 Protein Extraction from cultured cells

Cells from $75cm^3$ flask were trypsinized and pelleted by centrifugation followed by wash in PBS. The cells were subsequently pelleted and the supernatant was discarded and put on ice. About 100-500µl of ice cold RIPA lysis buffer (composed of 50mM, Tris HCl, pH 8.0, 150mM NaCl, 1% NP-40, 0.5%DOC,0.1%SDS) was added to the pellet and placed on ice for 20 minutes. This was followed by two cycles of freezing at -80°C and thawing at room temperature. The cell lysate was centrifuged at 13000rpm at 4°C for 10 minutes and the supernatant containing the cell lysate was transferred to a fresh ependorf tube for storage at -80°C.

2.3.6.1 Protein Quantification

Protein quantification was performed using BioRad D_c assay. To 30 µl of protein sample, 100 µl of reagent A' (prepared by mixing 1000 µl of A with

20 µl of reagent S). This was followed by addition of 800 µl of reagent B prior to vortexing to mix. The sample was incubated at room temperature for 15 minutes before measurement on BioRad spectrophotometer at 750nm for absorbance. BSA samples of known concentrations of 10, 20, 30 and 50 µg in RIPA buffer were used to plot a standard curve from which the concentration of protein samples were estimated.

2.3.6.2 Western Blot

Western blot of protein samples was carried out using NuPage system (from Invitrogen) in accordance with manufacturer's protocols. The gels and buffers used were all obtained from the same manufacturer.

To prepare protein samples for electrophoresis, NuPage LDS sample buffer was mixed with NuPage reducing agent prior to addition to protein samples. The protein sample mix was heated at 70°C for 10 minutes for SDS-polyacrilamide gel electrophoresis.

800ml of running buffer was prepared by adding 80ml of MOPS buffer to 40ml of methanol and addition of 680ml of SDW. The NuPage bis-tris gel's comb was removed from the wells and the wells were rinsed with running buffer before it was assembled in Xcell mini cell system. Its chambers were subsequently filled with running buffer. Protein samples were then loaded to the gels along with two markers namely prestained marker and MagicMarker. Prestained marker enables visualisation during electrophoresis and after transfer to PVDF membrane while MagicMarker reacts with secondary antibody to serve as internal standard for final western blot. The NuPage gel was run for 50 minutes at 200V.

Following separation of protein, NuPage gel was transferred to PVDF membrane using XCell II blot method. The PVDF membrane was soaked for 30 seconds in methanol followed by brief wash with SDW and left to soak in transfer buffer (prepared by mixing 80ml of methanol, 40ml of 20X transfer buffer and 680ml of SDW) for 5 minutes. The transfer buffer was also used to soak blotting pads for several minutes. This was followed by placing PVDF membrane on top of NuPage gel and they were sandwiched between blotting paper and soaked pads and placed in Xcell II Blot module. The iiner chamber was filled with transfer buffer with its outer chamber filled with SDW and the transfer was performed for 60 minutes at 25V.

After transfer, the membrane was washed twice and blocked overnight with 5% blotto solution in TBS-T. It was subsequently washed with distilled water and incubated with primary antibody for 4 hours. The membrane was then washed thrice with TBS-T prior to incubation with HRP-conjugated secondary antibody for 30 minutes. This was followed by three washes with TBS-T (prepared by mixing 4.0g of NaCl, with 10ml of Tris-HCl, 500ml of distilled water and 500µl of Tween-T). ECL solution (made up of 3ml of solution A and 75µl of solution B) was applied to the membrane on saran wrap for 5 minutes and its excess blotted with bloting paper. It was subsequently exposed to photographic film for protein bands detection.

2.4 Transgene generation and DNA transfer

Transgene splicing constructs generated previously by cloning gene segments into plasmid vectors were confirmed by sequencing. Subsequently, gene

transfer experiments were carried out using transgene constructs to transform bacterial cells, prior to transfection studies in C2C12 and human fibroblasts.

2.4.1 Splicing gene constructs

The splicing constructs used in this project for the primary assay were previously generated in the lab by Dr Javier Granados-Riveron from gene splicing construct containing reporters- green fluorescent protein (GFP) and Dioscorea red fluorescent protein (DsRed). Introns 2 of *CLCN1* with its flanking exons as well as intron 19 of *SERCA2* and its flanking exons were independently cloned into pEGFP-C1 plasmid of 4.7kb size to generate pGR-CLCN1 and pGR-SERCA2 respectively (Figure 2.1).

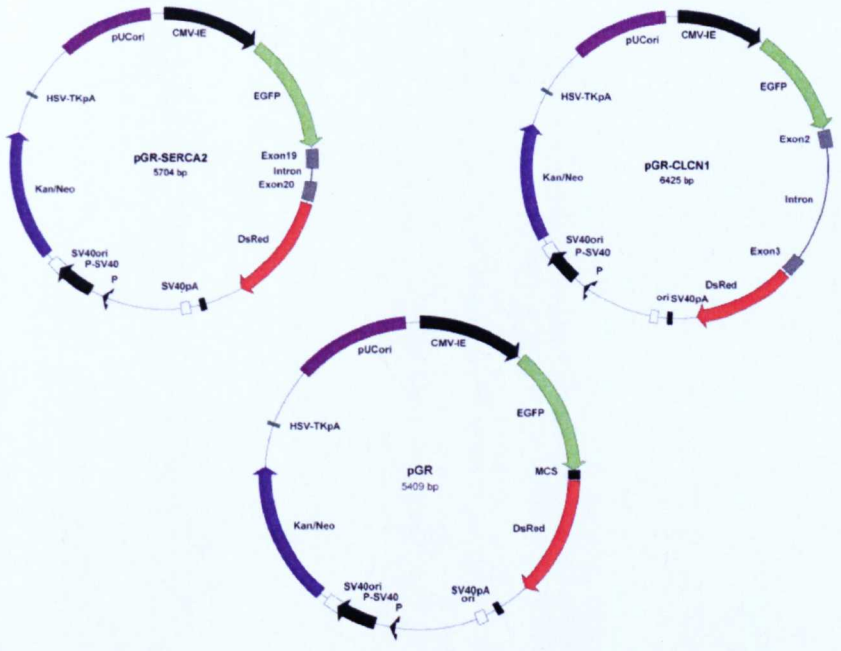

Figure 2.1: Transgene constructs pGR-CLCN1 and pGR-SERCA2 on pEGFP-C1 plasmids used for transformation of E. coli DH5α and subsequent transfection in fibroblasts for the splicing assay. pGR serves as the positive control of the splicing assay.

2.4.2 Transformation

Transformation of bacterial cells was carried out by electroporation. Previously prepared frozen stocks of electrocompetent E. coli strain DH5α were thawed on ice. 1µl of plasmid DNA was diluted at different concentrations (1/25, 1/50, 1/250) in different test tubes and chilled on ice and the cells and DNA were mixed together. Electroporation apparatus was set at 25µF capacitance and 2.5KV. The transformation mix was placed in the bottom of chilled cuvette and placed in the tray to subject it to electrical pulse. Immediately after electroporation, 200µl of SOC was added to the electroporated cells and subsequently transferred to a tube containing 800µl SOC and incubated at 37°C for an hour in a shaking incubator. Cells were harvested at 1000rpm for 10 minutes and resuspended in 200µl of LB. Aliquots

of the cells were taken and plated at room temperature and incubated overnight at 37°C under kanamycin selection.

2.4.3 Transfection

The C2C12 cell lines and human fibroblasts were transfected with plasmid DNA or siRNA using the Amaxa Nucleofection kit in accordance with manufacturer's instructions.

Cells in $75cm^3$ flasks were grown to a confluency of 80-90% cell density and the medium removed; washed with PBS, trypsinized and harvested. Aliquots of trypsinized cell suspension were taken for cell counts on a haemocytometer. A million cells per nucleofection sample were pelleted by centrifugation and the supernatant was discarded. This was followed by resuspension of cell pellets at room temperature in 100µl of nucleofector V solution. The cell suspension was subsequently mixed with 2µg of plasmid DNA or 100nM of siRNA and transferred into an Amaxa cuvette. The Amaxa Nucleofector programme B-032 was selected and used to electroporate C2C12 cells while U-23 programme was used to transfect human fibroblast. To reduce damage to cells, the cuvette was immediately removed after the electroporation and 500µl of pre-warmed culture medium was added to it. The contents of the cuvette were transferred into one of the six well plates and incubated in 37°C/5% CO_2 for 24 hours for expression of fluorescent proteins and subsequently selected for clones using G418 if plasmid DNA was used for transfection.

2.5 Microscopy

The imaging of cells in this project involved both widefield and confocal microscope as well as high content imaging device.

2.5.1 Widefield Microscopy

Cell imaging was performed using Zeiss inverted fluorescent microscope together with Olympus CK2 microscope with 4x, 10x and 40x objectives.

Green and red fluorescence in fixed cells on slide was examined using a Zeiss axioskop2 mot plus fluorescence microscope fitted with a digital camera having brightfield/ phase contrast as well as DAPI, green and red fluorescent filters. Fluorescence was analysed at 489nm excitation and 508nm emission combined filter for green fluorescence with 558nm excitation and 583nm emission wavelength for red fluorescence. Cells were viewed using 10x objectives. Analysis of fluorescent images was carried out using Openlab software.

Also, used for the imaging of fluorescence in cells, inverted fluorescent Nikon eclipse 7S 100 extra long working distances (ELWD) with 4x and 10x objectives were used and images were recorded on the computer screen.

2.5.2 Confocal Microscopy.

The fluorescent microscopes used to view fixed cells on slides include Zeiss LSM510 confocal head on a Zeiss Axiovert 100M microscope, fitted with Zeiss plan neofluar 40x/1.3 oil objective and Zeiss plan Apochromat 63x/1.4

oil objective. Images from these microscopes were analysed using LSM software.

2.5.3 High Throughput Imaging

The Molecular Devices Micro widefield high content plate reader fitted with Nikon 40x ELWD was used for high content imaging in high throughput screens of cells in immunofluorescence and RNA-*FISH* analysis. The plate reader consisted of 488nm Argon laser to excite GFP with band path of 505-530nm emission filter and 543nm Helium-Neon laser with long path 560nm emission filter for TRITC. Images from the plate reader were analysed using MetaXpress software.

For cells with transgene splicing double reporter construct, Molecular Devices Ultra widefield high content plate reader fitted with Nikon 40x ELWD was used for high content imaging of cellular fluorescence. The 488nm laser was used to view GFP at 525/50 emission filter; DAPI was excited with 405nm laser using 447/60nm filter; while DsRed was observed using Texas Red which was excited by 561nm laser with 593/40 emission filters.

2.6 Electronic Databases

Gene databases used to access nucleotide, transcripts and protein sequences were from the National Centre for Biotechnology Information (NCBI) and European Molecular Biology Laboratory (Ensembl). Primer sequences were designed using version 4.0 of primer3 Input.

CHAPTER THREE: DEVELOPMENT OF PRIMARY ASSAYS

3.1 Introduction

This chapter deals with developing a set of primary assays based on molecular events in myotonic dystrophy that can be utilised for screening on a large scale in high throughput screens of thousands of small molecules and chemical compounds to test their efficacy in reversing molecular features associated with the disease. The main molecular events in the disease under consideration in this section are ribonuclear foci formation by expanded repeat RNA and its association with RNA binding proteins (MBNL) to trig ger DM-like molecular cascades. The aim is to use nuclear foci as a tool for therapeutic screening of compounds that can reverse toxic RNA disease mediation in DM.

3.2 Nuclear foci assay

This assay was developed based on the pathogenic features of the mutant RNA containing expanded CUG or CCUG repeats which serve to sequester splicing factor MBNL1 leading to the formation of foci in DM cells thereby preventing it from performing its cellular functions of regulating splicing of a subset of pre-mRNAs. To test the idea that foci formation could be a convenient tool for therapeutic screening, lines of both DM1 and DM2 fibroblasts as well as control fibroblasts were initially screened for the appearance of foci and ribonuclear inclusions using a Cy3 fluorescently-labelled $(CAG)_{10}$ and $(CCAG)_{10}$ probe in RNA-*FISH* as well as for the

presence of ribonuclear inclusions using fluorescently-labelled MBNL1 antibodies.

The cells used for the screening were DM1, DM2 and wild type fibroblast lines which had been previously telomerised and are designated as DM1 Tel, DM2 Tel and wild type Tel respectively in this study. Furthermore, another cell used for the screens was telomerised DM1 fibroblast which had been induced with lentivirus containing MyoD, a muscle differentiation factor (designated as DM1 Tel MyoD) which is activated by doxycyclin to differentiate into myoblasts.

Cells were scored based on the appearance of foci and ribonuclear inclusions in both RNA-FISH and immunofluorescence respectively (figure 3.1).

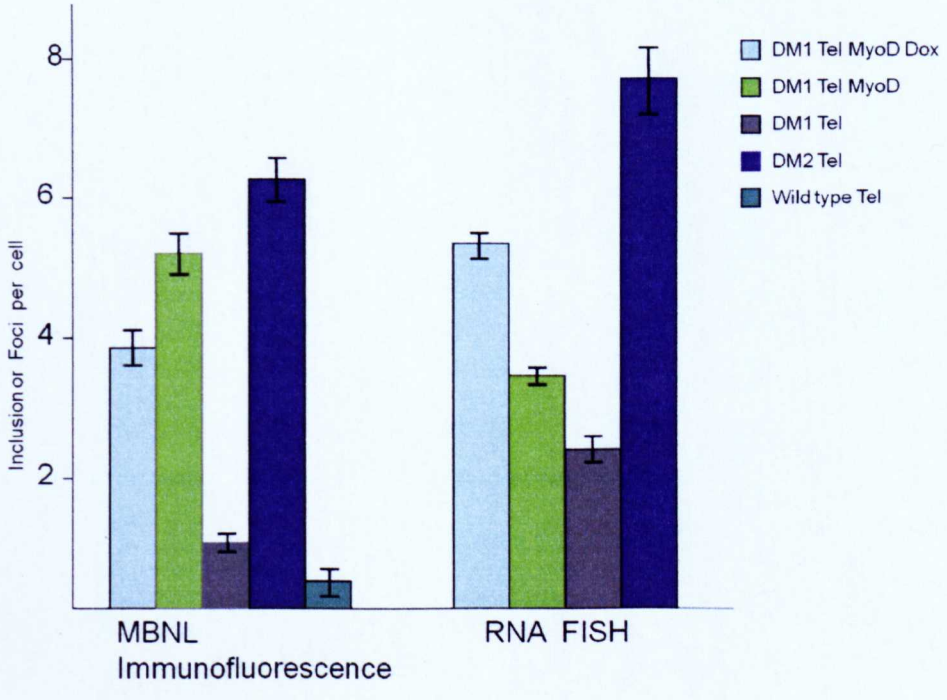

Figure 3.1: Schematic diagram showing average numbers of ribonuclear inclusion and foci distribution between wild type and DM cells. DM1 Tel MyoD is the fibroblast line containing MyoD, a muscle differentiation factor that can be activated by doxycyclin (Dox)

RNA-FISH was observed to be more robust than MBNL1 immunofluorescence because it could clearly distinguish between wild type and DM cells based on presence or absence of ribonuclear foci. In contrast with MBNL1 immunofluorescence which was found to have a leaky background as RNA-FISH had no such obvious limitations. In addition, the number of ribonuclear inclusions were low in immunofluorescent screens of wild type cells while foci was absent in wild type cells hence RNA-FISH analysis was more robust in clearly distinguishing between DM and wild type cells.

This was to determine the approach that could easily be utilized in high throughput screens (HTS) and also to establish baseline parameters for assessing if on treatment with chemical compounds, the cellular distribution of foci is reduced or absent.

Based on the ability of initial optimisation assays in clearly distinguishing DM cell from wild type cells, RNA-FISH was optimised for screens (figure 3.2) in HTS to determine if on treatment of the DM cells with compound, it can disrupt or dissociate interactions between MBNL1 and RNA expanded repeat units in foci leading to disappearance of foci.

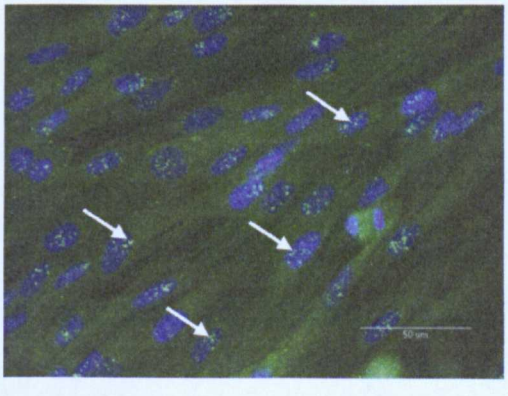

Figure 3.2: RNA-FISH screens for foci in DM2 cell. The arrows indicate foci in the nucleus represented by blue background. Scale bar in all figures represent 50μm.

The RNA-FISH showed that DM2 fibroblasts had more foci than DM1 fibroblast lines for telomerised cells and for those telomerised containing inducible MyoD. It could be possible that the increase in foci number per nuclei in DM2 over DM1 might be due to the presence of larger repeat expanded units in DM2.

Furthermore, it was observed that when DM1 fibroblasts containing inducible MyoD (a muscle differentiation factor) mediated by lentivirus having foci number of 3.1±0.2, were induced by doxycyclin to differentiate into myoblasts, the number of foci in its nuclei was increased to 4.8±1.0. This difference in nuclear foci number between DM1 fibroblasts and DM1 myoblasts which increases on differentiation is similar to the observation reported by Holt et al (2009) in which undifferentiated as well as differentiated DM1 myoblasts were used. This is due to induction of muscle genes and *DMPK* by MyoD which results in more foci.

Thus, differences in foci numbers between DM fibroblast nuclei as well as in myoblast nuclei could be exploited to assess the efficiency of any potential therapeutic agent for the disease condition.

3.3 Use of GFP-MBNL to Generate Clones for RNA-MBNL interactions in foci

As a parallel assay to the nuclear foci assay described above, pGFP-MBNL1 was used to transfect wild type and DM cells lines to generate clones for use in studying RNA-MBNL interactions in the nuclear foci. It has been previously demonstrated in transient transfections that MBNL co-localises with RNA repeat units in the foci in DM cells (Fardaei et al, 2001). The aim was to use

the clones generated for screening chemical compounds that can disrupt GFP-MBNL1 from interaction with repeat transcripts in the nuclei of DM cells, as foci are not seen in wild type cells. This assay would be ideal for therapeutic screening as it would facilitate the tracking of exogenous MBNL1 on treatment with compound to determine if it results in its redistribution or if it is still sequestered in nuclear foci.

Transient transfection of DM2 and wild type fibroblasts with GFP-MBNL1 showed that 32.2% and 39.8% respectively of the cells were positive for GFP after 48 hours. Unfortunately, GFP-MBNL1 was observed to kill all of the cells (both wild type and DM cells) it was transfected into after a period of three days. One possible explanation of this result is that the full length MBNL1 protein was toxic to the cells or GFP was toxic to the cells. In order to distinguish between these two possibilities and overcome this technical difficulty, *MBNL1* was cloned in pSNAP-tagged vector such that MBNL1 would be expressed as a fusion protein. Transient transfection studies in DM1 fibroblasts with both pGFP-MBNL1 and pSNAP-tagged MBNL1 showed 27% and 6.9% of the cells expressed GFP and SNAP proteins respectively (table 3.1) after 12 hrs post-transfection. At 24 hours post-transfection, the percentage of transfectants decreased to 19.4 for GFP-MBNL1 and 2.2% for SNAP-MBNL1. The transfectants all died by the third day due to the toxicity of MBNL1 constructs. Because SNAP- tagged MBNL1 was equally as toxic as GFP-MBNL1, no clones could be obtained for selection for study of exogenous MBNL1 interactions with RNA repeats in nuclear foci. It was thought that the full length MBNL protein might be toxic to the cells, so truncated versions were proposed for further study. The study above indicates that it was not GFP

that was causing the toxicity as the SNAP-tagged construct had similar toxicity to the GFP-expressing construct.

Post-transfection duration	GFP-MBNL1	SNAP tagged-MBNL1	Amaxa GFP (Control)
6 hours	4.3% (4 out of 94)	1.3% (1 out of 76)	26.3% (36 out of 137)
12 hours	27% (27 out of 100)	6.9% (5 out of 72)	56.4% (92 out of 163)
24 hours	19.4%(19 out of 98)	2.2% (2 out of 89)	72.8% (134 out of 184)
48 hours	5.0% (2 out of 40)	1.5% (1 out of 66)	54.0% (108 out of 200)

Table 3.1: Proportion of DM1 fibroblasts expressing GFP-MBNL1 and SNAP-tagged MBNL1 protein at different time points. The cells all died on the third day due to toxicity of constructs.

3.3.1 Construction of truncated GFP-MBNL

As a result of technical problems encountered in using pGFP-MBNL1 to generate cell clones, several deletions of GFP-MBNL1 were made (figure 3.3) alongside truncated versions of GFP-MBNL2.

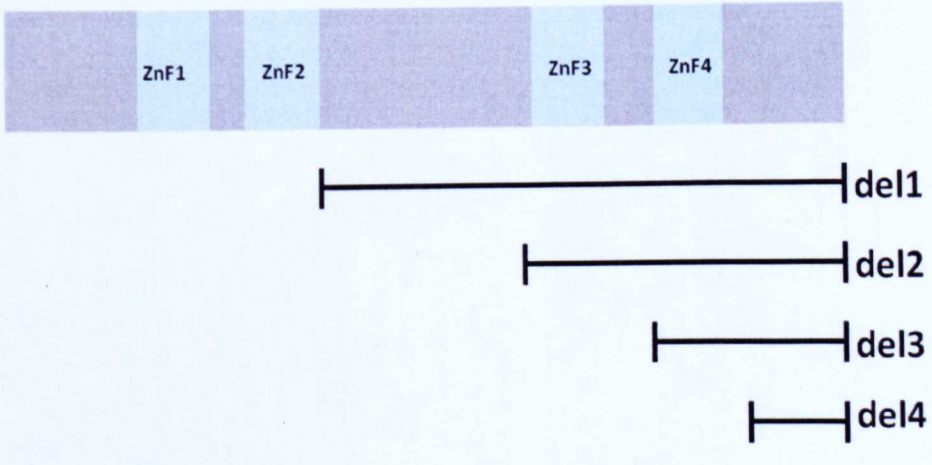

Figure 3.3:MBNL1 deletion in the pGFP-MBNL constructs showing deleted domains designated as deletion 1 (linker, zinc finger 3&4, C-terminus), deletion 2 (zinc finger3&4, C-terminus), deletion 3 (zinc finger4 & C-terminus) and deletion 4 (C-terminus).

The work described above suggested that full length MBNL1 was toxic to cells, thus various deletions of the two GFP-MBNL constructs based on their RNA-binding domains (Zinc fingers) were generated. Primers with flanking *Spe*1 restriction sites (table 3.2) were used to facilitate cloning. The sequences of these primers are listed in the appendix.

Reverse Primer for deletion	Forward primer for deletion	Region of deletion
MBNL1-D1r	pEGFP-C1delF	Linker, Zinc finger 3 &4 and C-terminus
MBNL1-D2r	pEGFP-C1delF	Zinc finger3 &4 and C-terminus
MBNL1-D3r	pEGFP-C1delF	Zinc finer4 and C-terminus
MBNL1-D4r	pEGFP-C1delF	C-terminus
MBNL2-D1r	pEGFP-C1delF	Linker, Zinc finger3 &4 and C-terminus
MBNL2-D2r	pEGFP-C1delF	Zinc finger3 &4 and C-terminus
MBNL2-D3r	pEGFP-C1delF	Zinc finer4 and C-terminus
MBNL2-D4r	pEGFP-C1delF	C-terminus

Table3.2: Truncated constructs were generated after PCR products were restricted and subsequently ligated in figure 3.4.

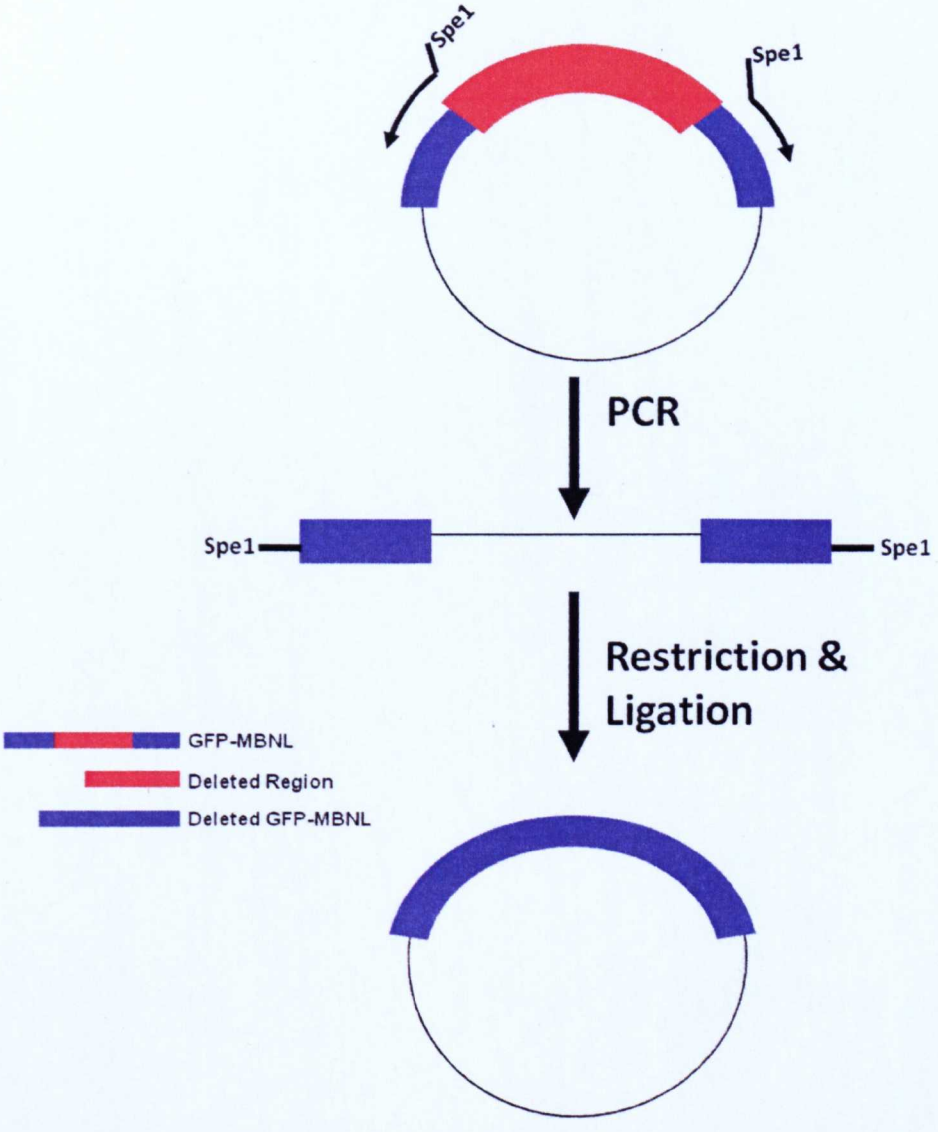

Figure 3.4: Schematic representation for generation of truncated versions GFP-MBNL

For MBNL1, two deletions 1 and 4 were generated. Deletions 1 and 2 were obtained for MBNL2. However, truncated versions of GFP-MBNL1 and 2 did not generate any clones in DM cells as they were equally as toxic as the full length protein. Furthermore, only wild type fibroblasts generated 4 and 7

clones for GFP-MBNL2 del1 and GFP-MBNL2 del2 respectively. Because of these difficulties, RNA-FISH became the only viable option that was adapted for use in high throughput screening in the primary assays.

Plasmid	Number of cells	GFP positive cells	% GFP cells
GFP-MBNL1del1	166	30	18.1
GFP-MBNL1del4	174	38	21.8
Amaxa GFP	134	94	70.1

Table 3.3: The proportion of DM1 fibroblast expressing truncated versions of GFP-MBNL1 after 24 hours. The cells all died under G418 selection.

Cell line	Plasmid	Number of cells	Number of GFP positive cells	% proportion of GFP
DM2	GFP-MBNL2del1	48	9	18.8
DM2	GFP-MBNL2del2	33	3	9.1
DM2	Amaxa GFP	93	27	29.0
WT	GFP-MBNL2del1	56	2	3.6
WT	GFP-MBNL2del2	47	3	6.4
WT	Amaxa GFP	91	28	30.8

Table 3.4: Truncated versions of GFP-MBNL2 in transiently transfected wild type (WT) and DM2 fibroblasts showing low expression levels of the constructs in these cells.

3.4 Splicing Construct Assays

In order to design a further assay that would be of use in primary high-throughput screening, we generated assays to determine the effect of compounds on alternative splicing. These assays were designed to screen for compounds that could correct the splicing misregulations that take place in DM. Transgenes constructs which were produced previously by Dr Javier Granados-Riveron in the lab, based on alternative splicing events involving

introns (figure 3.5) reported in muscle-specific chloride channel (*CLCN1*) and Sarcoplasmic-endoplasmic reticulum Ca^{2+} ATPase 2 (*SERCA2*).

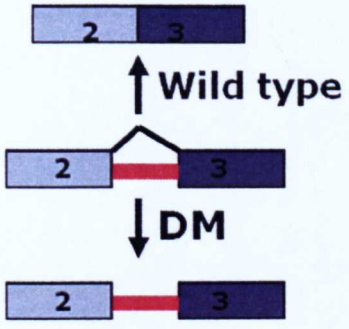

Figure 3.5: Schematic diagram showing alternative splicing of intron2 of *CLCN1* and intron 19 of *SERCA2* in DM patients and unaffected persons

The constructs generated contain segments of genes; intron 2 *CLCN1* with its flanking exons and intron 19 of *SERCA2*. The inserts were cloned into pEGFP-C1, a vector having green fluorescent protein (GFP) at its 5' end and a dioscorea red fluorescent protein (DsRed) at its 3' end. Two constructs were generated designated as pGR-CLCN1 and pGR-SERCA2 respectively. The third transgene constructs (pGR) serves as a positive control of the splicing assay was derived from pEGFP-C1 having both GFP and DsRed with no intron cloned into its multiple cloning sites.

The intron 2 of *CLCN1* contains a stop codon while intron 19 of *SERCA2* bases is not divisible by 3. In both cases, splicing of the introns result in translation of the single open reading frame of the transgene constructs to give chimeric product with green and red fluorescent activities. However, if no splicing occurs, the introns are retained and only green fluorescent activity is produced as a result of stoppage of translation by a stop codon in pGR-CLCN1

or out of frame translation leading to non-translation of red fluorescence by pGR-SERCA2 (figures 1.9).

3.4.1 *CLCN1* Splicing Construct Assay

This assay was designed based on intron 2 splicing of *CLCN1* which is altered in DM. The misregulated splicing of intron 2 of *CLCN1* in DM was first reported by Charlet et al (2002b) in which they demonstrated the retention of this intron in DM patients. Furthermore, Charlet et al (2002b) also reported that this intron contained Premature Termination Codons (PTCs) whose retention is induced in wild type cells following CUG-BP1 overexpression leading to DM-like splicing patterns to cause loss of CLCN1 function resulting in myotonia found in DM patients.

To develop this assay, a splicing construct designated as pGR-CLCN1 was generated from enhanced green fluorescent protein plasmid vector (pEGFP-C1) in which intron 2 with exon 2 and exon 3 was cloned into the *Xho1* and *Sal1* sites of its multiple cloning region. The intron 2 transgene was cloned into pEGFP-C1 coding for green fluorescent protein (GFP) at its 5' end and Dioscorea red fluorescent protein (DsRed) at its 3' end to generate pGR-CLCN1.

Based on the splicing model, pGR-CLCN1 will be spliced in wild type cells to produce green and red fluorescent activities by these cells because of the removal of intron 2 which contains PTC. However, in DM cells, there will be production of only green fluorescence and not red fluorescence because intron retention truncates the translation open reading frame as a result of PTCs contained in the intron. In addition, the reporter activities of GFP and DsRed

could be used to estimate the efficiency of the splicing assay based on DsRed:GFP ratios with those of wild type cells being one or almost approaching one while those of DM cells will be zero or very low.

3.4.2 *SERCA2* Splicing Construct Assay

The *SERCA2* splicing assay was derived from the work carried out by Kimura et al (2005). Kimura et al (2005) described a splice variant (SERCA2d) as containing intron 19 which they observed to occur in low proportions in DM1 skeletal muscle. Furthermore, it was suggested that the retention of intron 19 in *SERCA2* resulted in a frameshift leading to a PTC in exon 20.

The generation of *SERCA2* splicing constructs followed a similar protocol to that of pGR-CLCN1 in which intron19 along with its flanking exons 19 and 20 were cloned into the *Xho1* and *Sal1* sites of pEGFP-C1 with GFP at its 5' end and DsRed at its 3' end. The constructs were designated as pGR-SERCA2 and according to the splicing model, would undergo intron 19 splicing in wild type cells to produce green and red fluorescence.

By contrast in DM, retention of intron 19 in these cells introduces a frameshift in the open reading frame of pGR-SERCA2 resulting in only green fluorescence by the cells or very low red fluorescence/green fluorescence ratio.

3.4.3 Proof of Concept

The splicing constructs were tested in mouse muscle cells, C2C12. A proof of concept study of the transgene constructs was carried out in transient transfection using C2C12 cells. Figure 3.6 shows cells fluorescing with GFP and DsRed could be identified following transfection of both constructs, which

demonstrates splicing of the introns from the relevant gene constructs to give green and red fluorescent activities. This finding is consistent with the splicing model shown in figure 1.10.

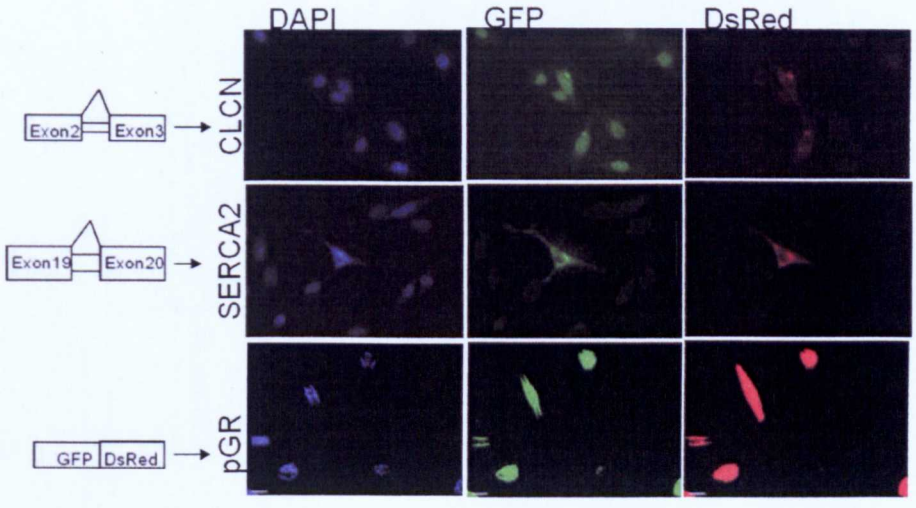

Figure 3.6: Mouse muscle C2C12 cells transfected with splicing constructs express both green and red fluorescence. This indicates the transgene construct has been spliced. pGR is the positive control for the study.

The transfected C2C12 cells were subsequently selected in G418. The presence of the plasmid was confirmed by PCR amplification of cell DNA using Oligos sinCLCN1f and DsRedOFr for *CLCN1*; with sinSERCA2f and DsRedOFr for *SERCA2*, pEGFP-C1F and DsRedOFr were used to amplify the pGR vector region consisting of GFP and DsRed. This confirmed that the integration of gene constructs into the cell genome had occurred.

3.5 Generation of Stable lines from Controls and DM fibroblast with transgenes

After validation of the splicing constructs in C2C12 cells, transgenes were subsequently transfected into wild type fibroblasts as well as DM1 and DM2

fibroblast lines. The transfected cells were then selected in 200μg/ml G418 and many of the clones were scanned for fluorescence. DNA from the clones was tested by PCR amplification to confirm the presence of the relevant transgenes using primers T1F and T1R for CLCN1, and *MIR*1-2f and *MIR*1-2r for pre-microRNA1-2, a house keeping gene, in genomic DNA to generate products of 208bp and 300bp, respectively, in a duplex reaction. For sinSERCA2, primers SERCA2f and DsRedORFr were used along with the pre-microRNA1-2 primers above to generate 423bp and 300bp products respectively (figure 3.7 & 3.8).

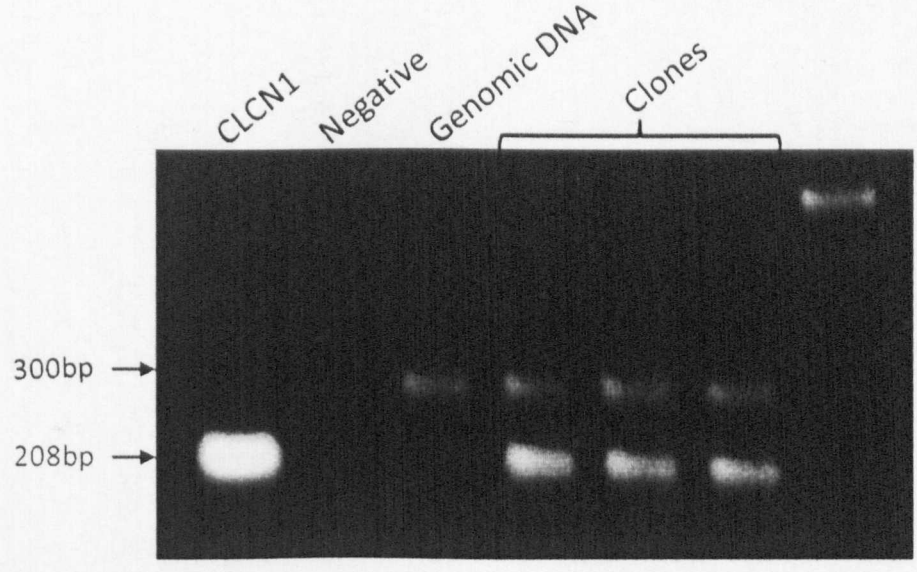

Figure 3.7: PCR amplification of cell clone DNA resolved on an agarose gel to confirm the presence of splicing construct pGR-CLCN1 in representative agarose gel for wild type and DM fibroblasts

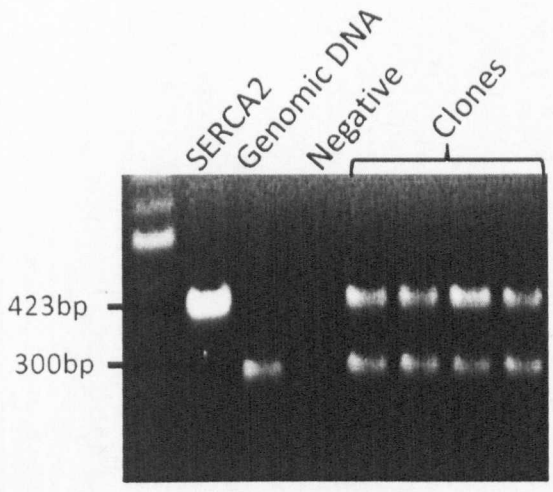

Figure 3.8: Confirmation of the presence of pGR-SERCA2 on a representative gel for isolated clones of wild type and DM fibroblasts

A total of 44 clones were obtained from human fibroblasts, pGR-CLCN1 was successfully introduced into all three cell lines (Table 3.5). Twenty six pGR-CLCN1 positive clones were derived from wild type fibroblasts, 4 clones from DM1 fibroblasts (KB TeloMyoD) and 1 clone for DM2 fibroblasts (KAGOTelo). For the pGR-SERCA2 construct, 11 clones were obtained for the wild type fibroblast line and 2 clones for the DM2 fibroblasts lines. As shown in figure 3.10 the wild type and the DM1 fibroblasts showed splicing of the pGR-CLCN1 transgene constructs in fluorescent scans that was similar to that demonstrated in C2C12. This shows the splicing of introns to produce the predicted fluorescence (figure 3.9).

Transgene	Cell line	Number of clones	Positive for transgene integration	Fluorescence
pGR-CLCN1	WT	67	26	6
pGR-CLCN1	DM1	11	4	2
pGR-CLCN1	DM2	1	1	-
pGR-SERCA2	WT	15	11	3
pGR-SERCA2	DM2	6	2	-

Table 3.5: Clonal cells generated by G418 selection from wild type and DM cells using transgene constructs. The dash indicates those which were not scanned for fluorescence.

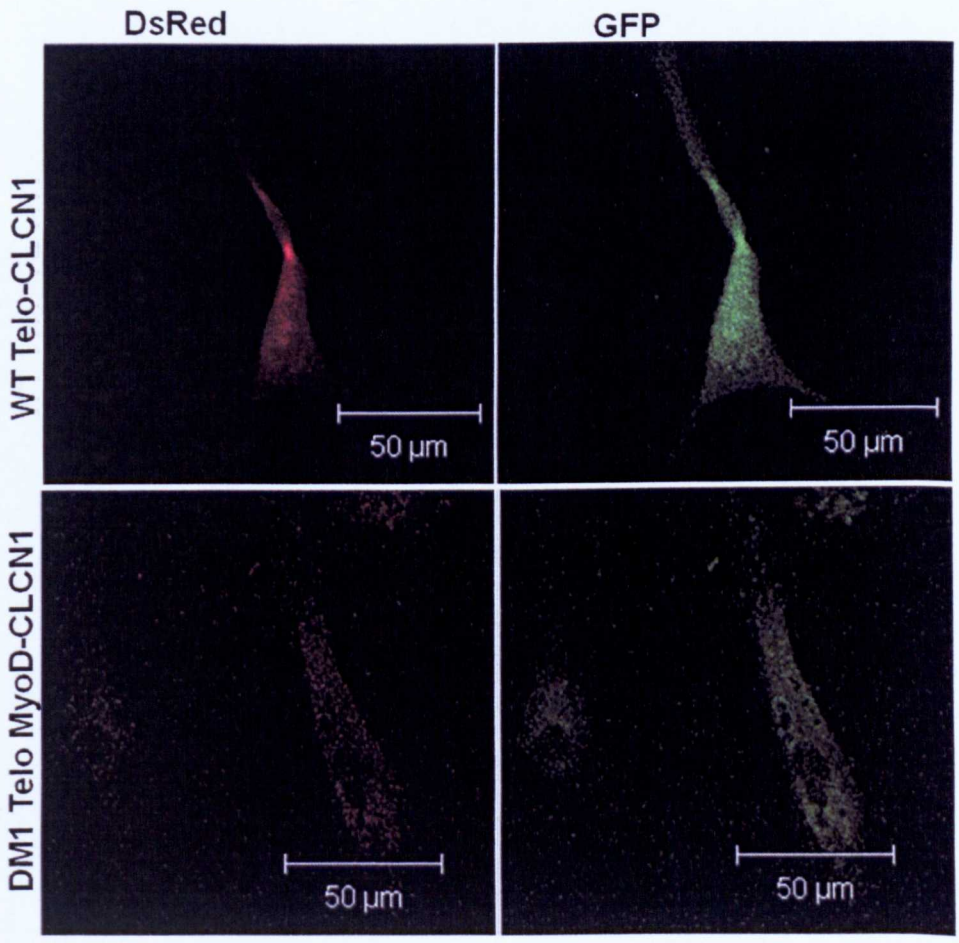

Figure 3.9: Fluorescent images of the cell clones transfected with transgene construct pGR-CLCN1 showing splicing of the construct and resulting fluorescence.

The clones obtained from these lines will be validated before use in therapeutic screening. Validation will involve differentiating DM1 clones containing splicing constructs to myoblasts to determine whether there are changes in the splicing ratio of green: red fluorescence. These cells will also be subjected to siRNA knockdown of *MBNL1* and *MBNL2* to assess its effect on splicing of constructs since MBNL knockdown in wild type myoblasts has been reported by Dansithong et al (2005) to alter *IR* splicing in addition to reducing foci number in DM cells.

3.6 Summary

Two assays have been developed in this chapter for primary screening of compounds for DM therapy. They include a nuclear foci assay and the use of transgene splicing reporter constructs. The nuclear foci assay has been optimised in high content imaging on the plate reader in both 96-well and 384-well format. Furthermore, clones with transgene splicing construct were confirmed for fluorescent expression in confocal imaging scans.

Both assays will be validated in the next chapter of this report for their applicability in HTS for compound screening by *MBNL* downregulation to assess its effect on these assays. In addition, DM1 clones with splicing construct will be subjected to differentiation to assess if it changes the fluorescent ratio when fibroblasts differentiate into myoblasts.

CHAPTER FOUR: VALIDATION OF PRIMARY ASSAYS AND COMPOUND SCREENING

4.1 Introduction

The assays generated in the previous chapter, namely nuclear foci and splicing construct assays were tested for confirmation of their efficiency and suitability for use in screening compounds. In one instance, DM1 clones containing the *CLCN1* splicing construct were differentiated to determine whether this altered the splicing profile. In another instance, wild type and DM1 clones containing the same splicing construct were subjected to MBNL downregulation to assess its effect on the splicing assay. Furthermore, in order to assess the efficiency of nuclear foci assay, DM1 cells were also subjected to MBNL downregulation to assess its effect on nuclear foci.

The primary assays were subsequently used for screening compounds and molecules following optimisation for high throughput screening (HTS).

4.2 Validation of Splicing construct assay

To validate the splicing construct assay, a DM1 cell clone containing the *CLCN1* splicing construct was subjected to differentiation to assess its effect on *CLCN1* splicing. In addition, clones of DM1 and wild type cells containing a *CLCN1* splicing construct were also subjected to MBNL downregulation to test its effect on *CLCN1* splicing in these clones. The fluorescence ratio (DsRed fluorescence/green fluorescence) was used as a measure of the rate of splicing in the *CLCN1* splicing constructs.

4.2.1 Differentiation of DM1 clones containing *CLCN1* splicing construct alters its splicing

The clone of DM1 fibroblasts containing a *CLCN1* splicing construct, which was generated in the previous chapter was subjected to differentiation by the presence of doxycyclin which induces MyoD expression, a muscle differentiation factor, to convert the fibroblasts into myoblasts.

Based on the splicing concept, it was hypothesized that the fluorescence ratio in the DM1 clone containing the *CLCN1* splicing construct, which gives an indication of the extent of splicing, would be altered as is reported in studies of splicing of transcripts upon differentiation of DM1 cells (Savkur et al, 2001; O'Leary et al, 2010).

Consistent with this proposal, the fluorescence ratio (ie DsRed to GFP) observed in the DM1 cells containing the *CLCN1* splicing construct changed from 1.0 (100.0%) in fibroblasts to 0.0 (0.0%) in confocal scans showing no red fluorescence in these cells after differentiation into myoblasts (figure 4.1).

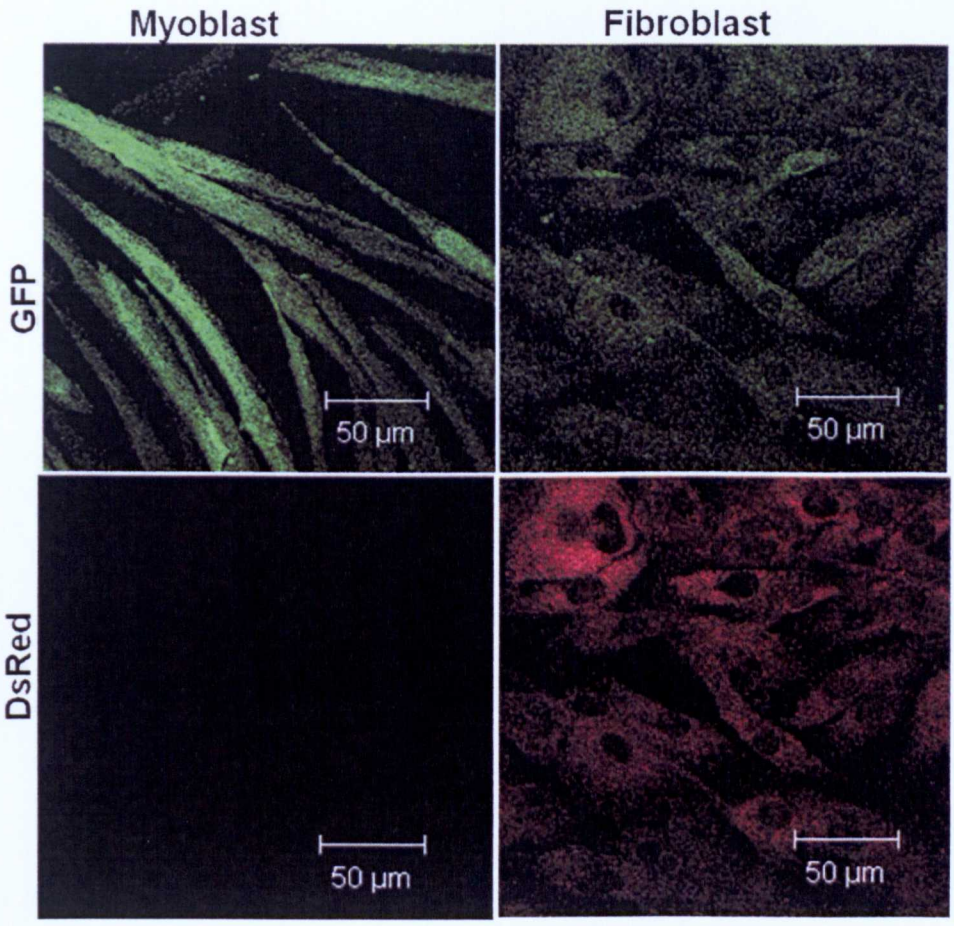

Figure 4.1: Intron 2 of *CLCN1* splicing transgene is spliced out in DM1 fibroblasts as shown by the expression of both GFP and DsRed in these cells. When fibroblasts undergo differentiation into myoblasts, intron2 of the splicing transgene is retained resulting in expression of only GFP. This represents a developmental switch from normal splice patterns in DM1 fibroblasts to DM1 splicing pattern in myoblasts.

The switch in splicing as shown by the expression of GFP and DsRed in DM1 fibroblasts compared to the GFP-only expression in myoblasts, derived from the same fibroblasts clonal lineage, is due to the retention of intron 2 of the *CLCN1* splicing construct in myoblasts. This leads to the termination of transgene transcript translation resulting in GFP expression only in the DM1 myoblasts. The intron2 retention in the DM1 myoblasts mimic the splicing

pattern associated with DM. This demonstrates that the clonal fibroblasts, which undergo developmental change to a DM-like splicing pattern on differentiation, were suitable for use in compound screening for DM therapy.

4.2.2 *CLCN1* splicing in DM1 fibroblasts clone is altered by MBNL downregulation but not in wild type clone

In order to downregulate MBNL levels in DM1 clone so as to assess its effect on the *CLCN1* splicing construct, siRNA whose sequence (appendix B) is directed against MBNL1 and MBNL2 mRNA was used with scrambled oligo, which is non-specific to any gene, as control. The siRNA binds to mRNA to prevent its translation.

DM1 clones demonstrated a decreased in DsRed/GFP ratio which was observed to give 0.174 for *MBNL* double knockdown, 0.250 for scrambled knockdown which was nonspecific to any gene while untreated was 0.251. This indicates that MBNL downregulation alters *CLCN1* splicing by promoting increased intron 2 retention in DM1 clones thereby shifting its splicing pattern towards that found in DM (Figure 4.2).

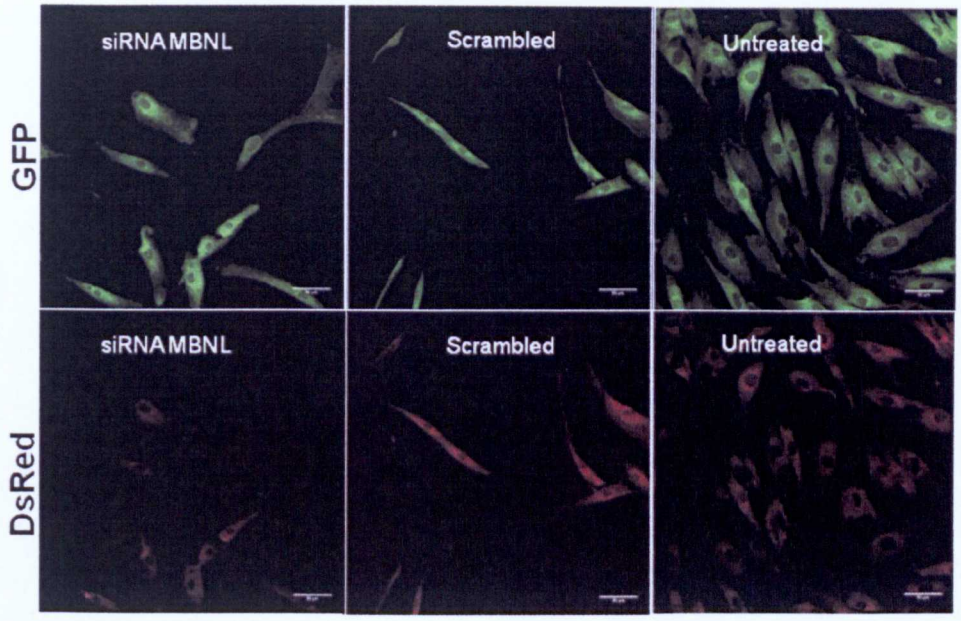

Figure 4.2: MBNL doubleknockdown (MBNL1 & 2) alters CLCN1 transgene splicing in DM1 fibroblast clones by reducing the intensity of DsRed fluorescence in HTS when compared to scrambled.

However, in wild type clones, MBNL downregulation did not show any effect on DsRed/GFP ratios as both MBNL and scrambled knockdown had the same ratio of 0.289 while untreated had a ratio of 0.228 (figure 4.3). This seems to suggest that MBNL downregulation did not have any effect on *CLCN1* splicing in wild type clones.

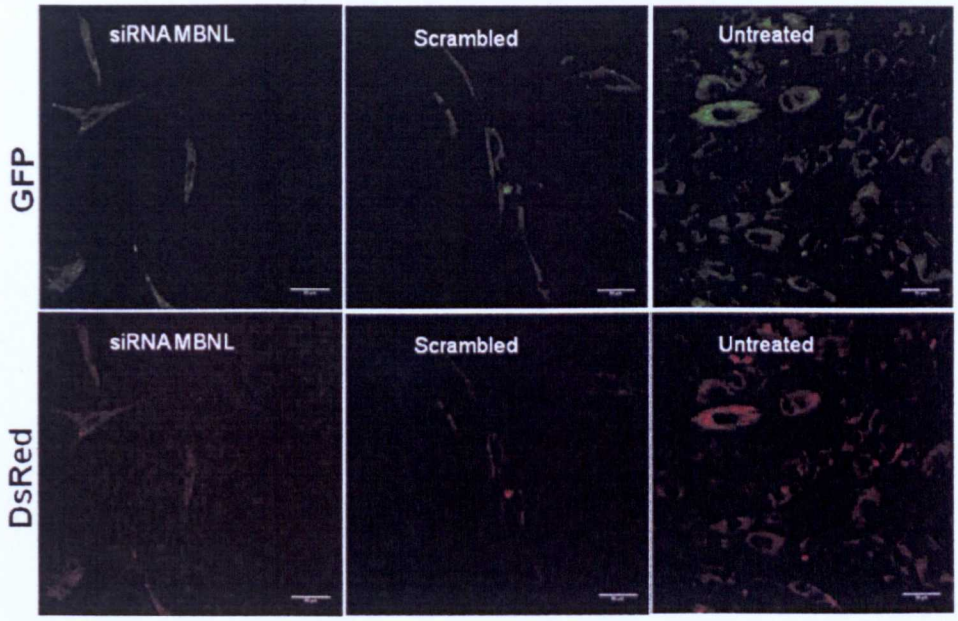

Figure 4.3: MBNL downregulation in wild type clone of CLCN1 transgene showing no effect on fluorescence ratio when compared to scrambled which serve as the control.

In order to confirm the possibility MBNL1 and 2 were actually downregulated in both wild type and DM1 fibroblast clones, western blotting of protein extracts from both MBNL double knockdown and scrambled knockdown samples were performed.

Western blotting results normalized to tubulin showed that MBNL1 was greater than 95% downregulated in DM1 fibroblasts clone (figure 4.4) and about 90% reduction was achieved in wild type clone (figure 4.5).

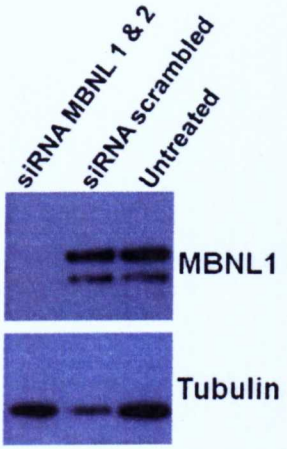

Figure 4.4: MBNL1 was reduced in MBNL doubleknockdown in DM1 clonal cells in comparison with controls (scrambled and untreated)

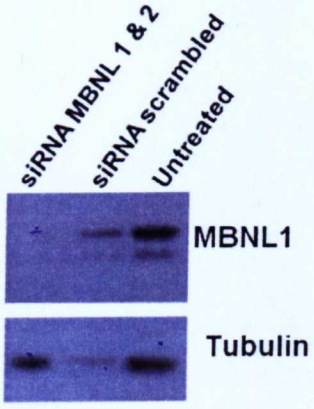

Figure 4.5: Downregulation of MBNL1 in wild type clonal cells confirmed on western blot normalised with tubulin as loading control.

The loading control (tubulin) was slightly less in scrambled knockdown than in MBNL knockdown in wild type clones suggesting that MBNL1 levels in scrambled knockdown is more than that observed on the blot and could be similar to levels seen in untreated samples.

On the other hand, MBNL2 was downregulated by 80-85% in both DM1 and wild type clones (figure 4.6 and 4.7).

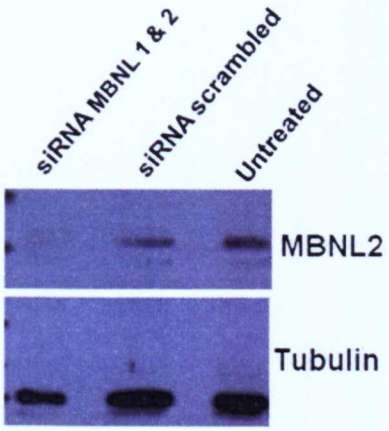

Figure 4.6: MBNL2 protein levels were decreased in MBNL doubleknockdown of DM1 clonal cells when compared to scrambled and untreated controls. Western blot was normalized with tubulin.

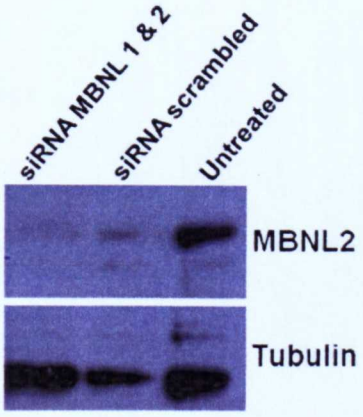

Figure 4.7: MBNL2 protein levels were reduced in MBNL doubleknockdown sample in comparison with controls (scrambled and untreated) with tubulin as loading control.

However, the loading control (tubulin) for scrambled knockdown indicates that the amount of MBNL2 protein is more than what is shown on the blot and could be similar to the levels seen in untreated sample.

Taken together, these results confirm that the splicing assay in DM1 clone is suitable for application in therapeutic screening of compounds that could reverse splicing defects seen in DM.

4.3 MBNL downregulation reduces Nuclear foci in DM1 cells

To validate the nuclear foci assay, DM1 fibroblasts were subjected to testing by *MBNL* knockdown using siRNA directed against its mRNA to assess its effect on nuclear foci number. The aim was to establish if MBNL depletion would result in reduction of nuclear foci as was previously demonstrated in a report by Dansithong et al (2005). This would provide a positive proof for the nuclear foci assay to justify its application in compound screening therapy in high throughput screens (HTS).

In accordance with this proposal, *MBNL1* and *MBNL2* double knockdown from four replicates demonstrated 59.3±9.7% reduction in nuclear foci of DM1 fibroblasts when compared to scrambled (99.3±5.7%), a nonspecific knockdown for any gene, which served as negative control (fig 4.8). This result shows that the nuclear foci assay lends itself to further application for compound screens.

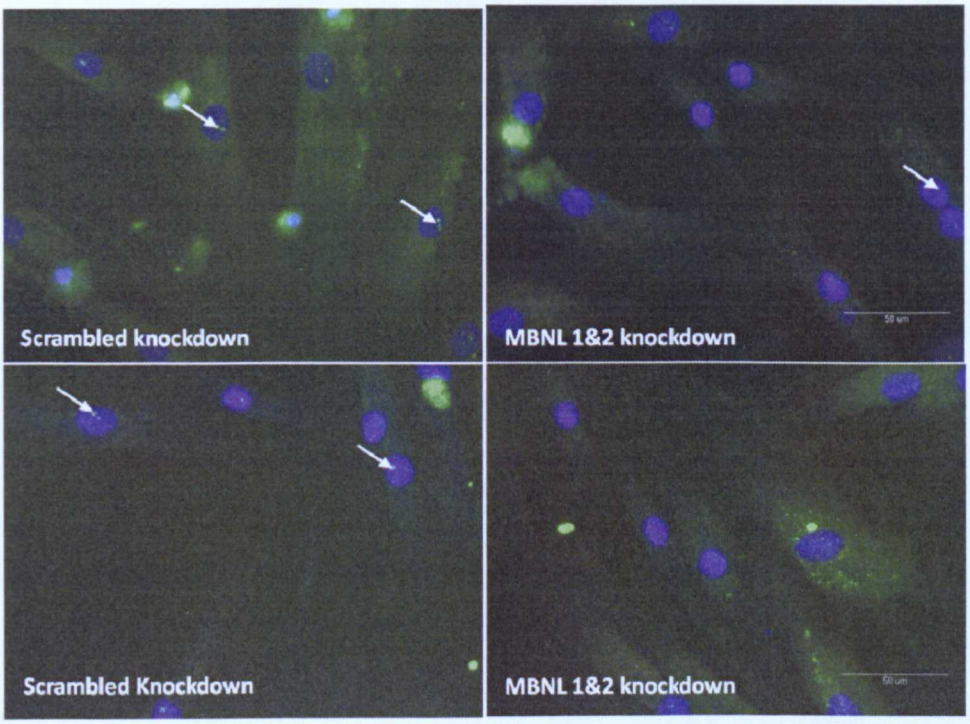

Figure 4.8: siRNA MBNL1 and 2 double knockdown reduces the number of nuclear foci while siRNA scrambled knockdown which is a nonspecific to any gene does not have any effect on nuclear foci in DM1 fibroblasts. Nuclear foci are indicated by the arrows.

4.4 Compound Screening

After validation, the primary assays were applied to screening compounds in the following sections for their efficacy in reduction or clearance of nuclear foci as well as in improving misregulated splicing in *CLCN1* reporter construct assays.

4.4.1 Compound Library for Screening

The initial library screen consisted of inhibitors of phosphatases and kinases. The kinase inhibitor collection consisted of 80 compounds including inhibitors of BTK, CaM Kinase II, CDK, CKI & II, EGFR, GSK, IKK, IR, JAK, JNK,

MAPK, MEK, MLCK, PI 3-kinase, PDGFR, PKA, PKC, RAF, SAPK, Src-family and VEGFR (Table 4.1). Some of these kinase inhibitors have been used by others to demonstrate their effect on alternative splicing. For instance, LY294002, an inhibitor of PI 3-kinase has been shown to block SRp40 phosphorylation and insulin-mediated exon inclusion of PKCβII isoform (Patel et al, 2001).

Kinase	Name
BTK	Bruton tyrosine kinase
CaM Kinase II	Calcium/calmodulin-dependent kinase II
CDK	Cyclin-dependent kinase
CKI & II	Casein kinase I & II
EGFR	Epidermal growth factor receptor
GSK	Glycogen synthase kinase
IKK	I Kappa B kinase
IR	Insulin receptor
JAK	Janus kinase
JNK	Jun N-terminal kinase
MAPK	Mitogen-activated protein kinase
MEK	MAPK/ERK kinase
MLCK	Myosin light-chain kinase
PI 3-kinase	Phosphatidylinositol-3-kinase
PKA	Protein kinase A
PKC	Protein kinase C
PDGFR	Platelet-derived growth factor receptor
RAF	Proto-oncogene serine/threonine-protein kinase
SAPK	Stress-activated protein kinase
Src- family	Non-receptor tyrosine kinase
VEGFR	Vascular endothelial growth factor receptor

Table 4.1: List of protein kinase inhibitors library and their respective names

The phosphatase inhibitor library was composed of 33 compounds including PP2B designated as calcineurin, CD45, CDC25, JSP-1, PP1, PP2A, PRL-1, PRL-3, PTEN etc (Table 4.2). One of the inhibitors in this group of compounds, calyculin A, an inhibitor of both protein phosphatase I (PPI) and

protein phosphatase 2A (PP2A) blocked alternative splicing of Bcl-x(L) and caspase 9b variants (Chalfant et al, 2002).

Phosphatase	Name
PP2B	Protein phosphatase 2B
CD45	Cluster for differentiation 45
CDC25	Cell division cycle 25
JSP-1	JNK stimulatory phosphatase 1
PP1	Protein phosphatase 1
PP2A	Protein phosphatase 2A
PRL-1	Pleiotropic regulatory locus 1
PRL-3	Pleiotropic regulatory locus 3
PTEN	Phosphatase and tensin homolog

Table 4.2: Phosphatase inhibitor library and its nomenclature

The initial screening library was made up of 113 compounds. Primary screens consisted of testing compounds at different concentrations of 48μM, 8μM and 1.6μM. Secondary screening tests were used to establish toxicity and sensitivity of the compounds in the screens.

The positive hits in HTS (defined as those which resulted in either clearance or 70% reduction of foci) obtained from the screening library were PKC inhibitors designated in the compound library as D8 and D9 and are named hypericin and Ro-31-8220 respectively. The optimal concentrations of D8 and D9 used in the screens were 50μM and 5μM respectively.

4.4.2 Protein Kinase C (PKC) Inhibitors

Protein kinase C has been shown to be activated by the expression of expanded CUG repeat containing RNA in its natural context of *DMPK* but the mechanism is yet to be understood (Kuyumcu-Martinez et al, 2007). Furthermore, it was demonstrated that PKC activation by expanded CUG

repeat induces hyperphosphorylation of CUG-BP1 leading to an increased half-life of the protein. It is the hyperphosphorylated forms of CUG-BP1 that are involved in alternative splicing.

PKCs are serine and threonine kinases that exist in twelve isoforms and are activated by phorbol esters like PMA (Mellor & Parker, 1998). A PKC inhibitor Ro-31-8220 was used in a functional study by Wang et al (2009) to test the role of CUG-BP1 in DM in an inducible cardiac-specific mouse model of the disease. Administration of PKC inhibitors to this mouse model was observed to relieve cardiac conduction defects as well as cardiac abnormalities. In addition, these inhibitors were found to reduce misregulated splicing events in exon21 of *Ank2* and exon16 of *Mtmr3* which are specifically regulated by CUG-BP1 (Wang et al, 2009). Taken together these reports demonstrate that inhibition of PKC activity could be a useful target for therapy of DM hence its justification for inclusion in the library of compounds used for DM therapy screening in this project.

4.5 PKC Inhibitors D8 and D9 clear nuclear foci from DM cells

Two of the compounds identified in our primary screens, D8 and D9, gave a positive result in compound screening assessment by clearance of foci in both DM1 and DM2 cells (figure 4.9) when compared to untreated cells which had nuclear foci.

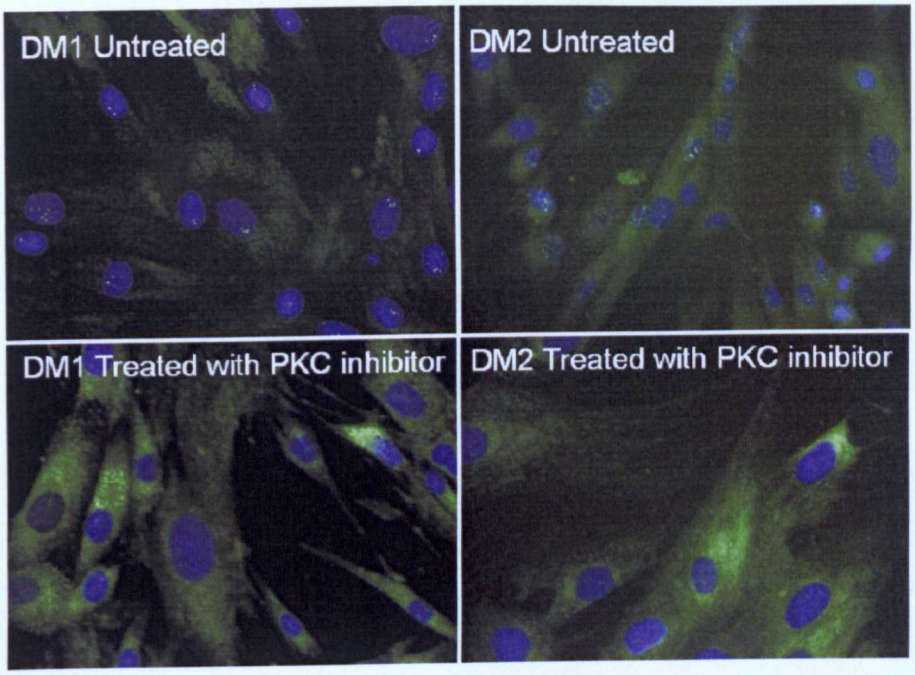

Figure 4.9: Compound screening analysis of DM cells showing the clearance of nuclear foci in both DM1 and DM2 fibroblasts by PKC inhibitor D9. D8 also gave similar effect on treatment.

These results demonstrate that D8 and D9 treatments could be of potential value in the therapy of DM. However, from this assay, it is not possible to determine whether D8 and D9 treatment results in the redistribution of MBNL1 following dissociation of nuclear foci.

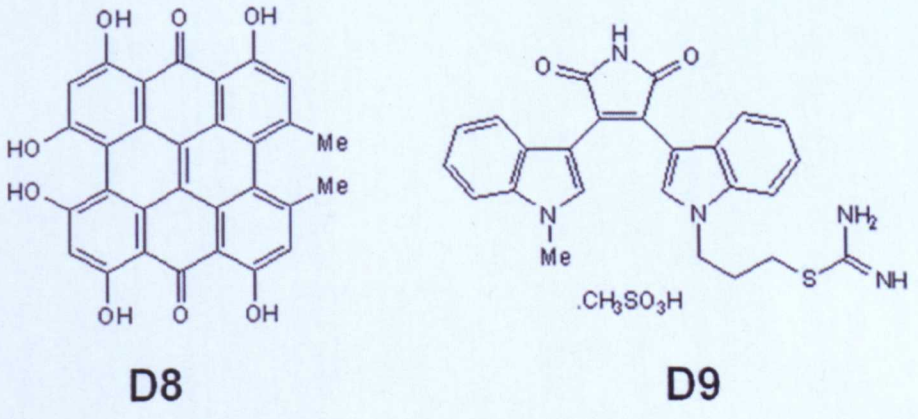

Figure 4.10: Chemical structures of PKC inhibitors D8 (hypericin) and D9 (Ro-31-8220).

Furthermore, we need to establish whether the RNA containing the expanded repeat units is released from the nuclei into the cytoplasm on clearance of foci from DM cells. The latter possibility will be tested in the next chapter of this report while the former can only be deduced based on data for the confirmation of positive hits by alternative splicing assays developed and tested in the next chapter of this report.

4.6 Correction of misregulated splicing in *CLCN1* reporter construct by PKC inhibitors D8 and D9 in DM1 myoblasts

In parallel, we applied the *CLCN1* splicing construct assay to assess compounds identified in the primary screening assay. This would serve as a double check against false positives for the identification of compound with therapeutic value in DM. Analysis of the expression of GFP and DsRed by DM1 myoblasts on treatment with compounds serves as a test for the effectiveness of compound treatment on correcting the DM-like splicing pattern. This would determine whether intron 2 of CLCN1 in the reporter splicing constructs is retained in DM1 differentiated cells (myoblasts) following treatment.

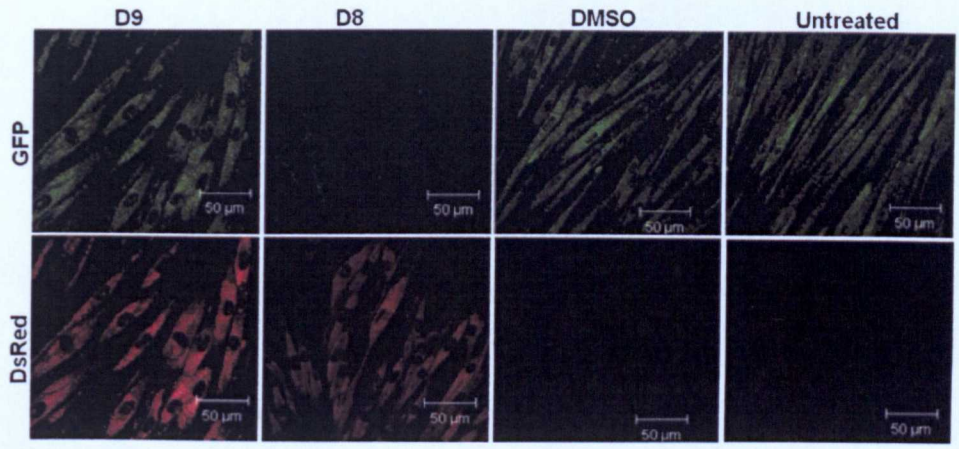

Figure 4.11: D8 and D9 treatment reverses DM-like splicing patterns of intron 2 retention of the *CLCN1* splicing transgene in DM1 myoblasts. Confocal images from laser scanning microscope are shown in treated and mock control (DMSO) and untreated myoblasts.

Both D8 and D9 treatments of differentiating DM1 fibroblasts restored *CLCN1* misregulated splicing in DM1 myoblasts (figure 4.11). The confocal images show the presence of both green and red fluorescent cells in contrast to mock control (DMSO treated) and untreated cells which exhibit only green fluorescence. The expression of only GFP in controls is an indicator of *CLCN1* misregulated splicing due to the retention of intron 2 which contains a premature termination codon leading to the truncated translation of the *CLCN1* open reading frame.

The assay was optimised on the Molecular Devices Ultra scanning device used for HTS which is more sensitive than laser scanning microscope. It showed different intensities of DsRed fluorescence in relation to GFP following treatment. The ratios of DsRed/GFP were quantified and analysed using metaXpress software multiwavelength cell scoring. D8 showed a greater DsRed/GFP ratio of 1.14 which was three times greater than that of D9 which was 0.36. Both DMSO treatments and untreated had fluorescence intensity

ratios of DsRed/GFP of 0.06 and 0.07, respectively, which were significantly less than the measures following D8 and D9 treatments. The HTS scans confirmed the result from confocal scans that both D8 and D9 treatments improved intron 2 splicing in differentiated DM1 reporter construct clones. Furthermore, D8 showed a greater effect on splicing than D9 with the *CLCN1* reporter splicing assays in HTS as demonstrated by higher DsRed/GFP ratio (figure 4.12).

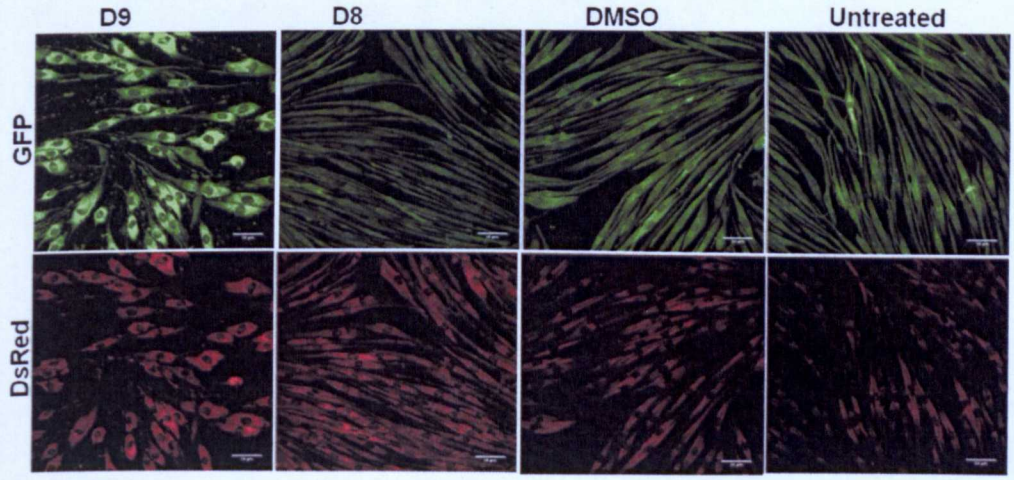

Figure 4.12: HTS scans on plate reader of DM1 myoblast containing *CLCN1* splicing construct showing diminished DsRed fluorescence in mock control (DMSO) and untreated in comparison with treatments (D8 and D9).

In addition, both DM1 fibroblasts and wild type fibroblasts containing the *CLCN1* splicing construct were analysed untreated by compounds as additional controls (figure 4.13 and 4.14). However, wild type myoblast were not used in these experiments as these cells would have served as a better control.

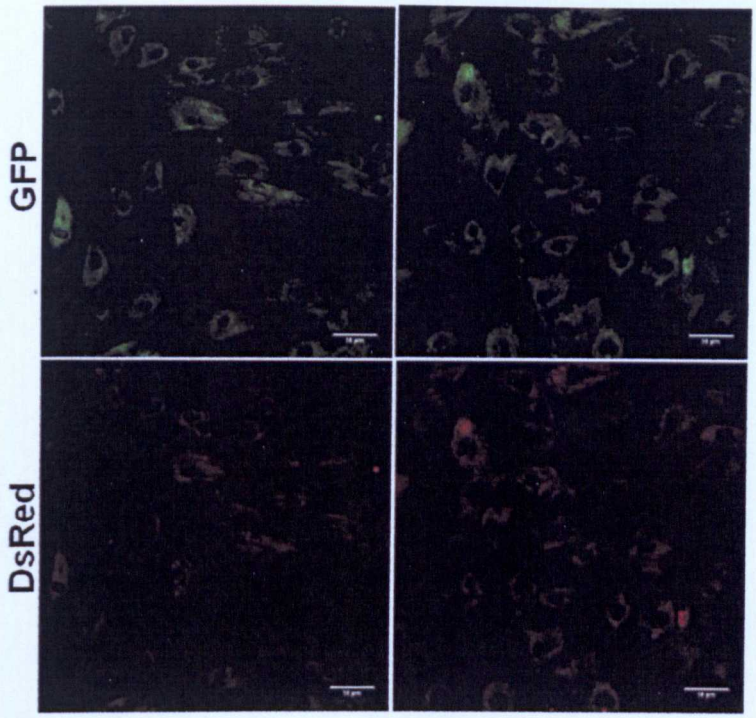

Figure 4.13: HTS scans of untreated wild type fibroblasts (non-DM) exhibiting GFP and DsRed fluorescence which is an indication of the extent of splicing of the *CLCN1* transgene construct in these cells.

In order to determine if the PKC inhibitors D8 and D9 affect splicing of the transgene in DM1 fibroblasts and wild type (non-DM fibroblasts), treatments of D8 and D9 were applied to these lines. The treatments in both wild type and DM1 fibroblasts showed that D9 had no effect on altering the splicing of the intron 2 of *CLCN1* construct while D8 seems to show a very minor alteration in intron 2 splicing (4.15 and 4.16). This implies that D9 does not affect *CLCN1* splicing in the fibroblast lines. However, due to the toxicity of D9 in the *CLCN1* splicing construct assay, the initial concentration was scaled down from 5μM to 3μM. Compound treatment was applied to differentiating myoblasts on day 5 of the six days differentiation period and DM1 myoblasts were exposed to 25 hour treatment before fixation for HTS. Both DM1 and

wild type fibroblast lines with the *CLCN1* splicing construct were subjected to 48 hour treatment exposure because these cell lines have a greater tolerance for D9 toxicity than DM1 myoblasts.

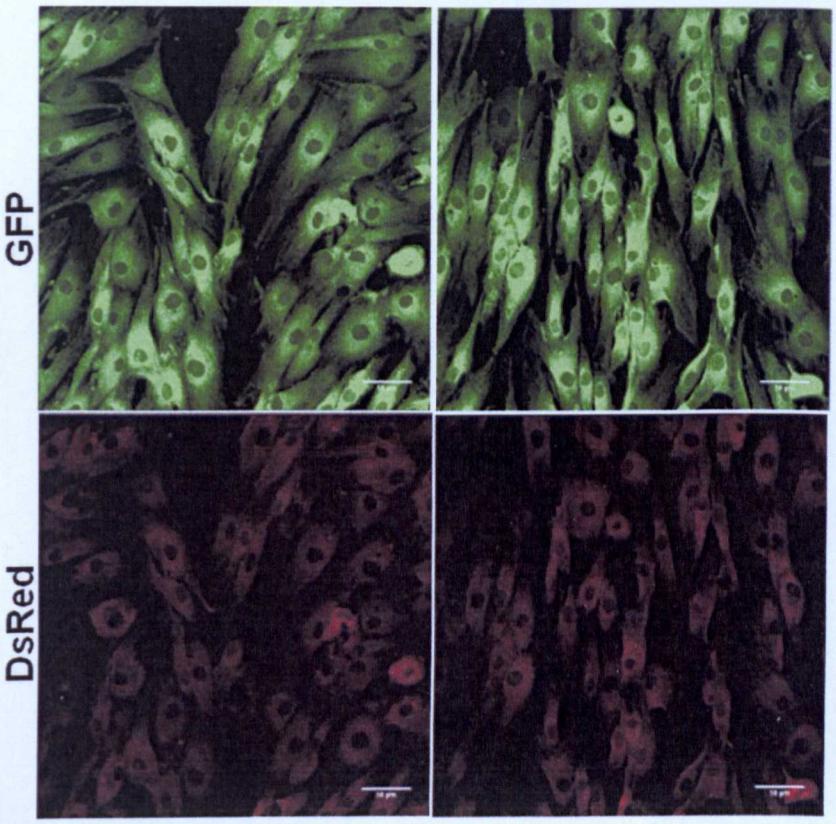

Figure 4.14: HTS imaging of DM1 fibroblast with *CLCN1* splicing transgene untreated with compounds showing splicing of intron 2 of CLCN1 transgene as shown by intensities of GFP and DsRed.

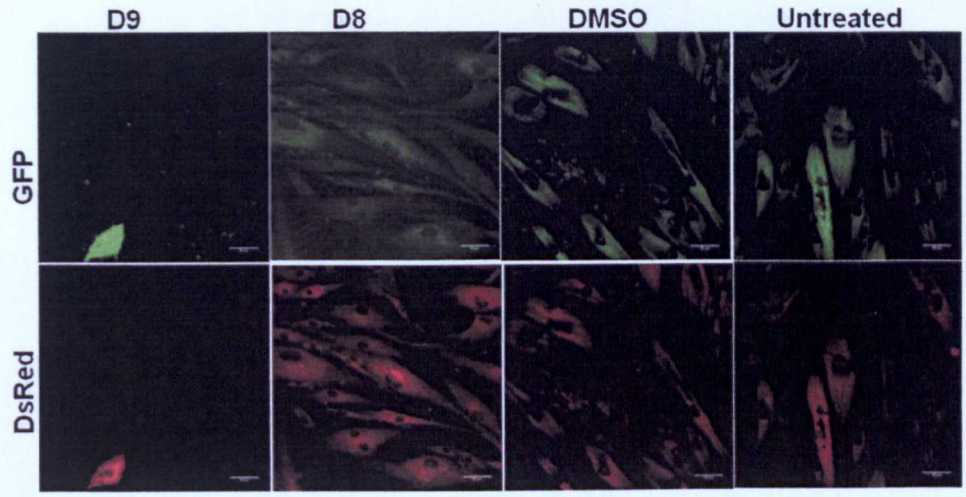

Figure 4.15: D9 treatments of wild type fibroblasts containing the *CLCN1* construct did not alter its splicing in comparison to controls (DMSO and untreated).

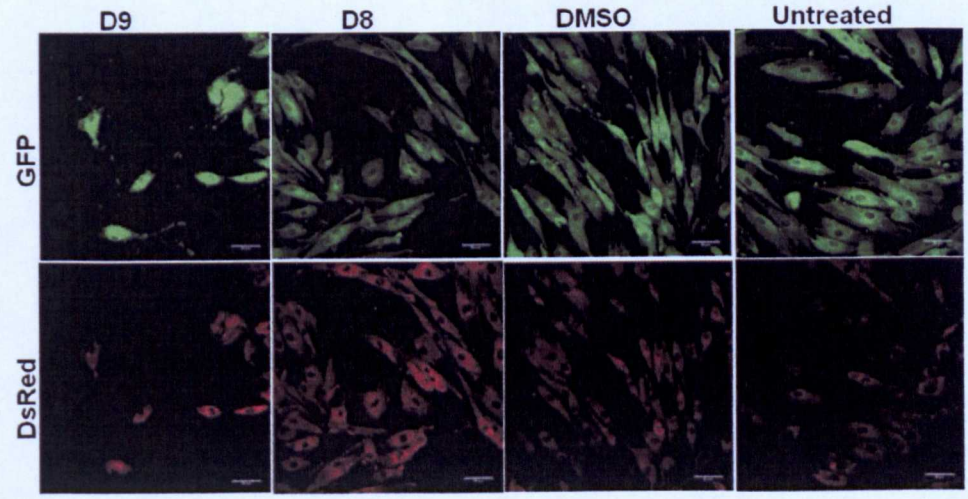

Figure 4.16: DM1 fibroblast containing *CLCN1* splicing construct showing a slight increase in its splicing on treatment with D8 and D9.

4.7 Summary

The applicability of the nuclear foci assay was confirmed by siRNA knockdown of *MBNL* on HTS prior to use in compound screening. The nuclear foci assay yielded two positive compound hits for clearance of nuclear foci

from the kinase and phosphatase inhibitor library. The compound hits obtained were D8 and D9 which are protein kinase C inhibitors.

In a parallel assay, the *CLCN1* splicing construct assay shows a suitable read-out with a developmental switch in its intron 2 to DM splicing patterns in myoblasts. Furthermore, DM1 fibroblasts clone of *CLCN1* splicing construct was confirmed by MBNL 1 and MBNL 2 downregulation for its effect on switching the splicing to DM pattern for optimisation on plate reader. Differentiating DM1 myoblasts containing the *CLCN1* splicing construct were used to confirm hits from the nuclear foci assay. Both D8 and D9 showed positive effects on reversing *CLCN1* intron 2 spliceopathy in differentiating DM1 myoblasts in both confocal scans and in HTS.

CHAPTER FIVE: DEVELOPMENT OF SECONDARY ASSAYS AND TESTING PUTATIVE HITS

5.1 Introduction

This section deals with assays developed based on downstream effects of ribonuclear foci formation in DM cells, namely entrapment of repeat expanded transcripts and spliceopathy which contribute to symptoms observed in DM patients. The assays developed were subsequently applied in testing the efficacy of putative compound hits (defined as compounds which cleared nuclear foci and corrected intron2 missplicing of *CLCN1* in DM1 myoblasts) obtained from primary screens in the preceeding chapter.

5.2 Secondary Assays

The aim was to develop a set of assays for DM therapy screening validation that follow on from primary assays for splicing misregulation and mutant *DMPK* transcripts that trigger DM-like molecular cascades. To enable validation of compound hits obtained from primary screens, secondary assays were developed based on analysis of compound effects on mutant allele of *DMPK* and splicing defects as the readout for the disease process.

5.2.1 Mutant *DMPK* analysis

Based on the effect of expanded repeat RNA containing *DMPK* transcripts in initiating molecular cascade of DM, two assays were developed for

optimisation. They include DNA mutation analysis and *BpmI* polymorphism which occur in mutant *DMPK* transcripts.

5.2.1.1 Mutational analysis of *DMPK* exon 10 for *BpmI* polymorphism

Initial DNA mutational analysis was carried out using PCR amplicons of *DMPK* exon10 from genomic DNA of DM1, DM2 and wild type fibroblasts in order to determine which cell was heterozygous for *BpmI* polymorphism by the presence of mutant and wild type allele of *DMPK* in these lines. Using primers (designated as GdmpkF and GdmpkR) located on flanking introns of exon10 (intron 9 and 10), a PCR product of 233bp was amplified, which was used for mutational analysis.

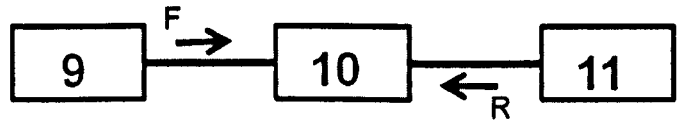

Figure 5.1: The location of primers on flanking introns of DMPK exon 10 used for amplification for analysis in dHPLC wave machine

Crude PCR amplicons from genomic DNA were subsequently subjected to 50 repeated cycles of heating at 98°C and cooling to -1.5 °C in order to promote heteroduplex formation. The products were then subjected to analysis in a denaturing HPLC Wave machine to produce elution profiles for the presence or absence of heterozygosity for *BpmI* polymorphism in fibroblasts defined by the presence mutant allele which has BpmI restriction site and normal allele of *DMPK* which lacks it. The elution profiles generate peaks for the normal allele

and mutant allele. Only one DM1 and one wild type fibroblast line were heterozygous for the *Bpm1* polymorphism which was present in mutant *DMPK* transcripts containing expanded repeats in this analysis showing the presence of two peaks in contrast to DM2 and another wild type line which showed a peak. The higher peak represents the normal *DMPK* allele while the lower bulging peak represents the mutant *DMPK* allele and the lower peak was absent in only DM2 fibroblast indicating it was not informative for *BpmI* polymorphism (figure 5.2).

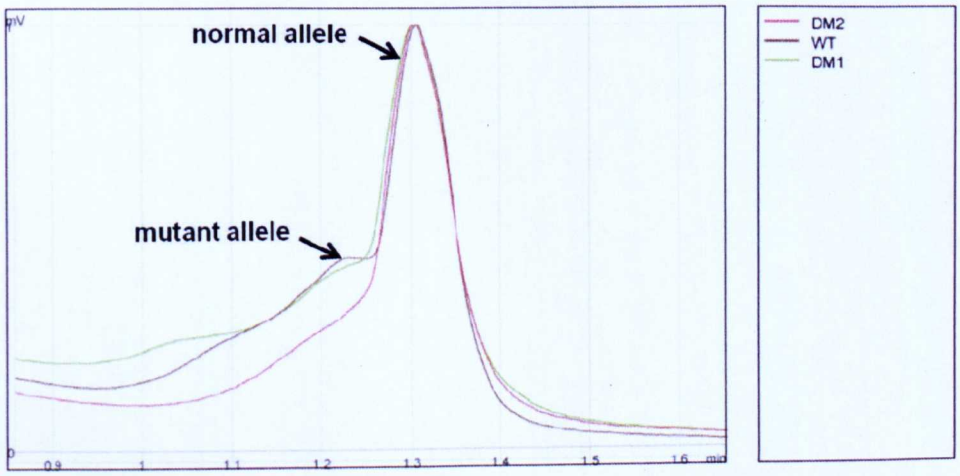

Figure 5.2 Elution profiles of mutational analysis of *BpmI polymorphism* of *DMPK* in wild type, DM1 and DM2 fibroblasts indicating the presence of the polymorphism in wild type and DM1 cells only

The mutational analysis was subsequently applied to cDNAs produced from nuclear and cytoplasmic RNA extracts from DM1 fibroblasts since it has been reported that the mutant *DMPK* transcripts are trapped in the nucleus hence are not transported to the cytoplasm (Hamshere et al, 1997; Davis et al, 1997).

These cDNAs were amplified using primers located on exon 9 and exon 10 to give a PCR product of 154bp for the mutational analysis.

Amplicons were heated and cooled for heteroduplex formation prior to dHPLC elution analysis which gave two peaks for the nuclear fraction, indicating the presence of normal and mutant *DMPK* alleles. On the other hand, the cytoplasmic fraction only gave a high peak showing the presence of only the normal *DMPK* transcripts (figure 5.3).

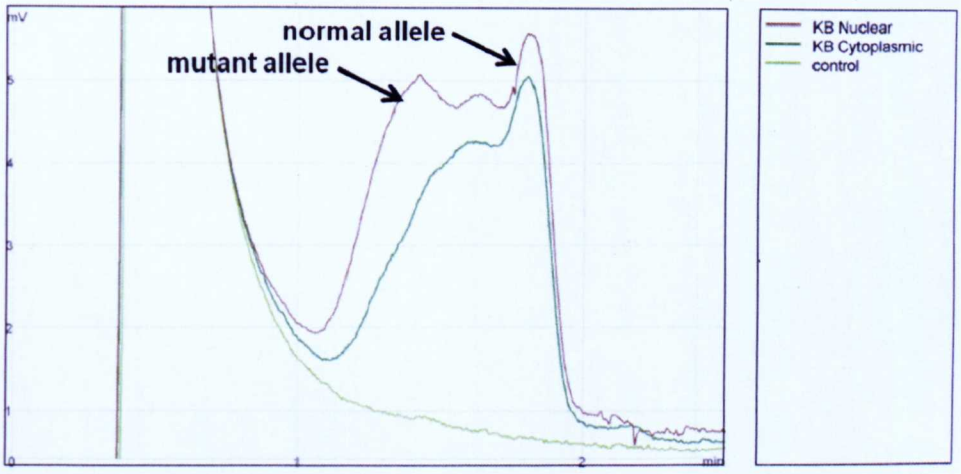

Figure 5.3: Mutational analysis of nuclear and cytoplasmic cDNAs of DM1 fibroblasts showing the presence of mutant *DMPK* transcripts in the nucleus which are absent in the cytoplasm

Subsequently, analysis was applied to compound treated cells whose nuclear and cytoplasmic RNA extracts were reverse transcribed, amplified by PCR and subjected to 50 cycles heating and cooling for heteroduplex formation. In addition, PCR amplicons of these reverse transcribed fractionated RNAs were sequenced to confirm results from dHPLC analysis.

Comparison of dHPLC elution profiles with sequencing analysis showed that every other sample exhibited similar results except for cytoplasmic sample from D9 treatment which demonstrated the presence of mutant *DMPK*

transcript in the cytoplasm (figure 5.4) which was not confirmed in the sequencing analysis. All mutational and sequencing analysis was carried out using PCR product of 32 cycles.

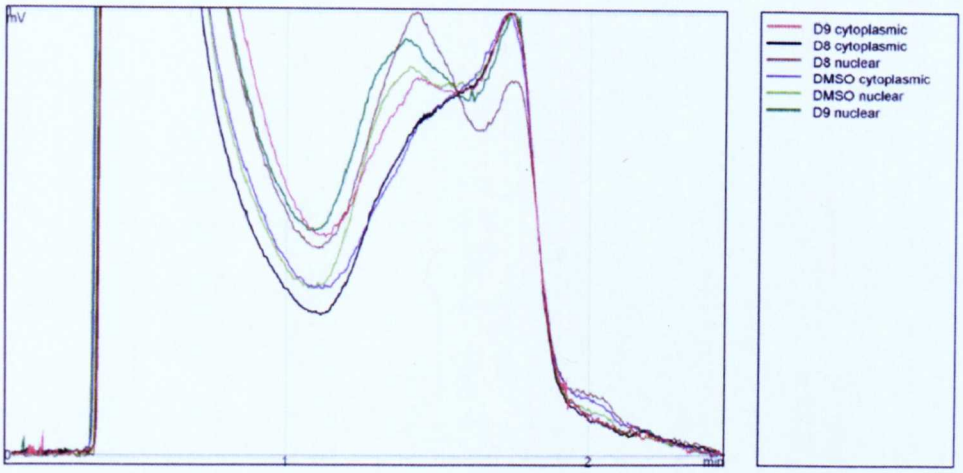

Figure 5.4 *DMPK* mutational analysis of nuclear and cytoplasmic cDNAs from PKC and DMSO treated DM cells showing that only D9 treatment effected the release of mutant transcript into the cytoplasm

Due to conflicting results for the cytoplasmic fraction of D9 treated cells in dHPLC analysis and sequencing which showed the presence of mutant transcript in cytoplasm in dHPLC which was not confirmed by sequencing, the wave machine mutational analysis was abandoned in favour of *BpmI* restriction analysis of *DMPK* for the mutant allele which will be discussed in the following section.

5.2.1.2 *BpmI* Restriction analysis

This was based on previous work in the lab reported in Hamshere et al (1997) in which primers flanking the polymorphic site on exon 10 of *DMPK* were designed on exon 9 and exon 10 (figure 1.11).

RNA extracted from nuclear and cytoplasmic fractions was reverse transcribed prior to PCR at 30 cycles. The RT-PCR amplicon yielded a 154bp product which was normalised to GAPDH as control.

The *BpmI* restriction site is present only in mutant *DMPK* transcripts containing expanded CUG repeat units but absent from the normal transcripts. *BpmI* restriction of 154bp amplicon gives 154bp and 138bp representing normal and mutant transcripts respectively on 3% agarose gel (figure 5.5).

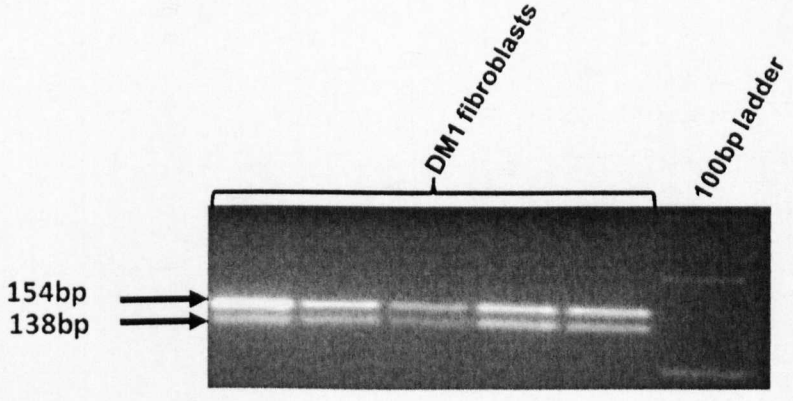

Figure 5.5: *Bpm I* restriction of RT-PCR amplicons from total RNA extracts of DM1 fibroblast showing the normal *DMPK* (154bp) and mutant transcripts (138bp)

This was applied to a DM1 line that was informative for the *BpmI* polymorphism and a wild type line that was a carrier for this polymorphism. *BpmI* restriction analysis of amplicons obtained from nuclear and cytoplasmic cDNAs showed the presence of mutant transcripts in the nucleus of DM cell

and its absence from the cytoplasm. However, in the wild type cells, the mutant transcript is present in both nuclear and cytoplasmic compartments of the cell.

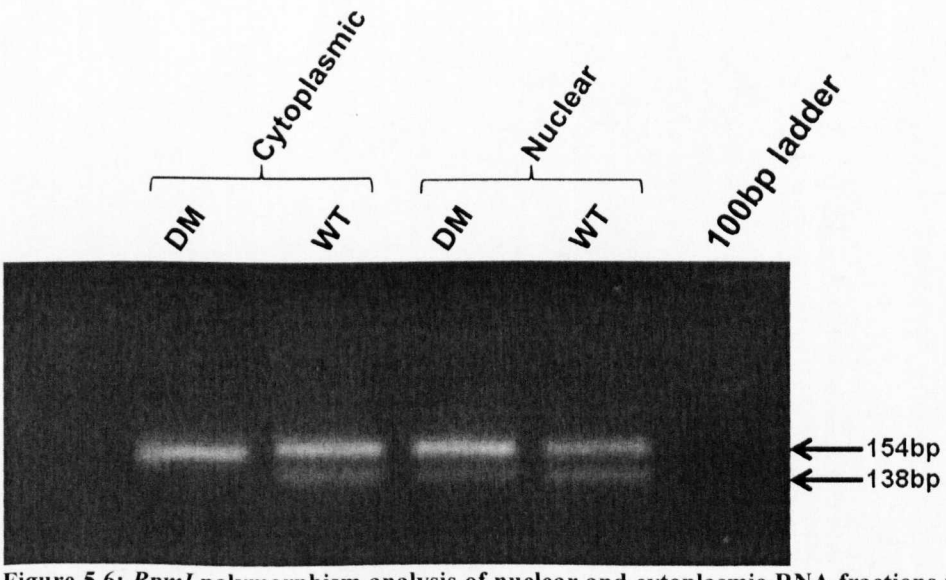

Figure 5.6: *Bpml* polymorphism analysis of nuclear and cytoplasmic RNA fractions from DM1 and wild type (WT) lines demonstrating the release of mutant *DMPK* transcripts into cytoplasm in wild type cells while that of DM1 cells is trapped in the nucleus.

5.2.2 Alternative Splicing assays

These assays were based on detecting the misregulated splicing events that contribute to the symptoms of DM phenotype. Alternative splicing events utilized in these assays were those involving insulin receptor (*IR*), sarcoplasmic/endoplasmic reticulum Ca^{2+}-ATPase1 (*SERCA1*), and muscleblind-like (*MBNL*).

5.2.2.1 Insulin Receptor Splicing assays

This assay is based on alternative splicing of exon 11 whose isoform is reduced in DM muscle cultures but increased in wild type muscles. Primers

used in this assay were located on exon 10 and exon 12, flanking the alternatively spliced exon 11. This generated RT-PCR products of 167bp and 131bp based on inclusion (IR-B) or exclusion of exon 11 (IR-A) respectively (figure 5.7).

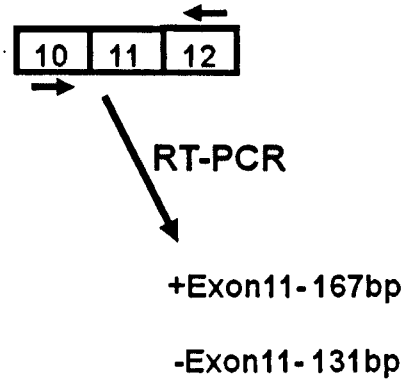

Figure 5.7: Alternative splicing scheme for *IR* involving exon 11 splicing analysis

Screening of DM1, DM2 and wild type fibroblast cDNAs was performed using PCR of 30 cycles. This showed a predominance of the isoform lacking exon 11 in DM2 fibroblasts. Wild type fibroblasts had almost equal proportion of both splice isoforms while DM1 fibroblasts had slightly more of the splice isoform containing exon 11 (figure 5.8).

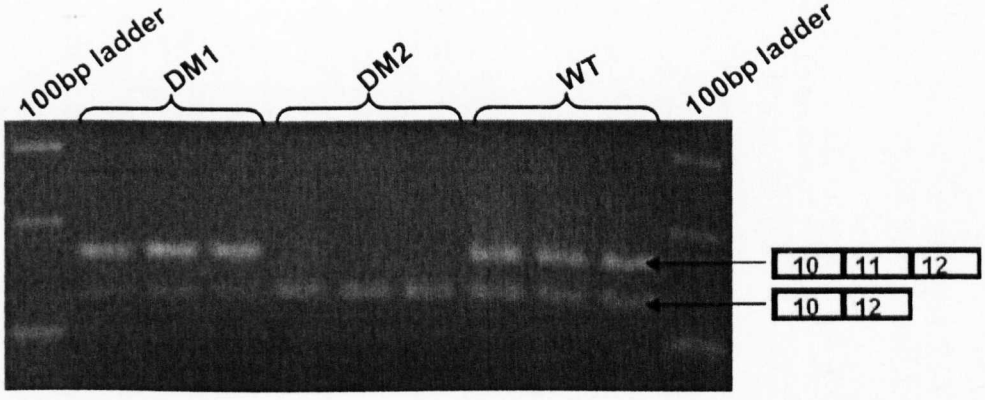

Figure 5.8: *IR* splicing screens of wild type, DM1 and DM2 fibroblast lines showing predominance of IR-A isoform in DM2 lines while IR-B is the major isoform in both DM1 and wild type fibroblasts.

Initial genescan analysis of *IR* splice isoforms in these fibroblast lines showed that the proportion of IR-B isoforms in DM1, DM2 and wild type fibroblasts were 52.3%, 10.8% and 49.1% respectively.

Only the DM1 fibroblasts, of those cell lines used above, contained an inducible MyoD transgene which in the presence of doxycyclin activates its myogenic programme to differentiate into myoblasts. The DM1 fibroblasts containing inducible MyoD were differentiated prior to *IR* alternative splicing analysis. It was observed that there was a splice isoform shift from IR-B, which occurred in DM1 fibroblasts to predominance of IR-A in differentiated myoblasts (figure 5.9).

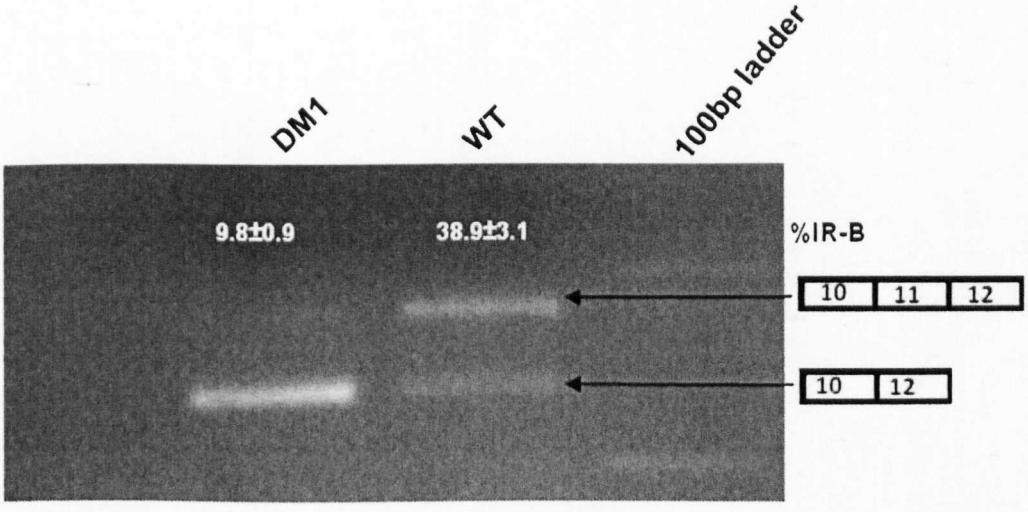

Figure 5.9: *IR* splice isoforms in DM1 and wild type myoblasts showing greater proportion of IR-A in patients' myoblast in contrast to wild type which show almost equal proportions of IR-A and IR-B.

The splice isoform quantification analysis of wild type fibroblasts, wild type myoblasts and DM1 myoblasts showed that the proportions of IR-B isoform were 56.8±1.1%, 38.9±3.1% and 9.8±0.9% respectively.

5.2.2.2 Sarcoplasmic/endoplasmic reticulum Ca^{2+}-ATPase 1 Splicing assay

In order to examine further the effect of compound treatment on DM molecular features, another assay was designed based on splicing of exon 22 of *SERCA1*. Alternative splicing of this exon generates two isoforms: SERCA1a which contains exon 22 and SERCA1b which lacks exon22. Primers designed for *SERCA1* splicing were located on exon 20 and exon 23 of the *SERCA1*. This generated RT-PCR products of 277bp and 235bp for SERCA1a and SERCA1b respectively (figure 5.10).

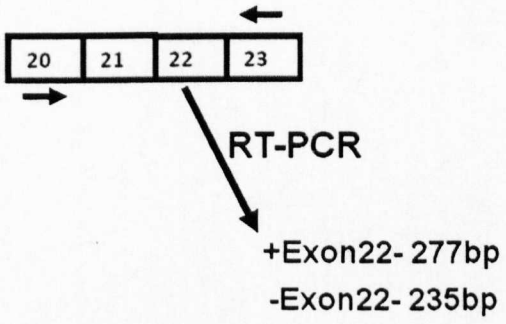

Figure 5.10: Scheme for SERCA1 alternative splicing analysis involving exon 22

The splicing assay was applied to DM and wildtype fibroblasts. Each of the cell lines showed predominance of the SERCA1a isoforms (figure 5.11).

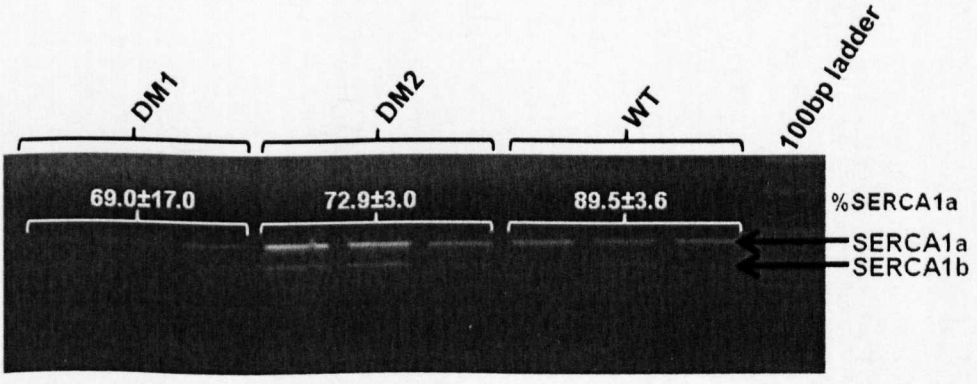

Figure 5.11: *SERCA1* splice isoforms in wild type and DM fibroblasts showing predominance of the SERCA1a isoforms.

Genescan quantification analysis of SERCA1a isoforms were 89.5±3.6%, 69.0±17.0% and 72.9±3.0% for wild type, DM1 and DM2 fibroblast respectively.

When DM1 fibroblasts were differentiated into myoblasts, there was a shift from splice isoform SERCA1a to SERCA1b. Wild type myoblasts demonstrated a slight increase in SERCA1a splice isoform over SERCA1b (figure 5.12).

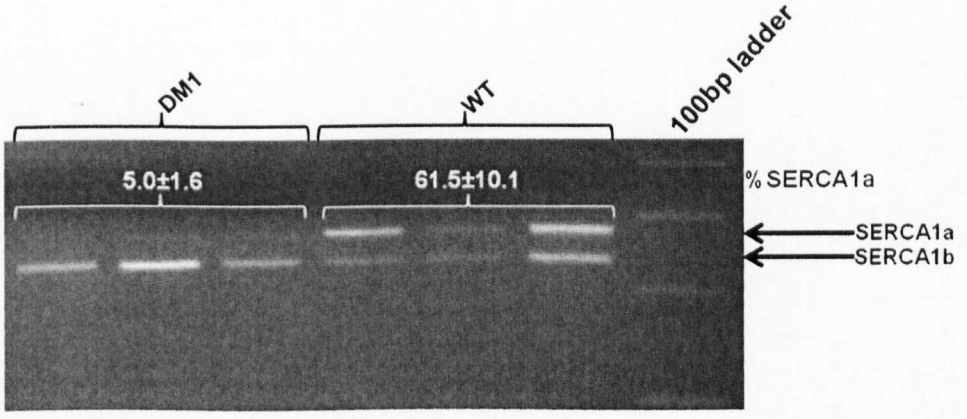

Figure 5.12: *SERCA1* splice isoforms in wild type and DM1 myoblasts. Wild type myoblasts display roughly equal proportions of the *SERCA1* splice isoforms whereas DM1 myoblasts display predominance of the SERCA1b isoform.

Quantification of the SERCA1a splice isoforms by Genescan analysis gave a value of 5.0±1.6% for DM1 myoblasts compared to 61.5±10.1% for wild type myoblast.

5.2.2.3 Muscleblind-like Splicing assay

Due to the significant role of MBNL proteins in splicing misregulation in DM as a result of its depletion, two assays for MBNL splicing were included for study.

5.2.2.3.1 Muscleblind-like 1 Splicing assay

The muscleblind-like 1 splicing assay was based on primers designed to exons 5 and 8 of the flanking alternately spliced exon7, which gives RT-PCR products of 270bp and 216bp for the presence and absence of alternatively spliced exon7 respectively.

In DM fibroblasts, as well as in wild type fibroblasts, there was less of the *MBNL1* exon 7 splice isoforms than the -7 isoform on 3% agarose gels (figure 5.13).

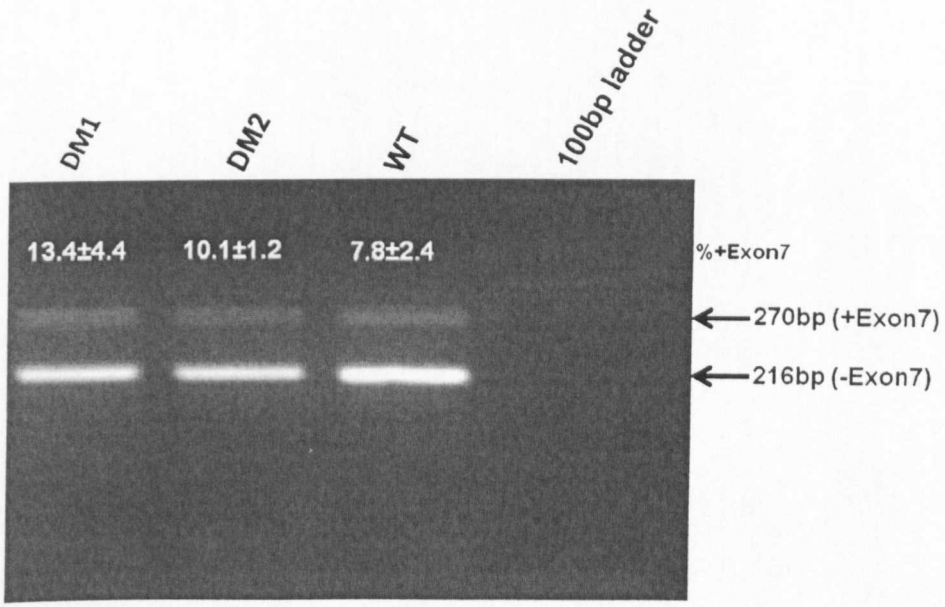

Figure 5.13: Wild type and DM fibroblasts showing similar decreased proportions of *MBNL1* exon7 isoforms on 3% agarose gel.

Analysis of exon 7 splice isoforms by Genescan showed 7.8±2.4%, 13.4±4.4% and 10.1±1.2% for the +7 isoform in wild type, DM1 and DM2 fibroblasts respectively.

However, when DM1 fibroblasts were differentiated into myoblasts, there was an increased proportion of the *MBNL1* plus exon 7 splice isoform in DM1 myoblasts compared to wild type myoblasts which showed a decrease in this splice isoform (figure 5.14).

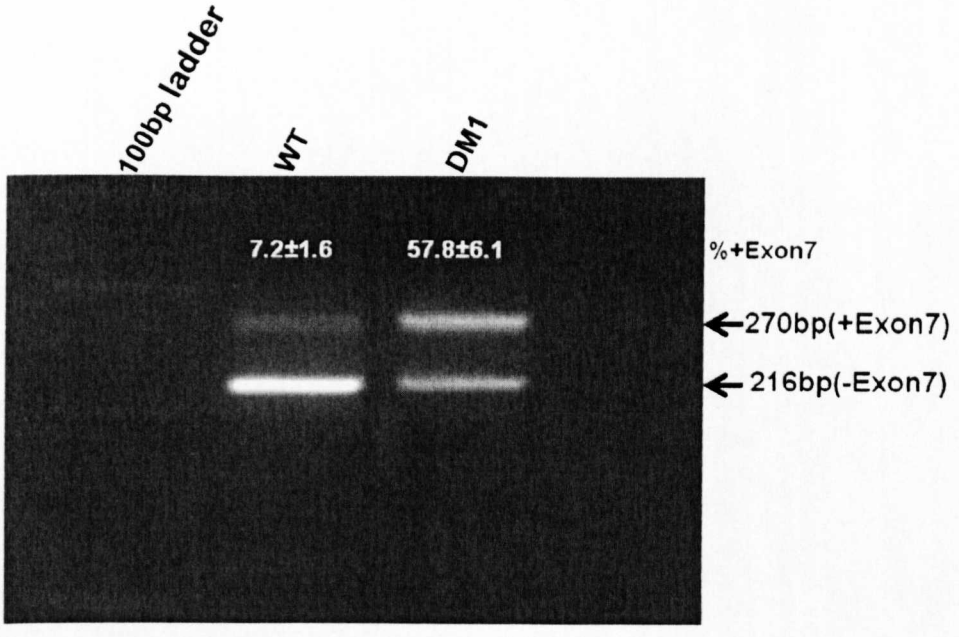

Figure 5.14: *MBNL1* splice isoforms in wild type and DM1 myoblasts showing greater proportion of +exon7 isoform in DM1 compared to wild type cells.

Genescan quantification analysis of the + exon 7 splice isoform revealed 7.2±1.6% for wild type myoblasts and 57.8±6.1% for DM1 myoblasts

5.2.2.3.2 Muscleblind-like 2 splicing assay

The *MBNL2* splice assay is based on the alternative splicing of exon7. Primers located in exon 5 and exon 8 and were designed to amplify a PCR product of 212bp for exclusion of alternately spliced exon 7 and 266bp for its inclusion. Fibroblasts from DM1 and DM2 patients show a similar decreased proportion of the exon 7 isoform while the wild type line is almost absent on 3% agarose gel (figure 5.15).

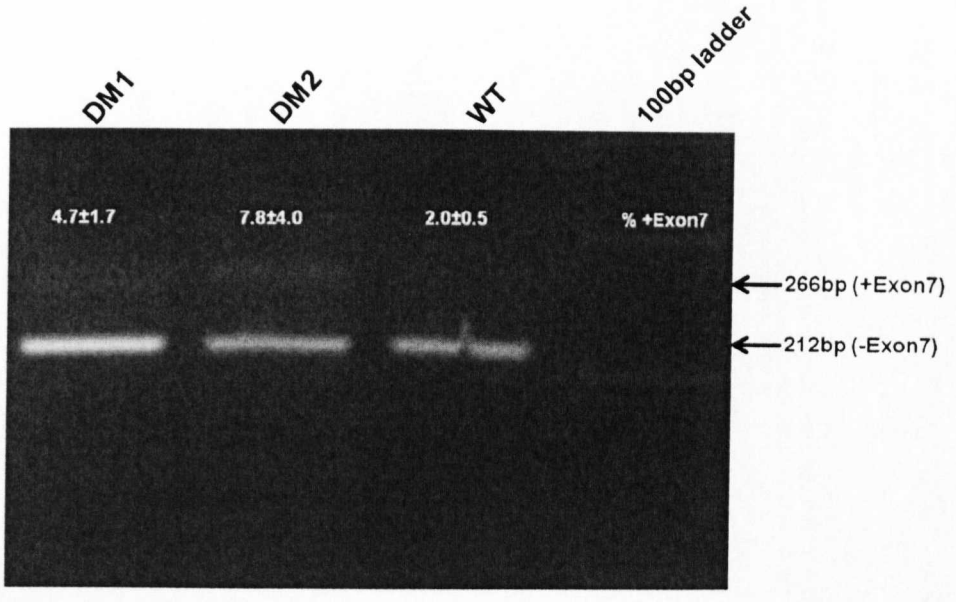

Figure 5.15: DM fibroblasts a showing decreased proportion of the +exon 7 isoform in comparison to wild type lines where it appears less on agarose gel.

The quantification of the +exon7 isoforms revealed 4.7±1.7%, 7.8±4.0% and 2.0±0.5% for DM1, DM2 and wild type fibroblast respectively.

In myoblasts, there is an increase in the proportion of the +exon 7 isoform in DM1 in contrast to the wild type where it is almost absent (figure 5.16). The quantification by Genescan shows that DM1 exhibits a greater proportion of the +exon 7 isoform (39.0±9.0%) while the wild type cells show a decreased proportion (2.1±0.6%).

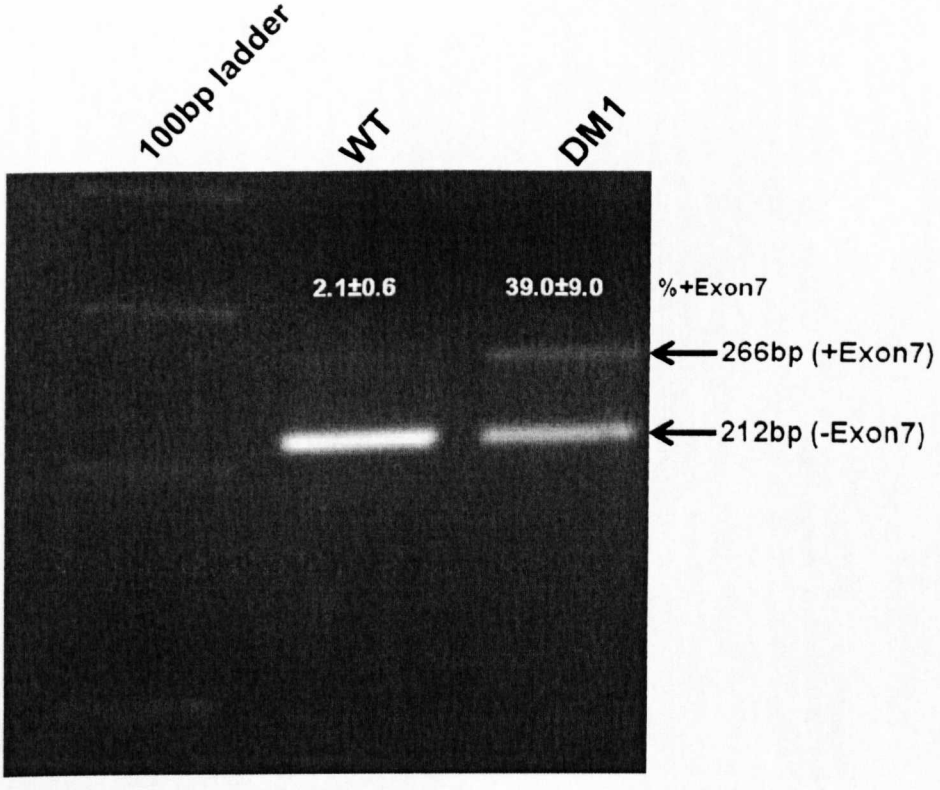

Figure 5.16: The DM1 cell line exhibited increased MBNL2 + exon 7 splice isoforms, which is almost absent from the wild type cell line.

5.3 Validation of Compounds

To test the hypothesis that compounds which clear or reduce nuclear foci in DM cells could lead to: (1) release of the RNA containing expanded repeat units into cytoplasm and, (2) produce a subsequent redistribution of MBNL1, released from foci, resulting in rescue of misregulated splicing, secondary screening assays were utilized. Secondary assays developed in the preceeding sections were used to validate positive compound hits from the HTS in primary screens. Among the positive hits obtained from the primary screens were protein kinase C (PKC) inhibitors designated as D8 and D9. These compounds

were applied to secondary assays that have been developed previously to test their effect on downstream targets of disease and are discussed below.

5.3.1.1 Mutant *DMPK* transcripts were not released into cytoplasm by *MBNL* downregulation

Since *MBNL1* and *MBNL2* double knockdown was demonstrated in chapter four of this report to effect 59.3±9.7% reduction in nuclear foci, it was also tested in *BpmI* polymorphism assay to determine if *MBNL* downregulation could effect the release of mutant *DMPK* containing expanded repeats. The siRNA double knockdown which was performed in parallel with nuclear foci assay showed that the mutant *DMPK* transcript was not released into the cytoplasm (figure 5.17).

However, the *MBNL* double knockdown effected a reduction in the proportion of mutant *DMPK* transcript in nucleus. Genescan analysis of normal and mutant DMPK transcripts showed that the percentage proportion of mutant allele in the nucleus was 18.0, 38.4 and 53.3 for MBNL double knockdown, nonspecific knockdown (scrambled) and untreated respectively. This correlates with what was observed on agarose gel (figure 5.18)

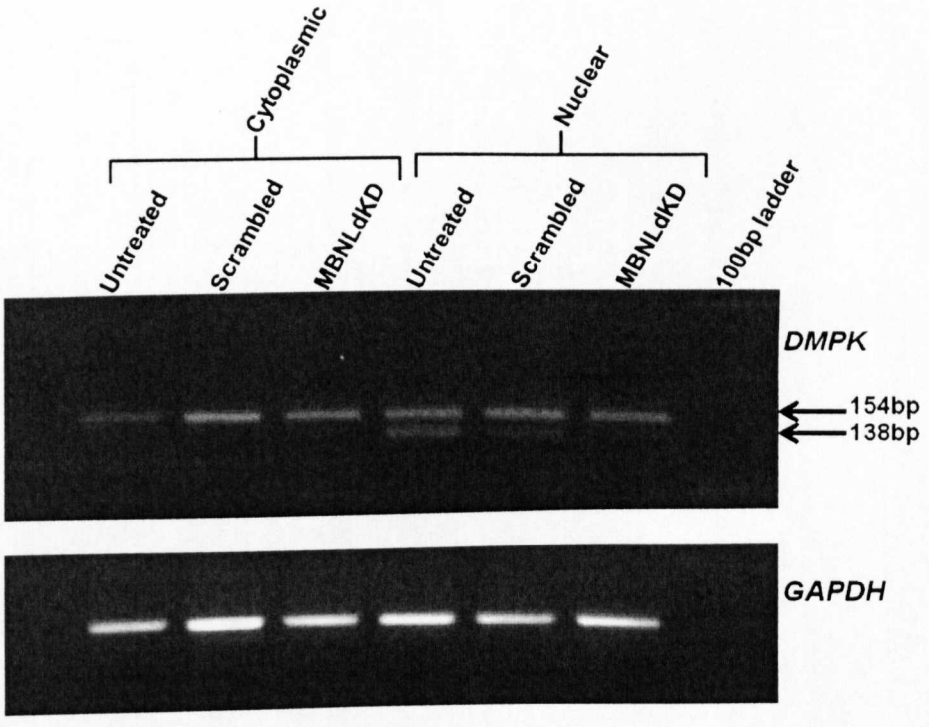

Figure 5.17: *MBNL* downregulation does not release mutant *DMPK* transcripts into cytoplasm but results in its reduction when compared to controls (scrambled which is a nonspecific knockdown and untreated)

5.3.1.2 PKC inhibitors do not release mutant transcripts into cytoplasm

In order to assess whether mutant transcripts are released from the nucleus following treatment with the hit compounds, *BpmI* polymorphism analysis was carried out on nuclear and cytoplasmic RNA following PKC inhibitor treatment of DM1 fibroblasts. Such treatment cleared nuclear foci from DM cells. Initial analysis showed that PKC inhibitors (D8 and D9) did not release the mutant transcripts into the cytoplasm indicating that these transcripts are still trapped in the nucleus (figure 5.18).

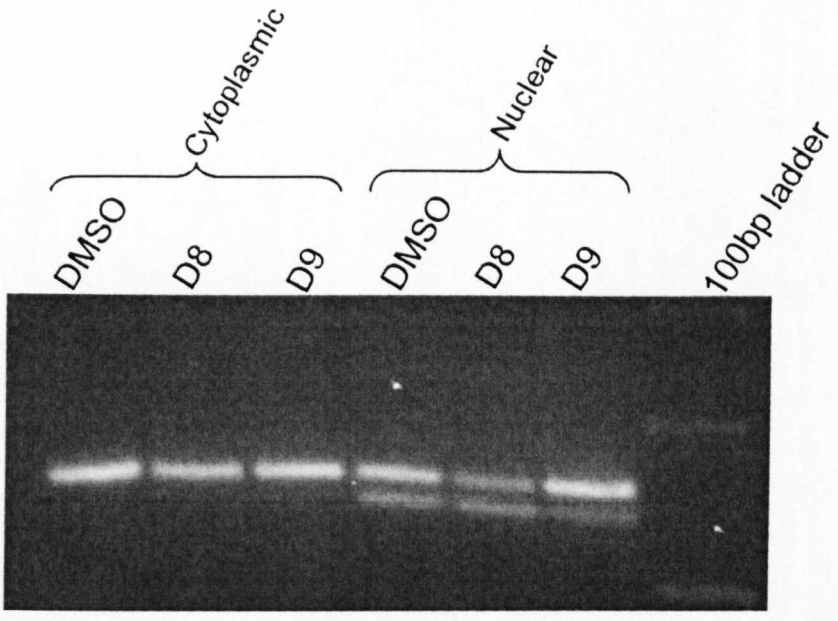

Figure 5.18: PKC inhibitor treatment of DM1 cells did not release the mutant transcript from the nucleus into the cytoplasm

Further analysis was carried out on DM1 fibroblasts in triplicate (figure 5.19a &b) which confirmed the results from the pilot study (figure 5.18).

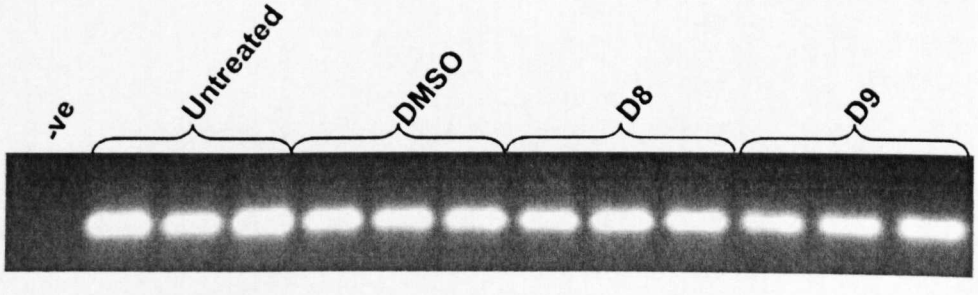

Figure 5.19a: Cytoplasmic *DMPK* showing non-release of the mutant *DMPK* transcript on treatment with PKC inhibitors

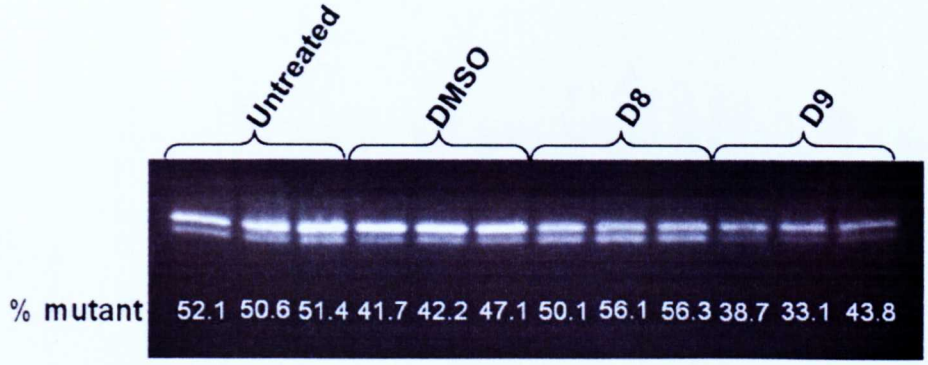

Figure 5.19b: PKC inhibitor D9 treatment shows a reduction of the mutant transcript in the nucleus which was not demonstrated in D8 treated DM1 fibroblasts.

Nuclear *DMPK* transcripts from these treatments were analysed using Genescan to quantify the relative proportions of the mutant and normal transcripts. Genescan analysis give peaks for the mutant and normal transcripts and the areas of the peaks were exported to calculate the relative proportions (figure 5.20).

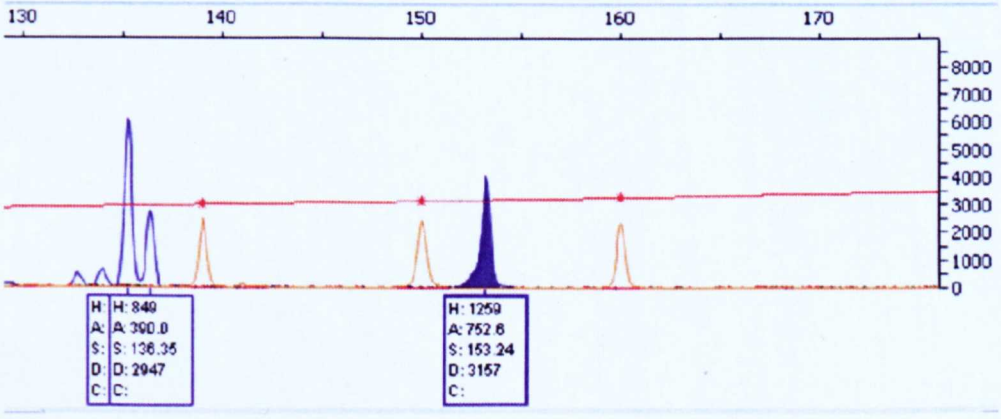

Figure 5.20: Analysis of the mutant *DMPK* (double peaks on the left) and normal allele (peak on the right) as shown by Genescan. Information below each peak gives the length in bp of product (S), height (H) and area (A) of the peak. The relative proportion was estimated using the area of the peaks for each allele. The yellow peaks are the size ladders.

The quantification of the *DMPK* transcript alleles on Genescan was carried out using PCR with 22-26 cycles in compound treated fibroblasts. The relative proportions of nuclear *DMPK* transcripts were assessed to determine whether compound treatment increased or decreased the proportion of mutant transcripts.

In DM1 fibroblasts, PKC inhibitor treatment affected the ratio of non-expansion transcripts to expansion *DMPK* transcripts. In nuclear RNA D9 produced 61.5±5.4% non-expansion transcripts compared to 45.8±3.5% following D8 treatment and 56.3±3.0% and 48.6±0.8% in DMSO and untreated cells respectively. The effect of D9 treatment was found to be statistically significant while D8 treatment was insignificant.

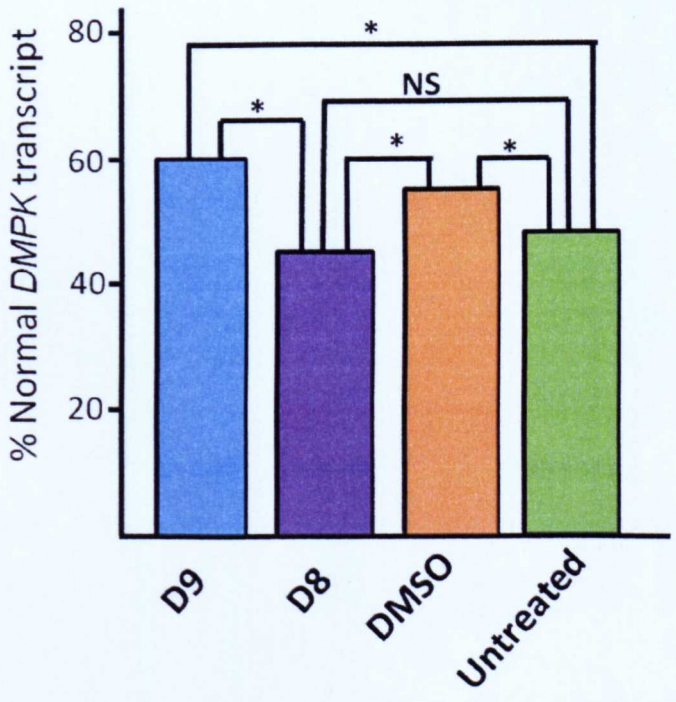

Figure 5.21: Statistical analysis of the effect of various treatments on nuclear *DMPK* in DM1 fibroblasts showing that only D9 had a significant effect on increasing the proportion of normal *DMPK* transcripts when compared to D8 treatment and untreated but it was not quite significant when compared to DMSO at p= 0.061.

The effect of PKC inhibitors was tested further in DM1 fibroblasts differentiated to myoblasts which also confirmed that they were not able to released mutant *DMPK* transcripts into the cytoplasm following treatment (figure 5.22 and 5.23).

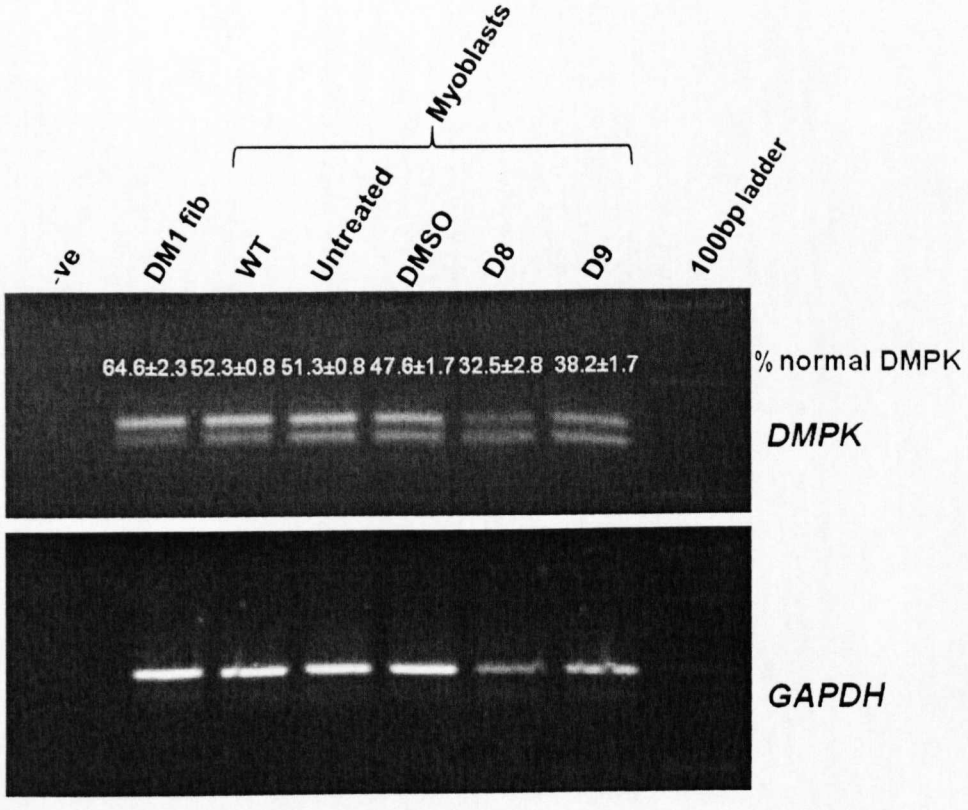

Figure 5.22: Analysis of nuclear *DMPK* following treatment of myoblasts showing that PKC inhibitors do not reduce the proportion of mutant *DMPK* transcript from the nuclear fraction. RT-PCR was normalised against *GAPDH*

In DM1 myoblasts, the proportions of mutant nuclear *DMPK* transcripts were increased in comparison to the relative amounts in fibroblasts (35.4±2.3% for fibroblasts and 48.7±0.8% for myoblasts). Furthermore, it appeared that D9 and D8 treated myoblasts had more *DMPK* mutant transcripts than controls. It

was also revealed by genescan analysis that D8 and D9 treatments did not reduce the proportion of mutant *DMPK* transcripts, neither did it release the mutant transcript into the cytoplasm when compared with wild type myoblasts (figure 5.23).

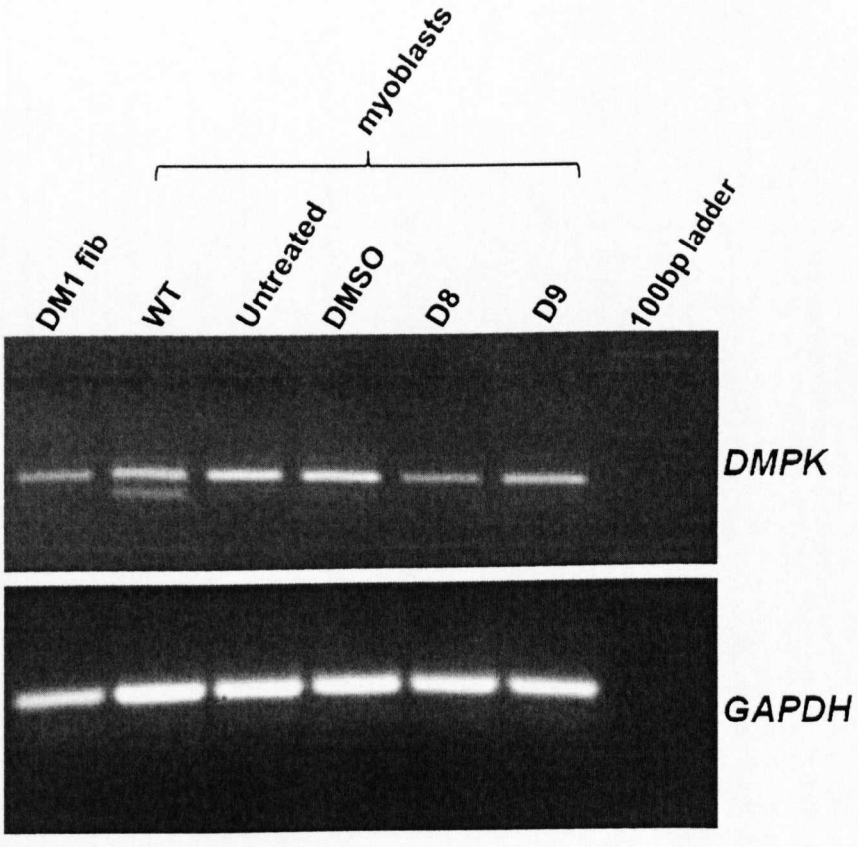

Figure 5.23: The non-release of mutant *DMPK* transcript into the cytoplasm of DM1 myoblasts following treatments by PKC inhibitors (D8 and D9). DM1 fibroblasts are included as controls on 3% agarose gel normalised to *GAPDH* as a control

The difference between D9 and DMSO treatments were statistically significant (p=0.037). In addition, a very significant difference was observed between D9 treatment and untreated controls (p=0.00509), as well as between D8 treatments and untreated controls (p=0.00395). Also, a very significant

difference was observed between D8 treatment and DMSO treatment (figure 5.24) which was a mock control (p=0.00227).

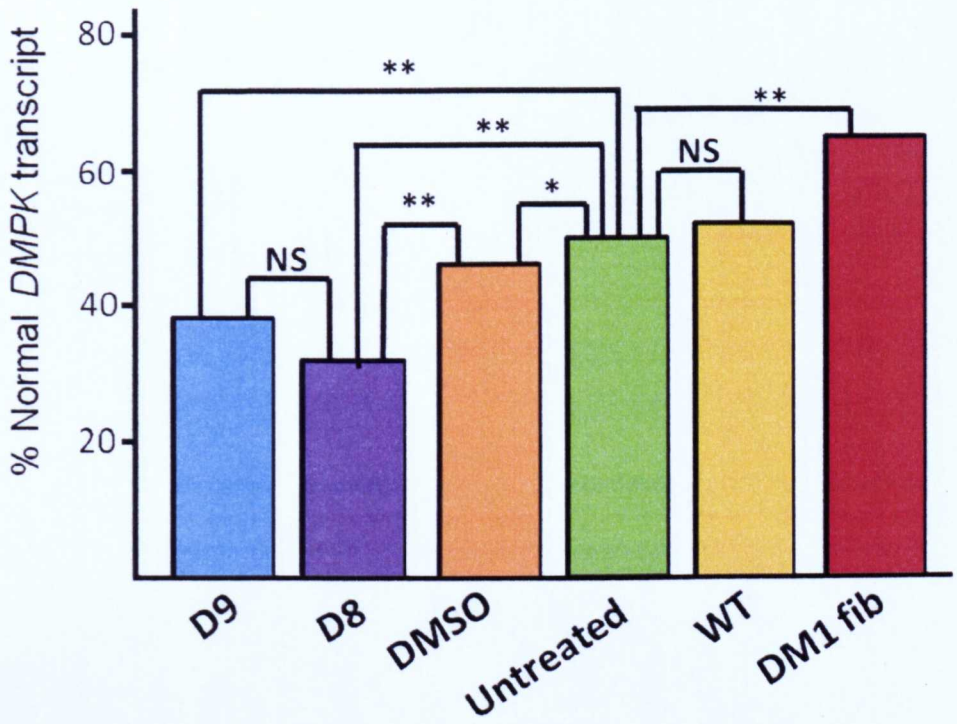

Figure 5.24: Statistical analysis of effect D8 and D9 treatments in comparison with controls showing that both PKC inhibitors have a negative effect of reducing normal *DMPK* in myoblast.

From the studies above, it would appear that both D8 and D9 treatments did not release mutant *DMPK* transcripts into the cytoplasm in both DM1 fibroblasts and myoblasts when compared to wild type fibroblasts and myoblasts in which mutant *DMPK* transcripts were released into cytoplasm.

5.3.2 D8 partially rescues *IR* splicing defect in DM1 myoblasts but not in DM2 fibroblasts

The *IR* splicing assay developed previously in section 5.2.2.1 was applied to compound treated DM2 fibroblasts and DM1 myoblasts to test its efficacy in reversing *IR* spliceopathy in DM. Initial application in DM2 fibroblasts showed that D8 treatment was effective in rescuing *IR* splicing as demonstrated by slightly increased IR-B isoform. D9 treatment has no such effect.

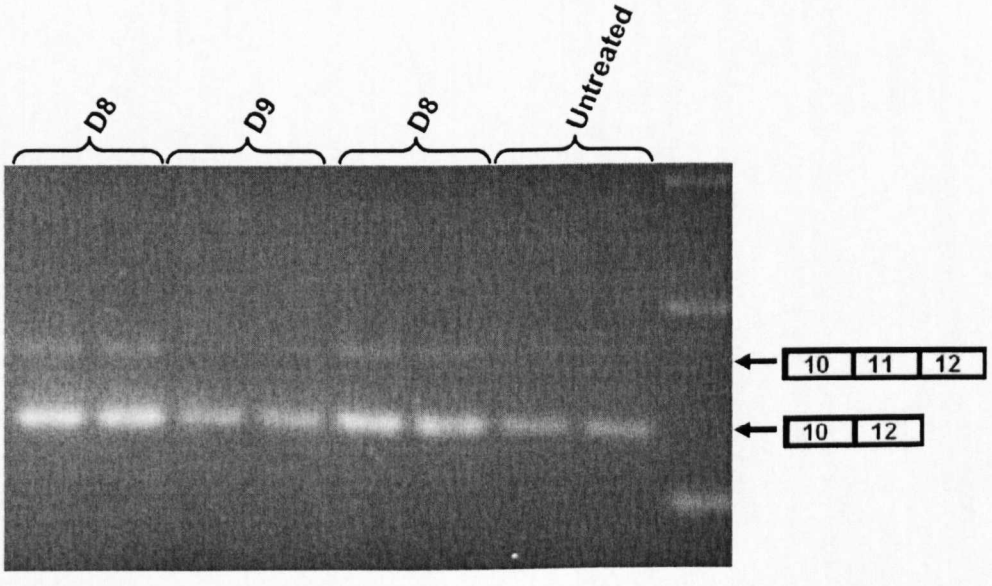

Figure 5.25: D8 shows partial reversal of *IR* splicing defect in DM2 fibroblast in the pilot study as indicated by the increased presence of IR-B.

However, replicating the above result in subsequent treatments of DM2 fibroblasts has been very challenging. Subsequent compound treatments of DM2 fibroblasts showed no difference between D8 and D9 treatments in comparison with controls (figure 5.26) following treatment with compounds for 24 hours.

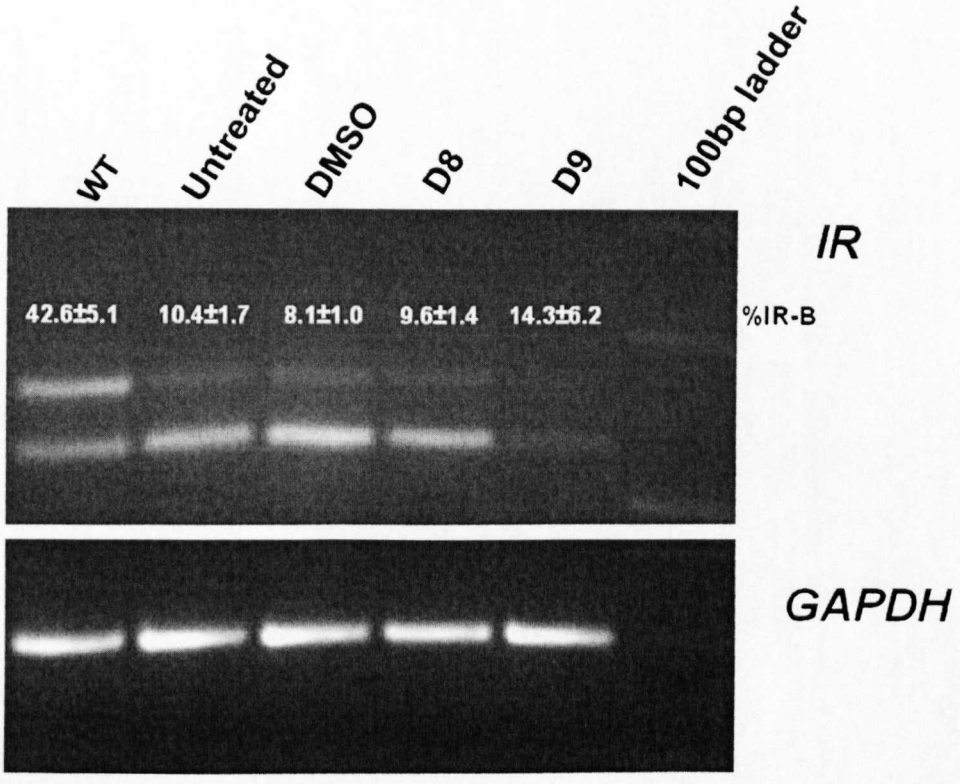

Figure 5.26: PKC inhibitors (D8 and D9) have no effect on improving the proportion of *IR* splice isoform B following treatment in DM2 fibroblast. RT-PCR was normalised using *GAPDH*

Isoform quantification of IR-B in triplicate treatments of D8, D9 and DMSO treated as well as untreated fibroblasts were 9.6±1.4%, 14.3±6.2%, 8.1±1.0% and 10.4±1.7% respectively. Wild type fibroblasts had IR-B proportion of 42.6±5.1%. Statistical analysis showed there was no difference between treatments (D8 and D9) on between treatments and controls (DMSO and untreated) (figure 5.27).

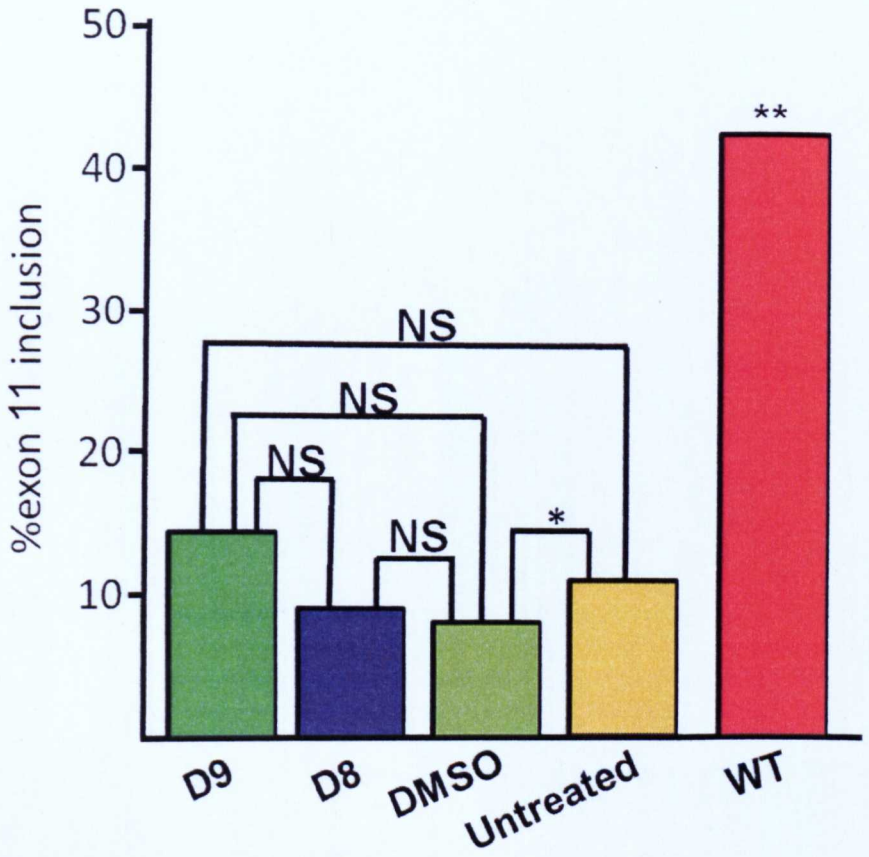

Figure 5.27: Analysis of *IR* splice isoforms in DM2 fibroblasts showing that PKC inhibitors D8 and D9 treatments did not have significant effects on the proportion of the IR-B isoform.

In DM1 differentiated myoblasts, D8 treatments slightly increased the proportion of IR-B splice isoform in comparison with controls (DMSO and untreated myoblasts). However, D9 treatment appeared to degrade both isoforms of *IR* by 48 hour of treatment (figure 5.28).

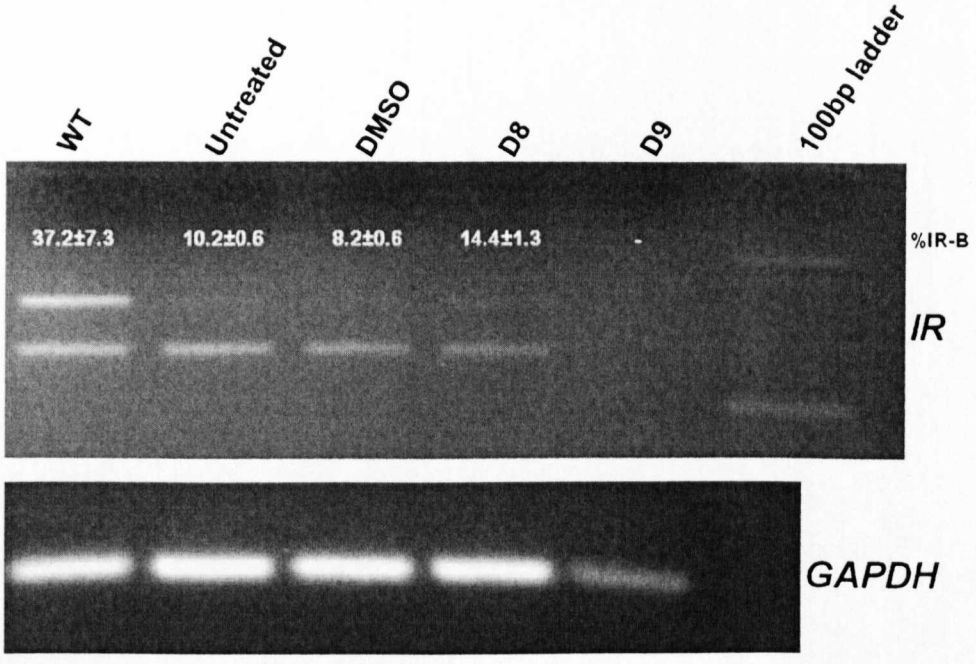

Figure 5.28: D8 treatment produces a slight increase in the IR-B isoform in DM1 myoblasts while D9 has a degradative effect on *IR* splicing when compared with controls (DMSO and untreated). *GAPDH* was used as loading control.

Splice isoform IR-B quantification gave values of 14.4±1.3%, 8.2±0.6%, 10.2±0.6% and 37.2±7.3% for triplicate treatments of D8, DMSO, untreated myoblasts and wild type respectively. Statistical analysis showed a very significant difference between D8 treatments and the mock control (DMSO) (figure 5.29) and there was also a significant difference when D8 treatment was compared with untreated myoblasts control ($p=0.02518$).

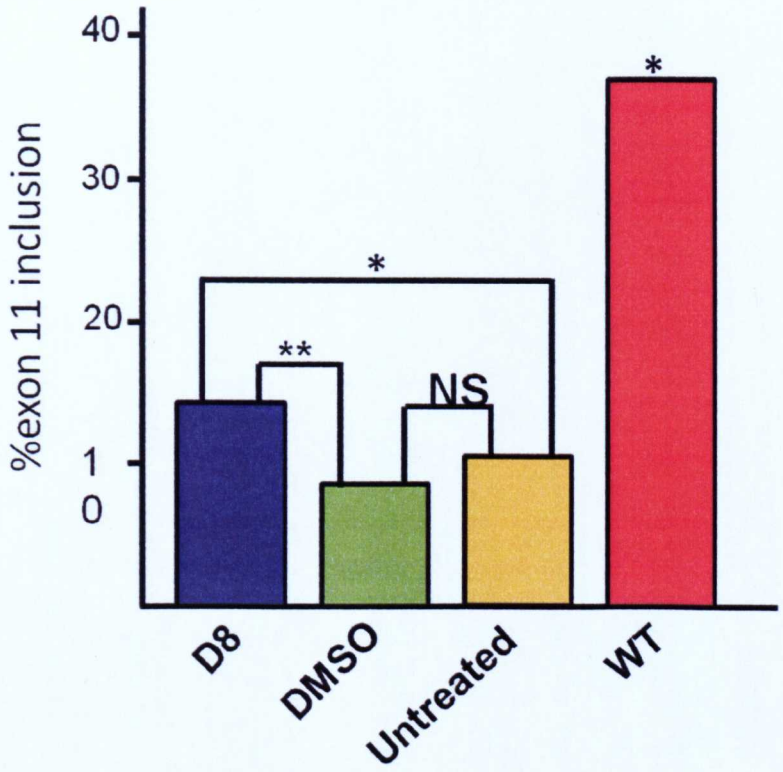

Figure 5.29: D8 treatment showed a statistically significant effect on the proportion of the IR-B isoforms in comparison to controls (DMSO and untreated) in DM1 myoblasts

5.3.3 PKC inhibitors do not increase *SERCA1* splicing in DM2 fibroblasts

In order to examine the effect of PKC inhibitors on another alternatively spliced transcript in DM, *SERCA1* splicing was assessed in triplicate compound-treated DM2 fibroblasts and controls. On a 3% agarose gels, there was no obvious shift in splice isoforms between compound treated DM2 fibroblasts and controls involving DMSO and untreated (figure 5.30).

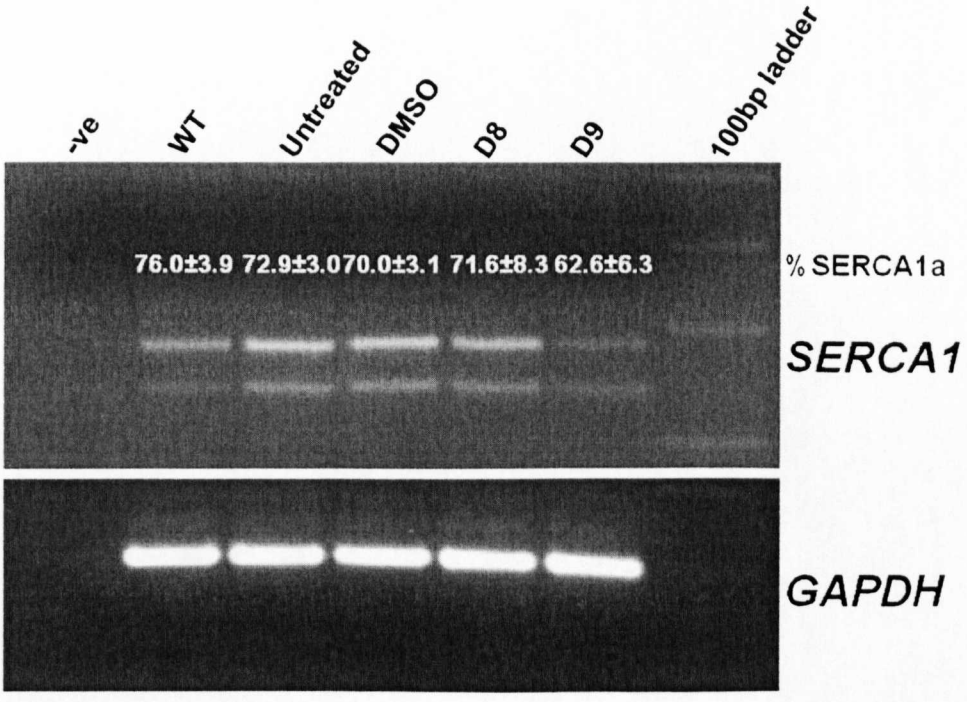

Figure 5.30: D8 treatment does not alter the ratio of *SERCA1* splice isoforms while D9 has the effect of reducing the isoform containing exon22 in DM2 fibroblasts in comparison to controls (DMSO and untreated) on agarose gel

Genescan analysis showed slight differences between compounds treatments (D8 and D9) as well as with controls. Exon22 splice isoform (SERCA1a) quantification analysis gave 62.6±6.3%, 71.6±8.3%, 70.0±3.1%, 72.9±3.0% and 76.0±3.9% for D9 treatments, D8 treatments, DMSO treated, untreated and wild type respectively on Genescan using PCR with 27-28 cycles. Statistical analysis of SERCA1a isoform using t-test showed no significant difference between treatments (D8 and D9) as well as between treatments and controls (DMSO and untreated). However, when treatments and controls were compared to wild type fibroblasts, D9 treatment was observed to be statistically significant (figure 5.31).

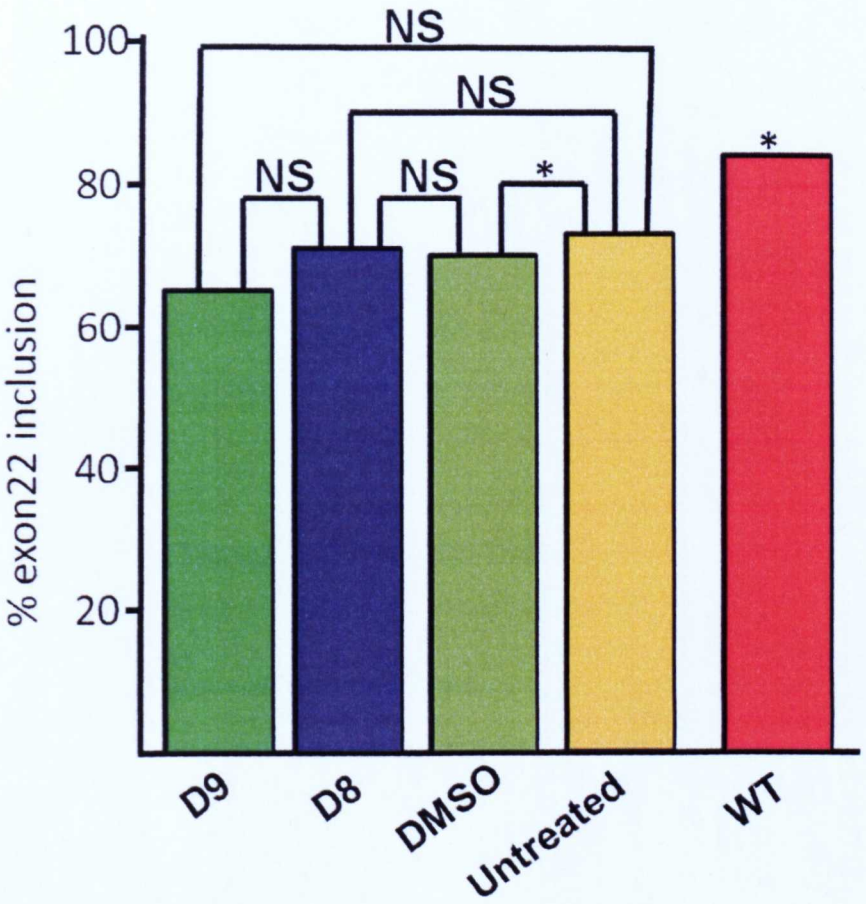

Figure 5.31: Analysis of SERCA1a isoforms showing no significant effect of PKC inhibitor treatments

5.3.3.1 D8 treatment increases *SERCA1* splicing in DM1 myoblasts

The *SERCA1* splicing assay was utilized in triplicate compound-treated differentiating myoblasts and controls. However, following D9 treatment, there was no evidence of any SERCA1a isoform due to degradation by 48 hours of treatment. In contrast to D9 treatment, D8 treatment showed a slight increase in the SERCA1a splice isoform in comparison to controls (figure 5.32).

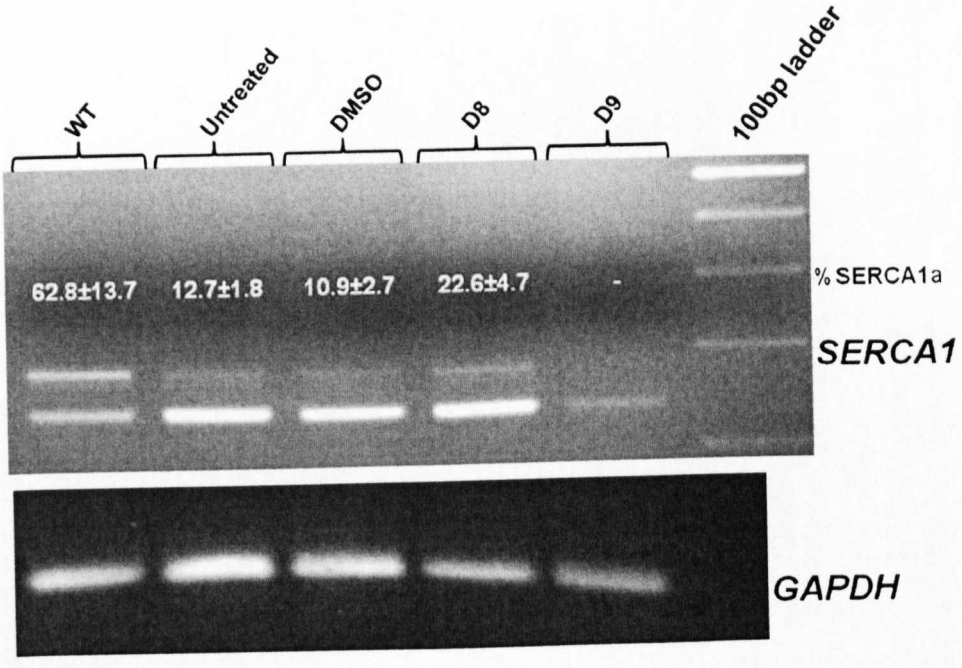

Figure 5.32: D9 treatment shows absence of SERCA1a isoforms while D8 treated DM1 myoblasts shows an increase in SERCA1a isoform when compared with controls on gel normalised using *GAPDH*

Genescan quantification analysis of SERCA1a (exon22) splice isoforms was observed to be 22.6±4.7%, 10.9±2.7%, 12.7±1.8% and 62.8±13.7% for D8, DMSO, untreated and wild type respectively. Statistically, there was a significant difference between D8 and DMSO treatments as well as D8 treatment compared to untreated myoblasts. In addition, there was a significant difference between D8 treatment and wild type ($p=0.01156$) as well as wild type compared to controls- DMSO treated and untreated myoblasts (figure 5.33).

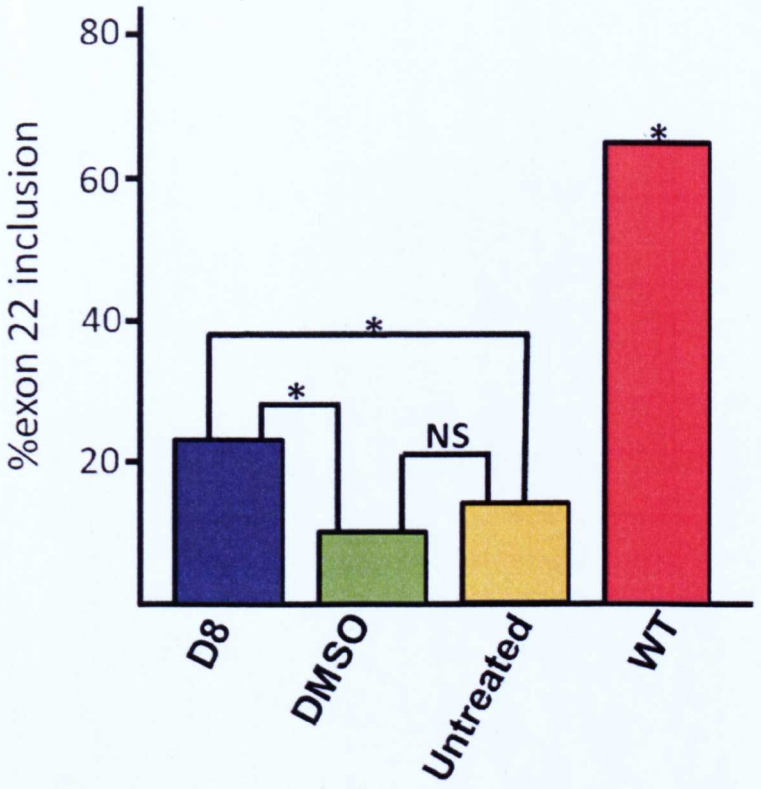

Figure 5.33: Statistical analysis shows that D8 treatment improves *SERCA1* splicing in DM1 myoblasts when compared to controls (DMSO treatment and untreated). The asterisks represent significant level of difference in the analysis.

5.3.4 D8 increases *MBNL1* splicing in DM1 myoblasts but not in DM2 fibroblasts

The analysis of efficacy of PKC inhibitors in reversing the spliceopathy of *MBNL1* splicing in DM was performed on compound treated DM2 fibroblasts and controls in triplicate. Only D9 treatment showed a very slight decrease of *MBNL1* +exon 7 isoform in comparison with D8 treatment and DMSO treatments, as well as untreated control (figure 5.34).

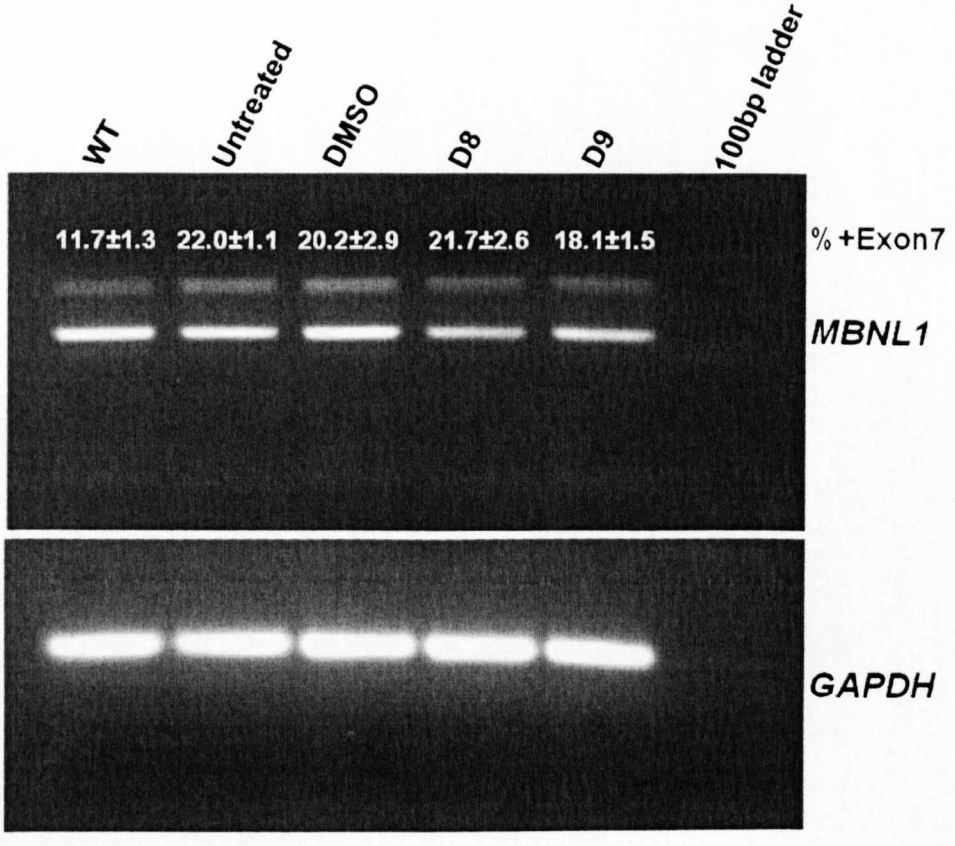

Figure 5.34: *MBNL1* splicing in PKC inhibitor treated DM2 fibroblasts and controls, demonstrating D8 and D9 treatments have no effect on its splicing. Fragments were analysed on 3% agarose gel normalised to *GAPDH*

This was confirmed by Genescan analysis of *MBNL1* splice isoforms, which showed that +exon7 isoform was present at 21.7±2.6%, 18.1±1.5%, 20.2±2.9%, 22.0±1.1% and 11.7±1.3% for D8-treated, D9-treated, DMSO, untreated and wild type respectively. Statistical analysis showed there was no significant difference when treatments (D8 and D9) were compared to controls (DMSO and untreated). However, there was significant difference between D8 and D9 treatments (figure 5.35).

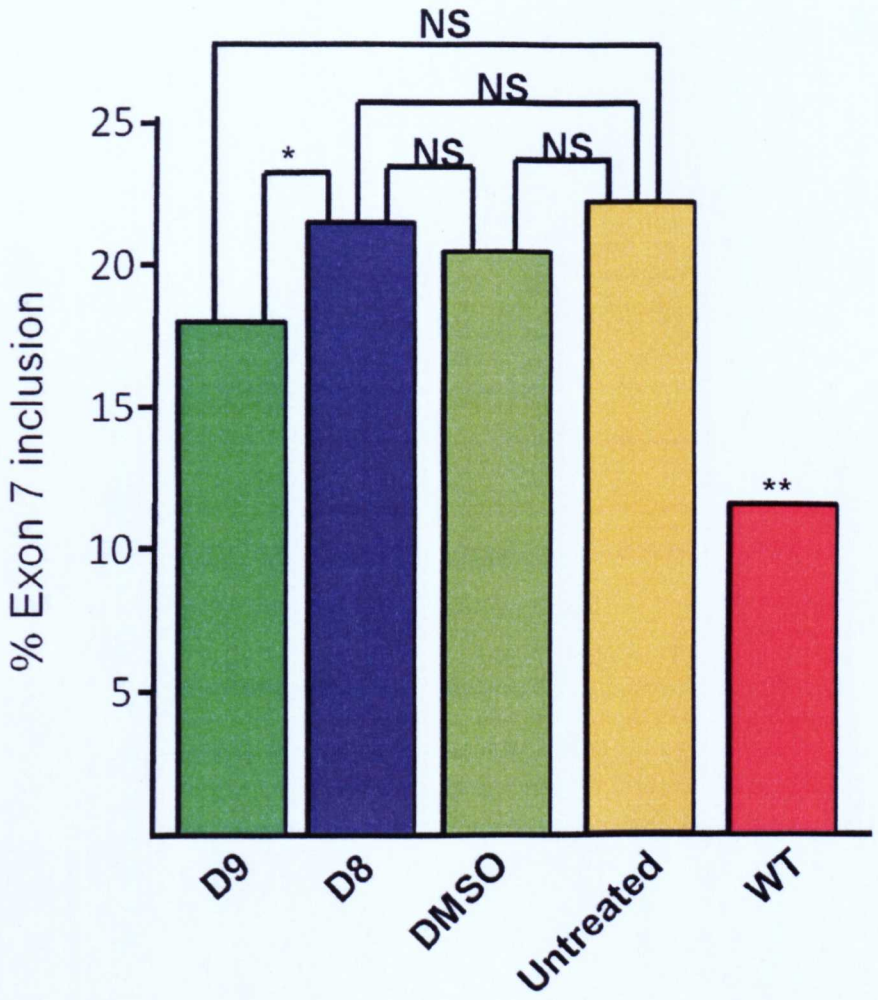

Figure 5.35: PKC inhibitors were ineffective in reversing missplicing of *MBNL1* +exon7 in comparison with controls.

On comparison of treatments and controls with wild type, it was observed that there was significant difference between DMSO treatment and wild type ($p=0.01046$) but the level of significance was higher between wild type and untreated controls ($p=0.00235$). In addition, a very significant difference was observed when wild type was compared to D9 treatments.

In DM1 differentiated myoblasts, triplicate treatments of D8 were observed to reduce the proportion of *MBNL1* exon 7 isoforms in comparison with D9 and DMSO treatments as well as untreated controls (figure 5.36).

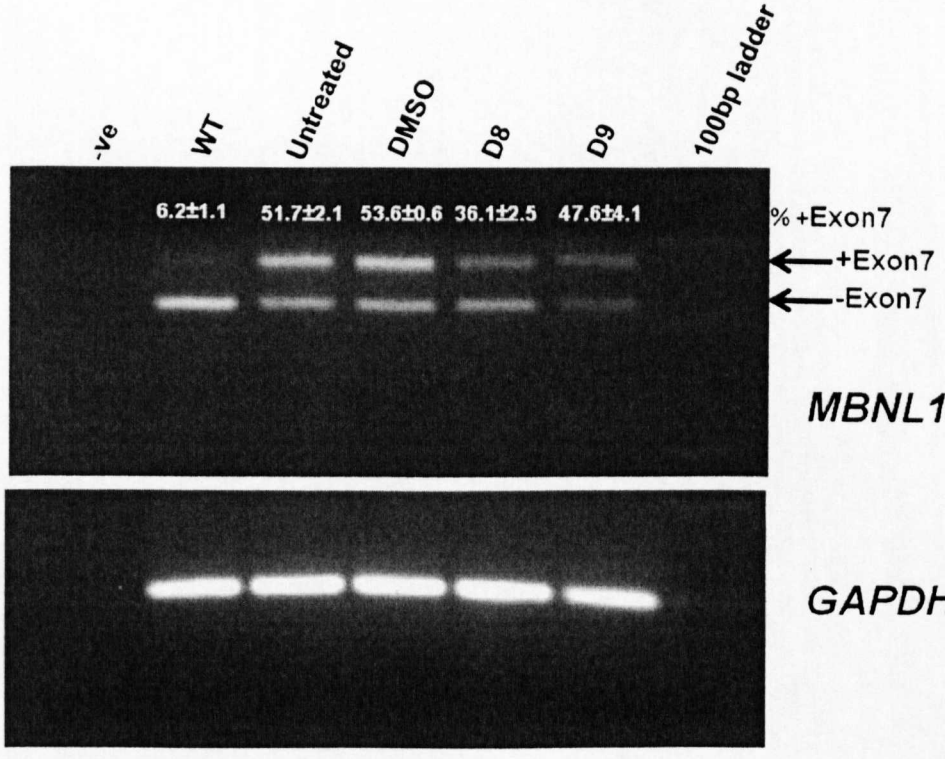

Figure 5.36: PKC inhibitor D8 treatment effects reversion of *MBNL1* exon 7 splicing while D9 treatment has a mild effect in DM1 myoblasts when compared with control.

This was confirmed by Genescan analysis of the *MBNL1* +exon 7 isoform which gave 36.1±2.5%, 47.6±4.1%, 53.6±0.6%, 51.7±2.1% and 6.2±1.1% for D8-treated, D9-treated, DMSO-treated, untreated and wild type respectively. Statistically, a very significant effect was observed between D8 and DMSO treatments as well as between D8 treatment and untreated control (figure 5.37).

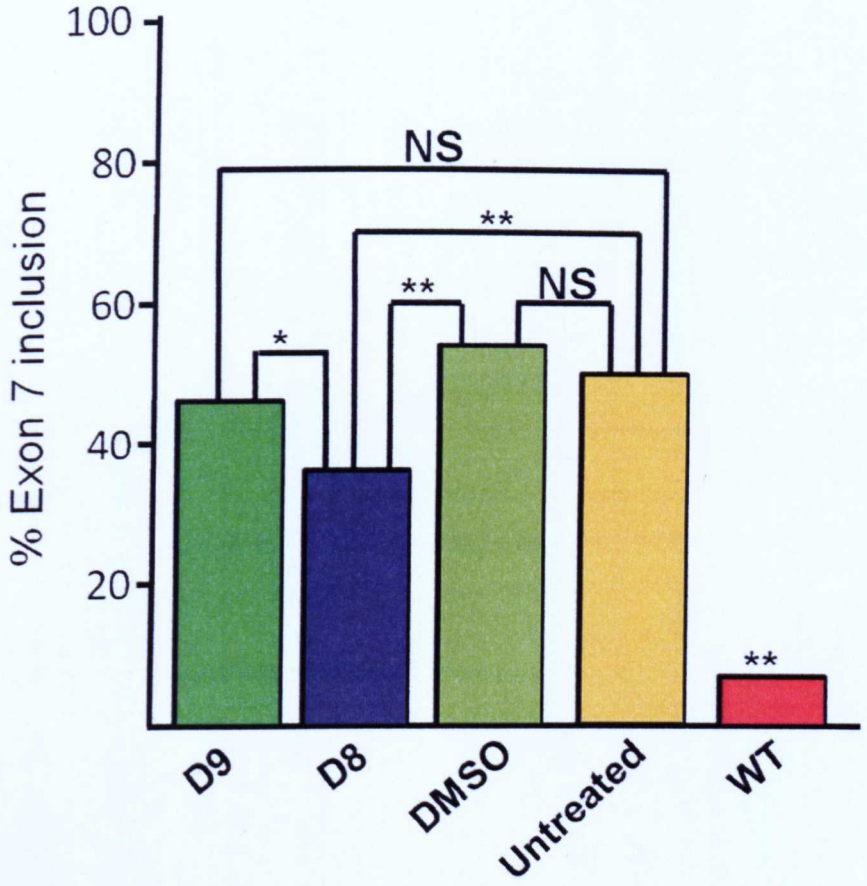

Figure 5.37: D8 treatment produces a very significant effect on *MBNL1* exon7 splicing in DM1 myoblasts in comparison with controls

In addition, there was a significant difference between D8 and D9 treatments as well as between D9 and DMSO treatments. Furthermore, a very significant difference was observed when wild type was compared with DMSO ($p=0.00022$) and untreated ($p=0.00029$). A very significant difference was also observed when treatments (D8 and D9) were compared to the wild type. However, there was no significant difference between D9 treatment and untreated or between DMSO treatments and untreated cells.

5.3.5 PKC inhibitors are ineffective in reversing *MBNL2* exon7 splicing in DM2 fibroblasts while D8 demonstrates marginal rescue in DM1 myoblasts

Next I examined the effect of PKC inhibitor treatments on alternative splicing of *MBNL2* exon7 splicing in both DM2 fibroblast and DM1 myoblasts.

Neither of the PKC inhibitor D8 showed any increase in *MBNL2* exon7 splice isoform in DM2 fibroblasts while D9 increases the proportion of this isoform (figure 5.38).

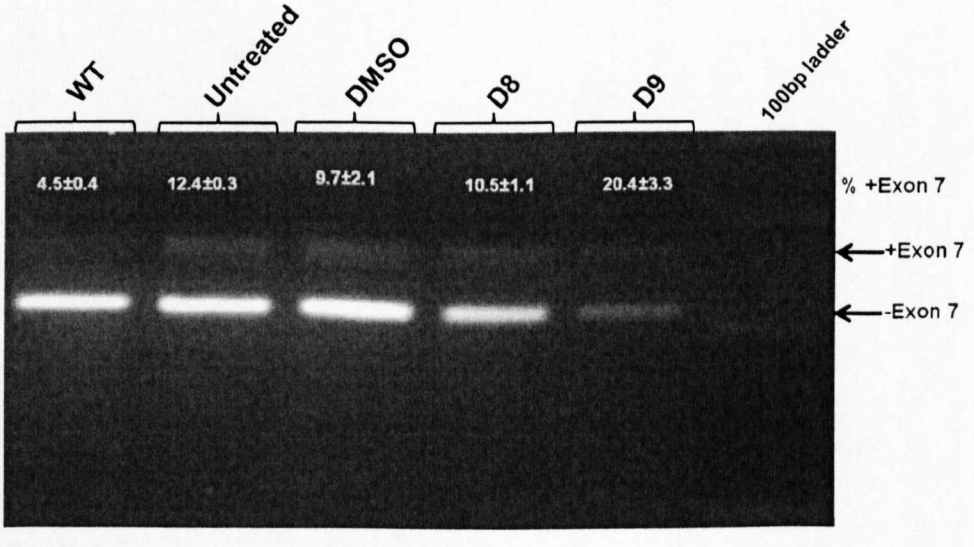

Figure 5.38: *MBNL2* exon7 splice isoform in DM2 fibroblasts is not affected by D8 treatment while D9 treatment seems to increase the proportion of this isoform. The wild type fibroblasts show decreased proportion of exon 7 isoform in comparison with DM2 fibroblasts.

Quantification analysis by Genescan for D9, D8, DMSO treatments as well as untreated showed 20.4±3.3%, 10.5±1.1%, 9.7±2.1% and 12.4±0.3% respectively for the +exon 7 isoform. The wild type cells which provided an additional control had 4.5±0.4% proportion of exon 7 isoform. Statistical analysis showed no significant effect of D8 treatment in comparison with

controls (DMSO and untreated). However, there was significant effect of D9 treatment compared to D8 and DMSO treatments (figure 5.39).

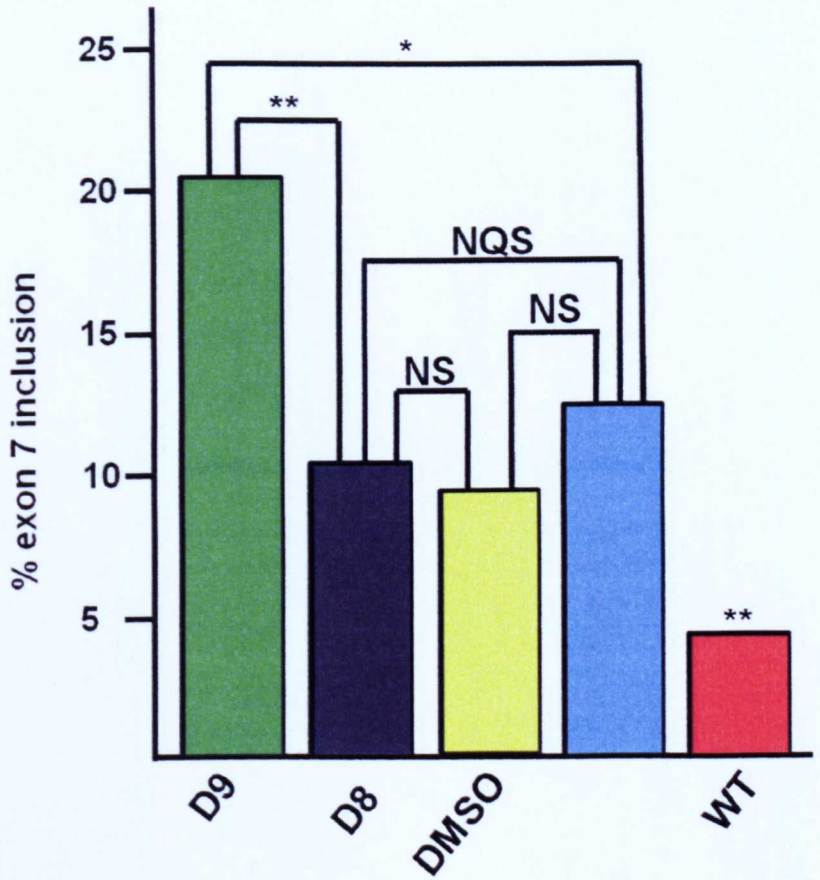

Figure 5.39: D8 treatment shows no significant effect while D9 treatment has a significant effect on *MBNL2* exon7 splicing in DM2 fibroblasts

In DM1 myoblasts, D8 treatment produced decreased proportion of the +exon 7 splice isoform while D9 treatment actually increased the isoform on agarose gel analysis (figure 5.40).

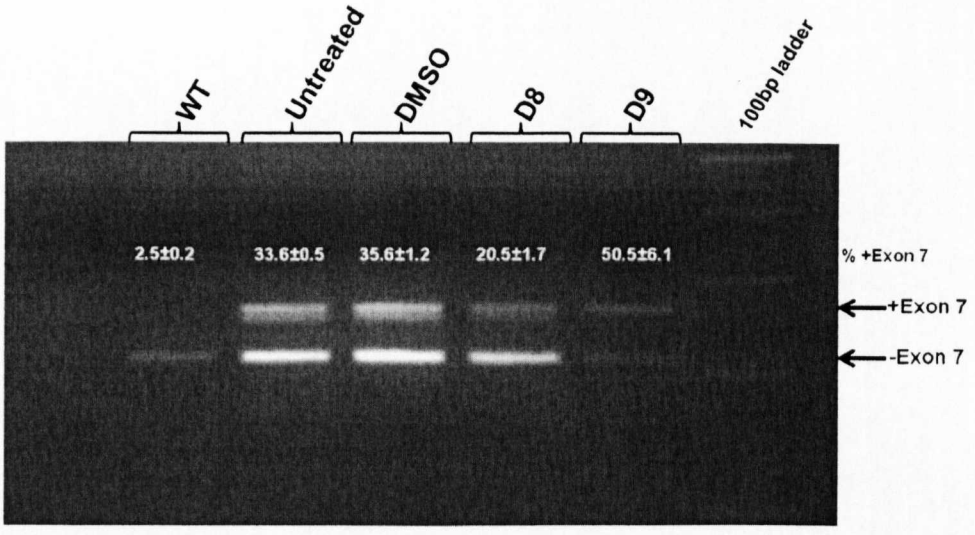

Figure 5.40: D8 treatment produced a decreased +exon 7 isoform of *MBNL2* when compared to controls (DMSO) while D9 treatment increases it in DM1 myoblasts. The wild type cell line which is an additional control lacks this isoform

The quantification of exon 7 splice isoforms by Genescan gave 50.5±6.1%, 20.5±1.7%, 35.6±1.2% and 33.6±0.5% for D9, D8, DMSO treatments and untreated respectively, for the +exon 7 isoforms indicating that D8 treatment has a significant effect in reducing this isoform. The wild type myoblast had 2.5±0.2% +exon 7 isoform proportion.

Statistical analysis demonstrated that D8 treatment had a very significant effect on the +exon 7 isoform splicing in comparison to untreated. D9 treatment had a significant negative effect in contrast to D8 treatment by increasing the proportion of +exon 7 splice isoform (figure 5.41).

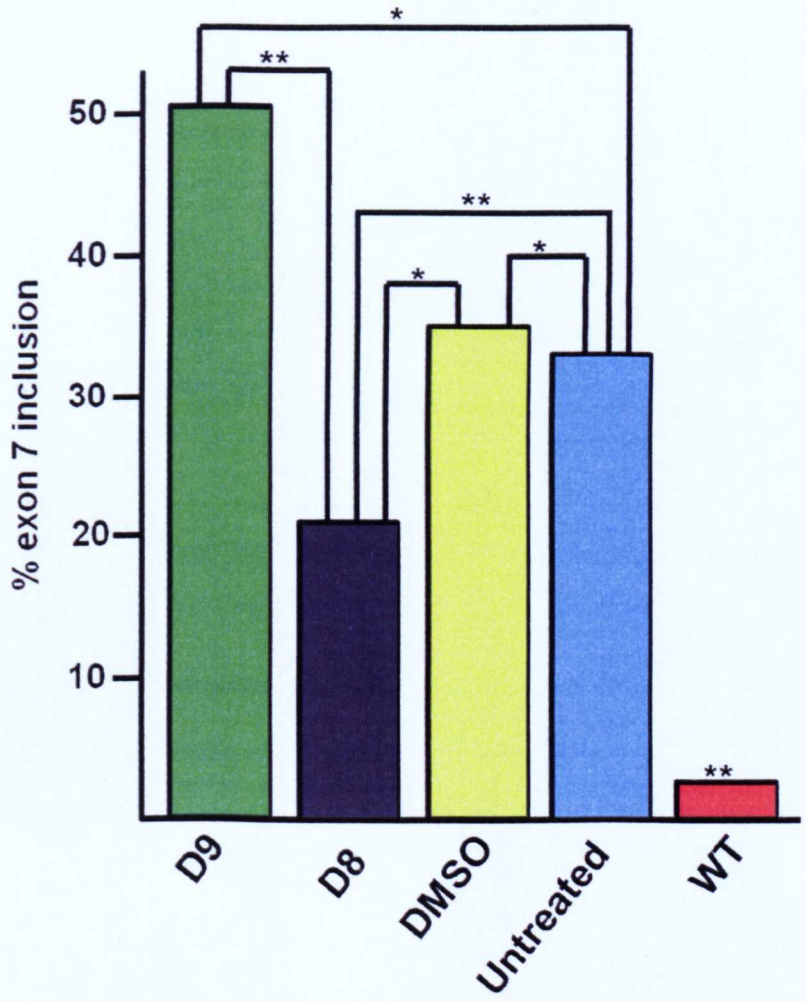

Figure 5.41: D8 showing a significant effect on exon7 splicing in DM1 myoblasts while the difference between wild type myoblast and the various treaments were very significant

5.4 Summary

Secondary assays were developed and applied in confirmation of positive compound hits obtained from primary assays in the previous chapter. The secondary assays used to validate testing of putative compound hits were *BpmI* polymorphism, *IR*, *SERCA1*, *MBNL1* and *MBNL2* splicing. *BpmI* polymorphism assay was utilized in assessing the effect of compounds on mutant *DMPK* containing expanded repeat RNA. Alternative splicing assays

(*IR*, *SERCA1*, *MBNL1* and *MBNL2*) were used to test the downstream effect of compound treatments in DM therapy screen.

From the studies in this chapter, D8 treatments were effective in reversing spliceopathy of *IR*, *SERCA1*, *MBNL1* and *MBNL2* in the DM1 myoblasts but not in DM2 fibroblasts. Furthermore, D9 treatments had no effect on improving spliceopathy of *IR*, *SERCA1*, *MBNL1* and *MBNL2* in both DM1 myoblasts and DM2 fibroblasts.

Finally, neither D8 and D9 treatments nor *MBNL* double knockdown effected the release of mutant transcript from the nucleus into the cytoplasm in DM1 cells. However, D9 treatment and MBNL double knockdown showed a reduction effect on the mutant *DMPK* transcript while D8 treatment showed no reduction on the same transcript.

CHAPTER SIX: DISCUSSION

6.1 Translocation of Nuclear mutant *DMPK* Transcript

The expanded CUG repeat RNA is localised in the nucleus of DM cells where it is proposed to be trapped in the nucleus to form foci due to its inability to be transported to the cytoplasm as is the case with the normal transcript (Hamshere et al, 1997; Davis et al, 1997). To track the location of the mutant *DMPK* transcript on treatment of DM cells with compounds, an assay was developed based on a *BpmI* polymorphism which occurs in the *DMPK* gene and as it is present in the mature mRNA, it permits identification of the location of wild type and expanded CUG repeat RNA in DM cells. Cells were screened for the presence of this polymorphism to assess the effect of compound treatment in the *BpmI* polymorphism assay.

To determine whether compound treatments that clear nuclear foci would liberate mutant *DMPK* transcripts from the nucleus into the cytoplasm, the *BpmI* polymorphism assay was used to examine the effects of treatment on the mutant allele. The data from chapter four demonstrates that both PKC inhibitors D8 and D9 remove nuclear foci. However, the mutant *DMPK* transcript was not released into cytoplasm as shown in chapter five of this report. In siRNA *MBNL1* and *MBNL2* double knockdown, which showed a reduction in nuclear foci, a similar effect was observed with non-release of the mutant transcript into the cytoplasm.

If compound treatment that reduces or clears nuclear foci in DM cells is not able to effect the translocation of the expanded CUG repeat RNA from nucleus to cytoplasm, then what is the possible effect of treatment on the mutant

DMPK that is still trapped in the nucleus? The possible answer to this question lies in the proposition that the compound treatments would either eliminate or inhibit the mutant *DMPK* transcripts in the nucleus from interacting with muscleblind-like proteins to form foci. To determine which of the two possibilities is valid for the treatments used in this study, analysis of the relative proportion of normal and mutant *DMPK* transcripts in the nucleus was performed. In DM1 fibroblasts, D9 treatment reduced the proportion of mutant *DMPK* transcripts while D8 treatment did not show any reduction in the mutant allele. This suggests that D9 either has a destructive effect on mutant *DMPK* or it could affect transcription mutant allele thereby resulting in low production of the same trancript while D8 inhibits expanded repeat RNA interactions with MBNL. Furthermore, when DM1 fibroblasts were differentiated into myoblasts, the proportion of the mutant transcripts in the nucleus was increased and this could account for the presence of more foci in DM1 myoblasts than in DM1 fibroblasts. MYOD induces the repertoire of muscle genes including *DMPK*. This gives more RNA and therefore more foci.

The result obtained from this study deviates from that reported by Wheeler et al (2009) which suggested that expanded CUG repeat RNA was transported to cytoplasm by CAG25 (a morpholino antisense oligonucleotide directed against CUG repeats) treatment resulting in an increase in its translation.

Indeed, the *BpmI* polymorphism assay could be a useful tool for assessing the effect of compound treatment on the mutant *DMPK* allele. Releasing the mutant transcript into the cytoplasm has been suggested to be beneficial in alleviating DM symptoms. It has been demonstrated that a woodchuck post-transcriptional regulatory element (WPRE) causes transport of expanded CUG

repeat RNA from nucleus into cytoplasm thereby alleviating its toxic effect on cell differentiation (Mastroyiannopoulos et al, 2005; Mastroyiannopoulos et al, 2008). This was further validated in a study by Dansithong et al (2008) which demonstrated that the cytoplasmic location of expanded CUG repeat RNA did not cause misregulated splicing and DM features in a mouse model even though it formed foci in the cytoplasm.

Thus any compound that induces the transport of expanded CUG repeat transcripts from the nucleus into cytoplasm would be useful in reversing DM1 symptoms and the *BpmI* polymorphism assay used in this study can facilitate identification of such compounds. It stands to reason that any compound that is capable of facilitating nuclear export of expanded CUG repeat RNA into the cytoplasm would have a disruptive effect on its hairpin formation. This is because in wild type cells *DMPK* transcripts with normal length CUG repeats are relatively short and do not fold to form secondary structures like hairpins. Hence, they are easily transported into the cytoplasm, as opposed to DM cells where long expanded repeats form hairpin structures. Indeed, a study by Garcia-Lopez et al (2011) has shown that D-amino acid hexapeptide (ABP1) reduced foci formation and causes the disruption of CUG hairpin to single-stranded CUG RNA. It would be interesting to test the effect of ABP1 in the *BpmI* polymorphism assay to determine if this compound can liberate expanded CUG RNA into cytoplasm of DM1 cells.

Since the expanded CCUG RNA in DM2 is intronic, application of this assay to test compound mediated export of expanded repeat transcripts would not be feasible.

6.2 Spliceopathy as a Potential Target for DM Therapy

In DM, alternative splicing is altered due to changes in the relative ratios of the splicing factors MBNL and CUG-BP1 (Kalsotra et al, 2009). To assess the use of alternative splicing of transcripts for DM therapy, lines of patient fibroblast cells were tested for their ability to mimic DM splicing patterns for subsequent application for screens. Since defective splicing of some transcripts has been associated with DM phenotypes, five alternative splicing events were utilized in therapeutic screenings in this study.

Four of the five alternative splicing events under consideration in this study were used in secondary screening. The splicing in these screens involves exon exclusion or inclusion. The splicing of *IR* and *SERCA1* involves exclusion of exon 11 and exon 22 respectively in DM while both *MBNL1* and *MBNL2* involve inclusion of exon 7 in DM.

Differentiated DM1 fibroblasts (DM1 myoblasts) and DM2 fibroblasts showed splicing patterns for *IR* similar to those observed in DM samples. However, only DM1 myoblasts demonstrated DM-like splice patterns for *SERCA1*, *MBNL1* and *MBNL2*.

Other defective splicing events that were considered were exon inclusion of *CLCN1* involving exon7a and *ZASP* exon 6a. This work was not included in this study because both *CLCN1* and *ZASP* are sarcomeric proteins which are absent from fibroblasts and derived myoblasts. However, *CLCN1* is present in derived myotubes and muscle biopsies of wild type and patients' cells (Charlet et al, 2002b; Mankodi et al, 2002; O'Leary et al, 2010). The cell lines used in this study have leaky expression of MyoD hence they can only differentiate

into myoblasts and not myotubes because only 90% of the cells were infected with inducible MyoD.

The other spliceopathy in DM used in this study is the intron retention which was utilized in the transgene splicing construct assay with double reporters (GFP and DsRed) for stable transfection in patient cell lines. This was applied to primary screens and optimised in HTS.

Spliceopathy of *CLCN1* and *SERCA1* have been used in screening therapy studies of DM (Mulders et al, 2009; Warf et al, 2009; Wheeler et al, 2009). Therapeutic reversal of spliceopathy in DM has been demonstrated using antisense RNA against CUG repeats (Francois et al, 2011), antisense oligonucleotides (Mulders et al, 2009; Wheeler et al, 2009), MBNL1 overexpression (Dansithong et al, 2005, Kanadia et al, 2006; Hino et al, 2007) and morpholino antisense oligonucleotide (Wheeler et al, 2007). This justifies the use of reversal of spliceopathy in DM as a measure of identifying molecules or drugs that can alleviate DM phenotypes.

In the screening analysis carried out on spliceopathy of DM in this project, only PKC inhibitor D8 treatments showed the potential to alleviate DM features in the cell model for all the five defective splicing events used in this study namely: exon11 of *IR*, exon 22 of *SERCA1*, exon 7 of both *MBNL1* and *MBNL2*, and intron 2 of *CLCN1*. D9 treatment only had a positive effect on correction of splicing in intron 2 of *CLCN1* and to a non-significant extent on *MBNL1*. However, it is very toxic to the cells as it resulted in 85-90% cell killing of DM1 myoblasts with splicing constructs, by 48 hours. As a consequence, D9 does not lend itself for further consideration as it was ineffective in other splicing assays beside *CLCN1*.

Based on the effect of the two PKC inhibitor treatments on alternative splicing assays for DM in this study, it is possible that D8 causes redistribution of MBNL1 as it improved the misregulated splicing of *IR* exon 11, *SERCA1* exon 22, exon 7 of both *MBNL1* and *MBNL2* as well as intron 2 of *CLCN1* in DM1 myoblasts. Western blotting of both nuclear and cytoplasmic protein obtained from PKC inhibitor-treated cells will clarify these possibilities. Furthermore, it is open to speculation that D8 could hinder phosphorylation of exon 7-containing isoforms of both *MBNL1* and *MBNL2* thus preventing its transport to the nucleus since exon 7 is necessary for its nuclear localisation and has affinity for sequestering MBNL1 to expanded CUG repeats (Botta et al, 2008; Cardani et al, 2009; Tran et al, 2011). Separation of MBNL1 and MBNL2 proteins on coomassie gel and their purification for mass spectrometry analysis will confirm this proposal.

However, in DM2 fibroblasts, both PKC inhibitors did not reverse splicing defects. This could be a result of low CUG-BP1 levels in DM2 in contrast to very high levels found in DM1 myoblast cultures (Savkur et al, 2001; Lin et al, 2006) hence PKC inhibition would be ineffective in DM2 as the spliceopathy could be accounted for primarily by MBNL1 sequestration alone and is not a contributory effect of *MBNL1* and CUG-BP1 as seen in DM1 (Kalsotra et al, 2009).

Finally, the expression levels of alternatively spliced transcripts were not the same across treatments as only D9 had a degradative effect on *IR* and *SERCA1* transcripts and to a lesser extent on *MBNL1* and *MBNL2* transcripts.

6.3 Cell-based model systems for HTS Drug Screens in DM

In this study, two model assays have been developed and successfully applied on a large scale in HTS. The first assay that was developed and optimised in HTS was the nuclear foci assay. The nuclear foci assay is a good workable model on the plate reader and shows compatibility in HTS as it is currently being used in 96-well plate and also in 384-well plates.

The second model assay system developed in this project is the splicing construct assay with double reporters for intron splicing. The *CLCN1* splicing construct assay used for compound screens in this study has the advantage over those of O'Leary et al (2010) because it is a double reporter system allowing quantification of the splicing efficiency of transgene construct in both DM1 fibroblast and DM1 myoblast. The quantification of splicing is absent from the luciferase *CLCN1* construct of O'Leary et al (2010) because it assesses the efficacy of compound by measuring its effect on intensity of the luciferase expression which is at the 3' end of the transgene construct. Their assay is limited by being qualitative in nature therefore the degree of efficacy of compound or drug can be estimated in the system reported here. Furthermore, the bichromatic fluorescent reporter system developed in this study differs from those used by Orengo et al (2006) by having both reporters in the same open reading frame as opposed to having the reporters in alternate reading frames used in their study. The splicing construct assay model system has been optimised for miniaturisation in HTS and the ratios of DsRed/GFP fluorescence intensity serve as a measure of the efficacy of compound treatment on *CLCN1* intron2 spliceopathy in this system.

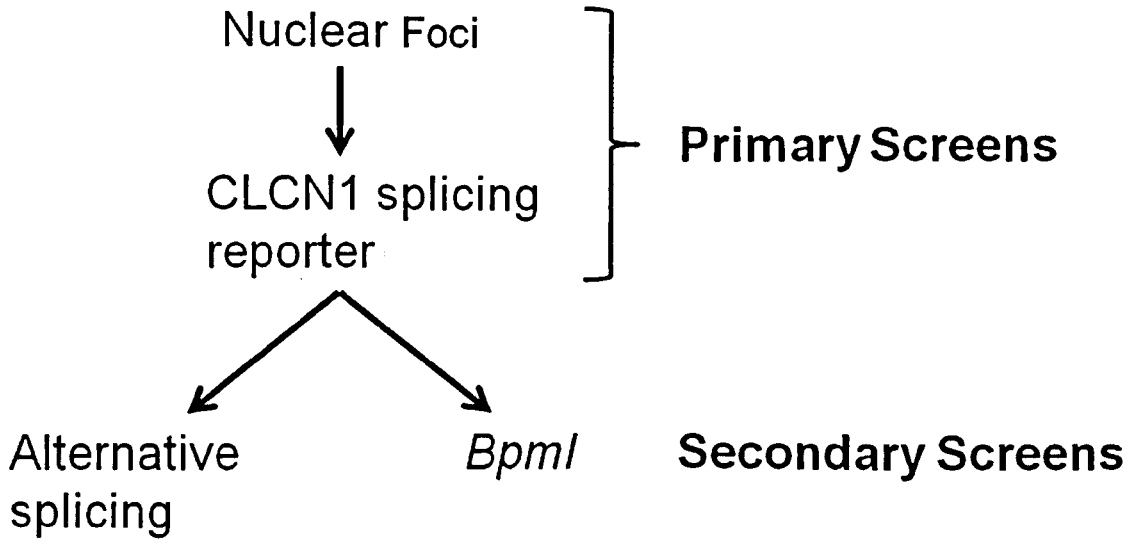

Figure 6.1: Model for compound screenings used in this study

6.4 Limitations of Study

The main technical limitation of this study was that the quantification of the isoforms for both the alternatively spliced transcripts and BpmI polymorphism was not linearly determined by qPCR but was performed by optimisation on Genescan. Furthermore, the expression levels of the various alternatively spliced transcripts from across different treatments were not equal. D9 treatments of DM1 myoblasts which in addition to showing degradative effect on transcript did show reduction in RNA pool in some treatments (figure 5.28) when normalised to *GAPDH.* It may have been due to side effects of the compound on RNA pool in the cell.

There was also a reduction in RNA from D8 treatment for the *DMPK* allele (figure 5.21) which was not observed in other independent replicates involving the same treatment.

6.5 Recommendations

Since MBNL1 and MBNL2 knockdown did not alter the *CLCN1* splicing in wild type clones to DM patterns, it would be necessary to subject the wild type clone to either combined MBNL1 & 2 knockdown with overexpression of CUG-BP1 or overexpression of CTG expanded repeat. The results obtained from chapter four of this report in wild type clone seem to indicate that DM molecular features are not due to MBNL sequestration alone. This therefore makes a case for combining both downregulation of MBNL with CUG-BP1 overexpression or CTG expanded repeat overexpression in the wild type clone to test its effect on altering *CLCN1* splicing. This is because it has been shown that overexpression of CUG-BP1, or overexpression of expanded CTG repeats or MBNL knockdown in wild type cells changes its splicing features to that of DM cells.

In order to determine if the PKC inhibitors D8 and D9 would be effective in correcting *CLCN1* missplicing in DM2, it would be necessary to apply the PKC inhibitor treatments to DM2 clones containing *CLCN1* splicing construct to determine if the treatment can also reverse intron 2 *CLCN1* spliceopathy. This would confirm whether PKC inhibitors which cleared nuclear foci from DM2 (figure 4.9) can reverse downstream consequences of ribinuclear foci formation.

6.6 Conclusion

The assays developed in this project have been utilized in compound screens and have been demonstrated to be relevant in identifying potential therapeutic hits that could alleviate DM features.

Based on the efficiency and ease of usage in primary screens in HTS, both nuclear foci assay and *CLCN1* double reporters are compatible good model assays. Both assay models have been demonstrated to be efficient and are directly applicable for high throughput analysis of compound libraries that reduces or removes completely nuclear foci and rescues misregulated splicing- both hallmarks of DM pathology.

Furthermore, other assays such as the *BpmI* polymorphism assay permit identification of molecules that can either inhibit, eliminate or remove expanded CUG repeat transcript from the nucleus.

The alternative splicing assays of transcripts developed and used in this study- *IR*, *SERCA1*, *MBNL1* and *MBNL2* are applicable to identifying therapeutic hits for DM with *SERCA1* and *MBNL1* which showed clearer effects with PKC inhibitor D8 treatment than others in many replicates.

Finally, the hit compounds identified by the assays from this project were PKC inhibitors D8 and D9. Both PKC inhibitors were effective in clearing nuclear foci from DM1 and DM2 fibroblasts but only D8 showed a therapeutic beneficial effect on the downstream consequences of expanded repeat RNA, i.e improving spliceopathy in all the alternative splicing assays tested in this project. The effectiveness of D8 treatment in reversing or improving splicing in DM1 myoblasts could be as a result of absence of CUG-BP1 mediated spliceopathy in DM2 since PKC inhibitors blocks CUG-BP1 activity.

Furthermore, even though both D8 and D9 clear nuclear foci from DM cells, D8 showed inhibition of mutant *DMPK* transcript in DM1 fibroblasts while D9 has a degradative effect on mutant *DMPK* transcript, is toxic and has some off-target effects namely- reduction of RNA in some treatments, degrades *IR* and *SERCA1* alternatively spliced transcripts and tends to increase the relative proportions of *MBNL2* isoforms associated with DM.

D8 could be used as positive control hit for comparison with other therapeutic hits in future drug screens for efficacy in DM therapy. Futhermore, D8 treatment could be applied to *in vivo* (mouse) models of DM to assess its efficacy in reversing DM symptoms in animal models.

REFERENCES

ALWAZZAN, M., HAMSHERE, M. G., LENNON, G. G. & BROOK, J. D. (1998) Six transcripts map within 200 kilobases of the myotonic dystrophy expanded repeat. *Mamm Genome,* 9, 485-7.

ALWAZZAN, M., NEWMAN, E., HAMSHERE, M. G. & BROOK, J. D. (1999) Myotonic dystrophy is associated with a reduced level of RNA from the DMWD allele adjacent to the expanded repeat. *Hum Mol Genet,* 8, 1491-7.

AMACK, J. D. & MAHADEVAN, M. S. (2001) The myotonic dystrophy expanded CUG repeat tract is necessary but not sufficient to disrupt C2C12 myoblast differentiation. *Hum Mol Genet,* 10, 1879-87.

AMACK, J. D., PAGUIO, A. P. & MAHADEVAN, M. S. (1999) Cis and trans effects of the myotonic dystrophy (DM) mutation in a cell culture model. *Hum Mol Genet,* 8, 1975-84.

ANDREADIS, A., BROWN, W. M. & KOSIK, K. S. (1992) Structure and novel exons of the human tau gene. *Biochemistry,* 31, 10626-33.

ARAMBULA, J. F., RAMISETTY, S. R., BARANGER, A. M. & ZIMMERMAN, S. C. (2009) A simple ligand that selectively targets CUG trinucleotide repeats and inhibits MBNL protein binding. *Proc Natl Acad Sci U S A,* 106, 16068-73.

ARIKAN, M. C., MEMMOTT, J., BRODERICK, J. A., LAFYATIS, R., SCREATON, G., STAMM, S. & ANDREADIS, A. (2002) Modulation of the membrane-binding projection domain of tau protein: splicing regulation of exon 3. *Brain Res Mol Brain Res,* 101, 109-21.

AROMATARIS, E. C. & RYCHKOV, G. Y. (2006) ClC-1 chloride channel: Matching its properties to a role in skeletal muscle. *Clin Exp Pharmacol Physiol,* 33, 1118-23.

ARTERO, R., PROKOP, A., PARICIO, N., BEGEMANN, G., PUEYO, I., MLODZIK, M., PEREZ-ALONSO, M. & BAYLIES, M. K. (1998) The muscleblind gene participates in the organization of Z-bands and epidermal attachments of Drosophila muscles and is regulated by Dmef2. *Dev Biol,* 195, 131-43.

BEGEMANN, G., PARICIO, N., ARTERO, R., KISS, I., PEREZ-ALONSO, M. & MLODZIK, M. (1997) muscleblind, a gene required for photoreceptor differentiation in Drosophila, encodes novel nuclear Cys3His-type zinc-finger-containing proteins. *Development,* 124, 4321-31.

BENDERS, A. A., GROENEN, P. J., OERLEMANS, F. T., VEERKAMP, J. H. & WIERINGA, B. (1997) Myotonic dystrophy protein kinase is involved in the modulation of the Ca2+ homeostasis in skeletal muscle cells. *J Clin Invest,* 100, 1440-7.

BERUL, C. I., MAGUIRE, C. T., ARONOVITZ, M. J., GREENWOOD, J., MILLER, C., GEHRMANN, J., HOUSMAN, D., MENDELSOHN, M. E. & REDDY, S. (1999) DMPK dosage alterations result in atrioventricular conduction abnormalities in a mouse myotonic dystrophy model. *J Clin Invest,* 103, R1-7.

BERUL, C. I., MAGUIRE, C. T., GEHRMANN, J. & REDDY, S. (2000) Progressive atrioventricular conduction block in a mouse myotonic dystrophy model. *J Interv Card Electrophysiol,* 4, 351-8.

BLANCHETTE, M. & CHABOT, B. (1997) A highly stable duplex structure sequesters the 5' splice site region of hnRNP A1 alternative exon 7B. *RNA,* 3, 405-19.

BOTTA, A., RINALDI, F., CATALLI, C., VERGANI, L., BONIFAZI, E., ROMEO, V., LORO, E., VIOLA, A., ANGELINI, C. & NOVELLI, G. (2008) The CTG repeat expansion size correlates with the splicing defects observed in muscles from myotonic dystrophy type 1 patients. *J Med Genet,* 45, 639-46.

BOUCHER, C. A., KING, S. K., CAREY, N., KRAHE, R., WINCHESTER, C. L., RAHMAN, S., CREAVIN, T., MEGHJI, P., BAILEY, M. E., CHARTIER, F. L. & ET AL. (1995) A novel homeodomain-encoding gene is associated with a large CpG island interrupted by the myotonic dystrophy unstable (CTG)n repeat. *Hum Mol Genet,* 4, 1919-25.

BROOK, J. D., MCCURRACH, M. E., HARLEY, H. G., BUCKLER, A. J., CHURCH, D., ABURATANI, H., HUNTER, K., STANTON, V. P., THIRION, J. P., HUDSON, T. & ET AL. (1992) Molecular basis of myotonic dystrophy: expansion of a trinucleotide (CTG) repeat at the 3' end of a transcript encoding a protein kinase family member. *Cell,* 68, 799-808.

BUEE, L., BUSSIERE, T., BUEE-SCHERRER, V., DELACOURTE, A. & HOF, P. R. (2000) Tau protein isoforms, phosphorylation and role in neurodegenerative disorders. *Brain Res Brain Res Rev,* 33, 95-130.

BUJ-BELLO, A., FURLING, D., TRONCHERE, H., LAPORTE, J., LEROUGE, T., BUTLER-BROWNE, G. S. & MANDEL, J. L. (2002) Muscle-specific alternative splicing of myotubularin-related 1 gene is impaired in DM1 muscle cells. *Hum Mol Genet,* 11, 2297-307.

BURK, S. E., LYTTON, J., MACLENNAN, D. H. & SHULL, G. E. (1989) cDNA cloning, functional expression, and mRNA tissue distribution of a third organellar Ca2+ pump. *J Biol Chem,* 264, 18561-8.

BUVOLI, M., COBIANCHI, F. & RIVA, S. (1992) Interaction of hnRNP A1 with snRNPs and pre-mRNAs: evidence for a possible role of A1 RNA annealing activity in the first steps of spliceosome assembly. *Nucleic Acids Res,* 20, 5017-25.

CARDANI, R., BALDASSA, S., BOTTA, A., RINALDI, F., NOVELLI, G., MANCINELLI, E. & MEOLA, G. (2009) Ribonuclear inclusions and MBNL1 nuclear sequestration do not affect myoblast differentiation but alter gene splicing in myotonic dystrophy type 2. *Neuromuscul Disord,* 19, 335-43.

CHALFANT, C. E., RATHMAN, K., PINKERMAN, R. L., WOOD, R. E., OBEID, L. M., OGRETMEN, B. & HANNUN, Y. A. (2002) De novo ceramide regulates the alternative splicing of caspase 9 and Bcl-x in A549 lung adenocarcinoma cells. Dependence on protein phosphatase-1. *J Biol Chem,* 277, 12587-95.

CHARLET, B. N., LOGAN, P., SINGH, G. & COOPER, T. A. (2002a) Dynamic antagonism between ETR-3 and PTB regulates cell type-specific alternative splicing. *Mol Cell,* 9, 649-58.

CHARLET, B. N., SAVKUR, R. S., SINGH, G., PHILIPS, A. V., GRICE, E. A. & COOPER, T. A. (2002b) Loss of the muscle-specific chloride channel in type 1 myotonic dystrophy due to misregulated alternative splicing. *Mol Cell,* 10, 45-53.

CHEN, C. D., KOBAYASHI, R. & HELFMAN, D. M. (1999) Binding of hnRNP H to an exonic splicing silencer is involved in the regulation of alternative splicing of the rat beta-tropomyosin gene. *Genes Dev,* 13, 593-606.

CHOU, M. Y., ROOKE, N., TURCK, C. W. & BLACK, D. L. (1999) hnRNP H is a component of a splicing enhancer complex that activates a c-src alternative exon in neuronal cells. *Mol Cell Biol,* 19, 69-77.

D'SOUZA, I. & SCHELLENBERG, G. D. (2000) Determinants of 4-repeat tau expression. Coordination between enhancing and inhibitory splicing sequences for exon 10 inclusion. *J Biol Chem,* 275, 17700-9.

D'SOUZA, I. & SCHELLENBERG, G. D. (2002) tau Exon 10 expression involves a bipartite intron 10 regulatory sequence and weak 5' and 3' splice sites. *J Biol Chem,* 277, 26587-99.

DANSITHONG, W., PAUL, S., COMAI, L. & REDDY, S. (2005) MBNL1 is the primary determinant of focus formation and aberrant insulin receptor splicing in DM1. *J Biol Chem,* 280, 5773-80.

DANSITHONG, W., WOLF, C. M., SARKAR, P., PAUL, S., CHIANG, A., HOLT, I., MORRIS, G. E., BRANCO, D., SHERWOOD, M. C., COMAI, L., BERUL, C. I. & REDDY, S. (2008) Cytoplasmic CUG RNA foci are insufficient to elicit key DM1 features. *PLoS One,* 3, e3968.

DAVIS, B. M., MCCURRACH, M. E., TANEJA, K. L., SINGER, R. H. & HOUSMAN, D. E. (1997) Expansion of a CUG trinucleotide repeat in the 3' untranslated region of myotonic dystrophy protein kinase transcripts results in nuclear retention of transcripts. *Proc Natl Acad Sci U S A,* 94, 7388-93.

DAY, J. W. & RANUM, L. P. (2005) RNA pathogenesis of the myotonic dystrophies. *Neuromuscul Disord,* 15, 5-16.

DISNEY, M. D., LEE, M. M., PUSHECHNIKOV, A. & CHILDS-DISNEY, J. L. The role of flexibility in the rational design of modularly assembled ligands targeting the RNAs that cause the myotonic dystrophies. *Chembiochem,* 11, 375-82.

FARDAEI, M., LARKIN, K., BROOK, J. D. & HAMSHERE, M. G. (2001) In vivo co-localisation of MBNL protein with DMPK expanded-repeat transcripts. *Nucleic Acids Res,* 29, 2766-71.

FARDAEI, M., ROGERS, M. T., THORPE, H. M., LARKIN, K., HAMSHERE, M. G., HARPER, P. S. & BROOK, J. D. (2002) Three proteins, MBNL, MBLL and MBXL, co-localize in vivo with nuclear foci of expanded-repeat transcripts in DM1 and DM2 cells. *Hum Mol Genet,* 11, 805-14.

FAUSTINO, N. A. & COOPER, T. A. (2003) Pre-mRNA splicing and human disease. *Genes Dev,* 17, 419-37.

FRANCOIS, V., KLEIN, A. F., BELEY, C., JOLLET, A., LEMERCIER, C., GARCIA, L. & FURLING, D. Selective silencing of mutated mRNAs in DM1 by using modified hU7-snRNAs. *Nat Struct Mol Biol,* 18, 85-7.

FRISCH, R., SINGLETON, K. R., MOSES, P. A., GONZALEZ, I. L., CARANGO, P., MARKS, H. G. & FUNANAGE, V. L. (2001) Effect of triplet repeat expansion on chromatin structure and expression of DMPK and neighboring genes, SIX5 and DMWD, in myotonic dystrophy. *Mol Genet Metab,* 74, 281-91.

FU, Y. H., FRIEDMAN, D. L., RICHARDS, S., PEARLMAN, J. A., GIBBS, R. A., PIZZUTI, A., ASHIZAWA, T., PERRYMAN, M. B., SCARLATO, G., FENWICK, R. G., JR. & ET AL. (1993) Decreased expression of myotonin-protein kinase messenger RNA and protein in adult form of myotonic dystrophy. *Science,* 260, 235-8.

FU, Y. H., PIZZUTI, A., FENWICK, R. G., JR., KING, J., RAJNARAYAN, S., DUNNE, P. W., DUBEL, J., NASSER, G. A., ASHIZAWA, T., DE JONG, P. & ET AL. (1992) An unstable triplet repeat in a gene related to myotonic muscular dystrophy. *Science,* 255, 1256-8.

FURLING, D., DOUCET, G., LANGLOIS, M. A., TIMCHENKO, L., BELANGER, E., COSSETTE, L. & PUYMIRAT, J. (2003) Viral vector producing antisense RNA restores myotonic dystrophy myoblast functions. *Gene Ther,* 10, 795-802.

FURLING, D., LEMIEUX, D., TANEJA, K. & PUYMIRAT, J. (2001) Decreased levels of myotonic dystrophy protein kinase (DMPK) and delayed differentiation in human myotonic dystrophy myoblasts. *Neuromuscul Disord,* 11, 728-35.

FUTATSUGI, A., KUWAJIMA, G. & MIKOSHIBA, K. (1995) Tissue-specific and developmentally regulated alternative splicing in mouse skeletal muscle ryanodine receptor mRNA. *Biochem J,* 305 (Pt 2), 373-8.

GABUT, M., CHAUDHRY, S. & BLENCOWE, B. J. (2008) SnapShot: The splicing regulatory machinery. *Cell,* 133, 192 e1.

GARCIA-LOPEZ, A., LLAMUSI, B., ORZAEZ, M., PEREZ-PAYA, E. & ARTERO, R. D. In vivo discovery of a peptide that prevents CUG-RNA hairpin formation and reverses RNA toxicity in myotonic dystrophy models. *Proc Natl Acad Sci U S A,* 108, 11866-71.

GAREISS, P. C., SOBCZAK, K., MCNAUGHTON, B. R., PALDE, P. B., THORNTON, C. A. & MILLER, B. L. (2008) Dynamic combinatorial selection of molecules capable of inhibiting the (CUG) repeat RNA-MBNL1 interaction in vitro: discovery of lead compounds targeting myotonic dystrophy (DM1). *J Am Chem Soc,* 130, 16254-61.

GOOD, P. J., CHEN, Q., WARNER, S. J. & HERRING, D. C. (2000) A family of human RNA-binding proteins related to the Drosophila Bruno translational regulator. *J Biol Chem,* 275, 28583-92.

HAMSHERE, M. G., NEWMAN, E. E., ALWAZZAN, M., ATHWAL, B. S. & BROOK, J. D. (1997) Transcriptional abnormality in myotonic dystrophy affects DMPK but not neighboring genes. *Proc Natl Acad Sci U S A,* 94, 7394-9.

HARLEY, H. G., BROOK, J. D., RUNDLE, S. A., CROW, S., REARDON, W., BUCKLER, A. J., HARPER, P. S., HOUSMAN, D. E. & SHAW, D. J. (1992) Expansion of an unstable DNA region and phenotypic variation in myotonic dystrophy. *Nature,* 355, 545-6.

HARPER, P. S. (2001) Myotonic Dystrophy 3rd edition. W. B. Saunders. London.

HINO, S., KONDO, S., SEKIYA, H., SAITO, A., KANEMOTO, S., MURAKAMI, T., CHIHARA, K., AOKI, Y., NAKAMORI, M., TAKAHASHI, M. P. & IMAIZUMI, K. (2007) Molecular mechanisms responsible for aberrant splicing of SERCA1 in myotonic dystrophy type 1. *Hum Mol Genet,* 16, 2834-43.

HO, T. H., BUNDMAN, D., ARMSTRONG, D. L. & COOPER, T. A. (2005a) Transgenic mice expressing CUG-BP1 reproduce splicing mis-regulation observed in myotonic dystrophy. *Hum Mol Genet,* 14, 1539-47.

HO, T. H., CHARLET, B. N., POULOS, M. G., SINGH, G., SWANSON, M. S. & COOPER, T. A. (2004) Muscleblind proteins regulate alternative splicing. *EMBO J,* 23, 3103-12.

HO, T. H., SAVKUR, R. S., POULOS, M. G., MANCINI, M. A., SWANSON, M. S. & COOPER, T. A. (2005b) Colocalization of muscleblind with RNA foci is separable from mis-regulation of alternative splicing in myotonic dystrophy. *J Cell Sci,* 118, 2923-33.

HOLT, I., JACQUEMIN, V., FARDAEI, M., SEWRY, C. A., BUTLER-BROWNE, G. S., FURLING, D., BROOK, J. D. & MORRIS, G. E. (2009) Muscleblind-like proteins: similarities and differences in normal and myotonic dystrophy muscle. *Am J Pathol,* 174, 216-27.

HUNTER, A., TSILFIDIS, C., METTLER, G., JACOB, P., MAHADEVAN, M., SURH, L. & KORNELUK, R. (1992) The correlation of age of onset with CTG trinucleotide repeat amplification in myotonic dystrophy. *J Med Genet,* 29, 774-9.

JANSEN, G., GROENEN, P. J., BACHNER, D., JAP, P. H., COERWINKEL, M., OERLEMANS, F., VAN DEN BROEK, W., GOHLSCH, B., PETTE, D., PLOMP, J. J., MOLENAAR, P. C., NEDERHOFF, M. G., VAN ECHTELD, C. J., DEKKER, M., BERNS, A., HAMEISTER, H. & WIERINGA, B. (1996) Abnormal myotonic dystrophy protein kinase levels produce only mild myopathy in mice. *Nat Genet,* 13, 316-24.

JANSEN, G., WILLEMS, P., COERWINKEL, M., NILLESEN, W., SMEETS, H., VITS, L., HOWELER, C., BRUNNER, H. & WIERINGA, B. (1994) Gonosomal mosaicism in myotonic dystrophy patients: involvement of mitotic events in (CTG)n repeat variation and selection against extreme expansion in sperm. *Am J Hum Genet,* 54, 575-85.

KALSOTRA, A., XIAO, X., WARD, A. J., CASTLE, J. C., JOHNSON, J. M., BURGE, C. B. & COOPER, T. A. (2008) A postnatal switch of CELF and MBNL proteins reprograms alternative splicing in the developing heart. *Proc Natl Acad Sci U S A,* 105, 20333-8.

KANADIA, R. N., JOHNSTONE, K. A., MANKODI, A., LUNGU, C., THORNTON, C. A., ESSON, D., TIMMERS, A. M., HAUSWIRTH, W. W. & SWANSON, M. S. (2003) A muscleblind knockout model for myotonic dystrophy. *Science,* 302, 1978-80.

KANADIA, R. N., SHIN, J., YUAN, Y., BEATTIE, S. G., WHEELER, T. M., THORNTON, C. A. & SWANSON, M. S. (2006) Reversal of RNA missplicing and myotonia after muscleblind overexpression in a mouse poly(CUG) model for myotonic dystrophy. *Proc Natl Acad Sci U S A,* 103, 11748-53.

KELLERER, M., LAMMERS, R., ERMEL, B., TIPPMER, S., VOGT, B., OBERMAIER-KUSSER, B., ULLRICH, A. & HARING, H. U. (1992) Distinct alpha-subunit structures of human insulin receptor A and B variants determine differences in tyrosine kinase activities. *Biochemistry,* 31, 4588-96.

KIM, D. H., LANGLOIS, M. A., LEE, K. B., RIGGS, A. D., PUYMIRAT, J. & ROSSI, J. J. (2005) HnRNP H inhibits nuclear export of mRNA

containing expanded CUG repeats and a distal branch point sequence. *Nucleic Acids Res,* 33, 3866-74.

KIMURA, T., NAKAMORI, M., LUECK, J. D., POULIQUIN, P., AOIKE, F., FUJIMURA, H., DIRKSEN, R. T., TAKAHASHI, M. P., DULHUNTY, A. F. & SAKODA, S. (2005) Altered mRNA splicing of the skeletal muscle ryanodine receptor and sarcoplasmic/endoplasmic reticulum Ca2+-ATPase in myotonic dystrophy type 1. *Hum Mol Genet,* 14, 2189-200.

KINO, Y., MORI, D., OMA, Y., TAKESHITA, Y., SASAGAWA, N. & ISHIURA, S. (2004) Muscleblind protein, MBNL1/EXP, binds specifically to CHHG repeats. *Hum Mol Genet,* 13, 495-507.

KLESERT, T. R., CHO, D. H., CLARK, J. I., MAYLIE, J., ADELMAN, J., SNIDER, L., YUEN, E. C., SORIANO, P. & TAPSCOTT, S. J. (2000) Mice deficient in Six5 develop cataracts: implications for myotonic dystrophy. *Nat Genet,* 25, 105-9.

KLESERT, T. R., OTTEN, A. D., BIRD, T. D. & TAPSCOTT, S. J. (1997) Trinucleotide repeat expansion at the myotonic dystrophy locus reduces expression of DMAHP. *Nat Genet,* 16, 402-6.

KOSHELEV, M., SARMA, S., PRICE, R. E., WEHRENS, X. H. & COOPER, T. A. Heart-specific overexpression of CUGBP1 reproduces functional and molecular abnormalities of myotonic dystrophy type 1. *Hum Mol Genet,* 19, 1066-75.

KROL, J., FISZER, A., MYKOWSKA, A., SOBCZAK, K., DE MEZER, M. & KRZYZOSIAK, W. J. (2007) Ribonuclease dicer cleaves triplet repeat hairpins into shorter repeats that silence specific targets. *Mol Cell,* 25, 575-86.

KUYUMCU-MARTINEZ, N. M., WANG, G. S. & COOPER, T. A. (2007) Increased steady-state levels of CUGBP1 in myotonic dystrophy 1 are due to PKC-mediated hyperphosphorylation. *Mol Cell,* 28, 68-78.

LADD, A. N., CHARLET, N. & COOPER, T. A. (2001) The CELF family of RNA binding proteins is implicated in cell-specific and developmentally regulated alternative splicing. *Mol Cell Biol,* 21, 1285-96.

LADD, A. N. & COOPER, T. A. (2002) Finding signals that regulate alternative splicing in the post-genomic era. *Genome Biol,* 3, reviews0008.

LADD, A. N., STENBERG, M. G., SWANSON, M. S. & COOPER, T. A. (2005) Dynamic balance between activation and repression regulates pre-mRNA alternative splicing during heart development. *Dev Dyn,* 233, 783-93.

LANDER, E. S., LINTON, L. M., BIRREN, B., NUSBAUM, C., ZODY, M. C., BALDWIN, J., DEVON, K., DEWAR, K., DOYLE, M., FITZHUGH, W., FUNKE, R., GAGE, D., HARRIS, K., HEAFORD, A., HOWLAND, J., KANN, L., LEHOCZKY, J., LEVINE, R., MCEWAN, P., MCKERNAN, K., MELDRIM, J., MESIROV, J. P., MIRANDA, C., MORRIS, W., NAYLOR, J., RAYMOND, C., ROSETTI, M., SANTOS, R., SHERIDAN, A., SOUGNEZ, C., STANGE-THOMANN, N., STOJANOVIC, N., SUBRAMANIAN, A., WYMAN, D., ROGERS, J., SULSTON, J., AINSCOUGH, R., BECK, S., BENTLEY, D., BURTON, J., CLEE, C., CARTER, N., COULSON, A., DEADMAN, R., DELOUKAS, P., DUNHAM, A., DUNHAM, I., DURBIN, R., FRENCH, L., GRAFHAM, D., GREGORY,

S., HUBBARD, T., HUMPHRAY, S., HUNT, A., JONES, M., LLOYD, C., MCMURRAY, A., MATTHEWS, L., MERCER, S., MILNE, S., MULLIKIN, J. C., MUNGALL, A., PLUMB, R., ROSS, M., SHOWNKEEN, R., SIMS, S., WATERSTON, R. H., WILSON, R. K., HILLIER, L. W., MCPHERSON, J. D., MARRA, M. A., MARDIS, E. R., FULTON, L. A., CHINWALLA, A. T., PEPIN, K. H., GISH, W. R., CHISSOE, S. L., WENDL, M. C., DELEHAUNTY, K. D., MINER, T. L., DELEHAUNTY, A., KRAMER, J. B., COOK, L. L., FULTON, R. S., JOHNSON, D. L., MINX, P. J., CLIFTON, S. W., HAWKINS, T., BRANSCOMB, E., PREDKI, P., RICHARDSON, P., WENNING, S., SLEZAK, T., DOGGETT, N., CHENG, J. F., OLSEN, A., LUCAS, S., ELKIN, C., UBERBACHER, E., FRAZIER, M., et al. (2001) Initial sequencing and analysis of the human genome. *Nature,* 409, 860-921.

LANGLOIS, M. A., LEE, N. S., ROSSI, J. J. & PUYMIRAT, J. (2003) Hammerhead ribozyme-mediated destruction of nuclear foci in myotonic dystrophy myoblasts. *Mol Ther,* 7, 670-80.

LEE, J. E. & COOPER, T. A. (2009) Pathogenic mechanisms of myotonic dystrophy. *Biochem Soc Trans,* 37, 1281-6.

LEE, M. M., CHILDS-DISNEY, J. L., PUSHECHNIKOV, A., FRENCH, J. M., SOBCZAK, K., THORNTON, C. A. & DISNEY, M. D. (2009a) Controlling the specificity of modularly assembled small molecules for RNA via ligand module spacing: targeting the RNAs that cause myotonic muscular dystrophy. *J Am Chem Soc,* 131, 17464-72.

LEE, M. M., PUSHECHNIKOV, A. & DISNEY, M. D. (2009b) Rational and modular design of potent ligands targeting the RNA that causes myotonic dystrophy 2. *ACS Chem Biol,* 4, 345-55.

LEROY, O., DHAENENS, C. M., SCHRAEN-MASCHKE, S., BELARBI, K., DELACOURTE, A., ANDREADIS, A., SABLONNIERE, B., BUEE, L., SERGEANT, N. & CAILLET-BOUDIN, M. L. (2006) ETR-3 represses Tau exons 2/3 inclusion, a splicing event abnormally enhanced in myotonic dystrophy type I. *J Neurosci Res,* 84, 852-9.

LEWIS, B. P., GREEN, R. E. & BRENNER, S. E. (2003) Evidence for the widespread coupling of alternative splicing and nonsense-mediated mRNA decay in humans. *Proc Natl Acad Sci U S A,* 100, 189-92.

LIN, X., MILLER, J. W., MANKODI, A., KANADIA, R. N., YUAN, Y., MOXLEY, R. T., SWANSON, M. S. & THORNTON, C. A. (2006) Failure of MBNL1-dependent post-natal splicing transitions in myotonic dystrophy. *Hum Mol Genet,* 15, 2087-97.

LIQUORI, C. L., RICKER, K., MOSELEY, M. L., JACOBSEN, J. F., KRESS, W., NAYLOR, S. L., DAY, J. W. & RANUM, L. P. (2001) Myotonic dystrophy type 2 caused by a CCTG expansion in intron 1 of ZNF9. *Science,* 293, 864-7.

LUECK, J. D., MANKODI, A., SWANSON, M. S., THORNTON, C. A. & DIRKSEN, R. T. (2007) Muscle chloride channel dysfunction in two mouse models of myotonic dystrophy. *J Gen Physiol,* 129, 79-94.

LYTTON, J., WESTLIN, M., BURK, S. E., SHULL, G. E. & MACLENNAN, D. H. (1992) Functional comparisons between isoforms of the sarcoplasmic or endoplasmic reticulum family of calcium pumps. *J Biol Chem,* 267, 14483-9.

MACHUCA-TZILI, L., BROOK, D. & HILTON-JONES, D. (2005) Clinical and molecular aspects of the myotonic dystrophies: a review. *Muscle Nerve,* 32, 1-18.

MACHUCA-TZILI, L., THORPE, H., ROBINSON, T. E., SEWRY, C. & BROOK, J. D. (2006) Flies deficient in Muscleblind protein model features of myotonic dystrophy with altered splice forms of Z-band associated transcripts. *Hum Genet,* 120, 487-99.

MAHADEVAN, M., TSILFIDIS, C., SABOURIN, L., SHUTLER, G., AMEMIYA, C., JANSEN, G., NEVILLE, C., NARANG, M., BARCELO, J., O'HOY, K. & ET AL. (1992) Myotonic dystrophy mutation: an unstable CTG repeat in the 3' untranslated region of the gene. *Science,* 255, 1253-5.

MAHADEVAN, M. S., YADAVA, R. S., YU, Q., BALIJEPALLI, S., FRENZEL-MCCARDELL, C. D., BOURNE, T. D. & PHILLIPS, L. H. (2006) Reversible model of RNA toxicity and cardiac conduction defects in myotonic dystrophy. *Nat Genet,* 38, 1066-70.

MANKODI, A., LIN, X., BLAXALL, B. C., SWANSON, M. S. & THORNTON, C. A. (2005) Nuclear RNA foci in the heart in myotonic dystrophy. *Circ Res,* 97, 1152-5.

MANKODI, A., LOGIGIAN, E., CALLAHAN, L., MCCLAIN, C., WHITE, R., HENDERSON, D., KRYM, M. & THORNTON, C. A. (2000) Myotonic dystrophy in transgenic mice expressing an expanded CUG repeat. *Science,* 289, 1769-73.

MANKODI, A., TAKAHASHI, M. P., JIANG, H., BECK, C. L., BOWERS, W. J., MOXLEY, R. T., CANNON, S. C. & THORNTON, C. A. (2002) Expanded CUG repeats trigger aberrant splicing of ClC-1 chloride channel pre-mRNA and hyperexcitability of skeletal muscle in myotonic dystrophy. *Mol Cell,* 10, 35-44.

MANKODI, A., URBINATI, C. R., YUAN, Q. P., MOXLEY, R. T., SANSONE, V., KRYM, M., HENDERSON, D., SCHALLING, M., SWANSON, M. S. & THORNTON, C. A. (2001) Muscleblind localizes to nuclear foci of aberrant RNA in myotonic dystrophy types 1 and 2. *Hum Mol Genet,* 10, 2165-70.

MARGOLIS, J. M., SCHOSER, B. G., MOSELEY, M. L., DAY, J. W. & RANUM, L. P. (2006) DM2 intronic expansions: evidence for CCUG accumulation without flanking sequence or effects on ZNF9 mRNA processing or protein expression. *Hum Mol Genet,* 15, 1808-15.

MARTORELL, L., MARTINEZ, J. M., CAREY, N., JOHNSON, K. & BAIGET, M. (1995) Comparison of CTG repeat length expansion and clinical progression of myotonic dystrophy over a five year period. *J Med Genet,* 32, 593-6.

MARTORELL, L., MONCKTON, D. G., GAMEZ, J., JOHNSON, K. J., GICH, I., LOPEZ DE MUNAIN, A. & BAIGET, M. (1998) Progression of somatic CTG repeat length heterogeneity in the blood cells of myotonic dystrophy patients. *Hum Mol Genet,* 7, 307-12.

MASTROYIANNOPOULOS, N. P., CHRYSANTHOU, E., KYRIAKIDES, T. C., UNEY, J. B., MAHADEVAN, M. S. & PHYLACTOU, L. A. (2008) The effect of myotonic dystrophy transcript levels and location on muscle differentiation. *Biochem Biophys Res Commun,* 377, 526-31.

MASTROYIANNOPOULOS, N. P., FELDMAN, M. L., UNEY, J. B., MAHADEVAN, M. S. & PHYLACTOU, L. A. (2005) Woodchuck post-transcriptional element induces nuclear export of myotonic dystrophy 3' untranslated region transcripts. *EMBO Rep,* 6, 458-63.

MAYEDA, A., MUNROE, S. H., CACERES, J. F. & KRAINER, A. R. (1994) Function of conserved domains of hnRNP A1 and other hnRNP A/B proteins. *EMBO J,* 13, 5483-95.

MCCLAIN, D. A. (1991) Different ligand affinities of the two human insulin receptor splice variants are reflected in parallel changes in sensitivity for insulin action. *Mol Endocrinol,* 5, 734-9.

MCCULLOUGH, A. J. & BERGET, S. M. (1997) G triplets located throughout a class of small vertebrate introns enforce intron borders and regulate splice site selection. *Mol Cell Biol,* 17, 4562-71.

MEISSNER, G. (1994) Ryanodine receptor/Ca2+ release channels and their regulation by endogenous effectors. *Annu Rev Physiol,* 56, 485-508.

MELACINI, P., VILLANOVA, C., MENEGAZZO, E., NOVELLI, G., DANIELI, G., RIZZOLI, G., FASOLI, G., ANGELINI, C., BUJA, G., MIORELLI, M. & ET AL. (1995) Correlation between cardiac involvement and CTG trinucleotide repeat length in myotonic dystrophy. *J Am Coll Cardiol,* 25, 239-45.

MELLOR, H. & PARKER, P. J. (1998) The extended protein kinase C superfamily. *Biochem J,* 332 (Pt 2), 281-92.

MICHALOWSKI, S., MILLER, J. W., URBINATI, C. R., PALIOURAS, M., SWANSON, M. S. & GRIFFITH, J. (1999) Visualization of double-stranded RNAs from the myotonic dystrophy protein kinase gene and interactions with CUG-binding protein. *Nucleic Acids Res,* 27, 3534-42.

MILLER, J. W., URBINATI, C. R., TENG-UMNUAY, P., STENBERG, M. G., BYRNE, B. J., THORNTON, C. A. & SWANSON, M. S. (2000) Recruitment of human muscleblind proteins to (CUG)(n) expansions associated with myotonic dystrophy. *EMBO J,* 19, 4439-48.

MOSTHAF, L., GRAKO, K., DULL, T. J., COUSSENS, L., ULLRICH, A. & MCCLAIN, D. A. (1990) Functionally distinct insulin receptors generated by tissue-specific alternative splicing. *EMBO J,* 9, 2409-13.

MULDERS, S. A., VAN DEN BROEK, W. J., WHEELER, T. M., CROES, H. J., VAN KUIK-ROMEIJN, P., DE KIMPE, S. J., FURLING, D., PLATENBURG, G. J., GOURDON, G., THORNTON, C. A., WIERINGA, B. & WANSINK, D. G. (2009) Triplet-repeat oligonucleotide-mediated reversal of RNA toxicity in myotonic dystrophy. *Proc Natl Acad Sci U S A,* 106, 13915-20.

NAKAMORI, M., KIMURA, T., FUJIMURA, H., TAKAHASHI, M. P. & SAKODA, S. (2007) Altered mRNA splicing of dystrophin in type 1 myotonic dystrophy. *Muscle Nerve,* 36, 251-7.

NAKIELNY, S. & DREYFUSS, G. (1999) Transport of proteins and RNAs in and out of the nucleus. *Cell,* 99, 677-90.

NAPIERALA, M. & KRZYZOSIAK, W. J. (1997) CUG repeats present in myotonin kinase RNA form metastable "slippery" hairpins. *J Biol Chem,* 272, 31079-85.

NILSEN, T. W. (2003) The spliceosome: the most complex macromolecular machine in the cell? *Bioessays,* 25, 1147-9.

NOVELLI, G., GENNARELLI, M., ZELANO, G., PIZZUTI, A., FATTORINI, C., CASKEY, C. T. & DALLAPICCOLA, B. (1993) Failure in detecting mRNA transcripts from the mutated allele in myotonic dystrophy muscle. *Biochem Mol Biol Int,* 29, 291-7.

O'LEARY, D. A., VARGAS, L., SHARIF, O., GARCIA, M. E., SIGAL, Y. J., CHOW, S. K., SCHMEDT, C., CALDWELL, J. S., BRINKER, A. & ENGELS, I. H. HTS-Compatible Patient-Derived Cell-Based Assay to Identify Small Molecule Modulators of Aberrant Splicing in Myotonic Dystrophy Type 1. *Curr Chem Genomics,* 4, 9-18.

ORENGO, J. P., BUNDMAN, D. & COOPER, T. A. (2006) A bichromatic fluorescent reporter for cell-based screens of alternative splicing. *Nucleic Acids Res,* 34, e148.

ORENGO, J. P., CHAMBON, P., METZGER, D., MOSIER, D. R., SNIPES, G. J. & COOPER, T. A. (2008) Expanded CTG repeats within the DMPK 3' UTR causes severe skeletal muscle wasting in an inducible mouse model for myotonic dystrophy. *Proc Natl Acad Sci U S A,* 105, 2646-51.

OTTEN, A. D. & TAPSCOTT, S. J. (1995) Triplet repeat expansion in myotonic dystrophy alters the adjacent chromatin structure. *Proc Natl Acad Sci U S A,* 92, 5465-9.

PASCUAL, M., VICENTE, M., MONFERRER, L. & ARTERO, R. (2006) The Muscleblind family of proteins: an emerging class of regulators of developmentally programmed alternative splicing. *Differentiation,* 74, 65-80.

PATEL, N. A., CHALFANT, C. E., WATSON, J. E., WYATT, J. R., DEAN, N. M., EICHLER, D. C. & COOPER, D. R. (2001) Insulin regulates alternative splicing of protein kinase C beta II through a phosphatidylinositol 3-kinase-dependent pathway involving the nuclear serine/arginine-rich splicing factor, SRp40, in skeletal muscle cells. *J Biol Chem,* 276, 22648-54.

PAUL, S., DANSITHONG, W., KIM, D., ROSSI, J., WEBSTER, N. J., COMAI, L. & REDDY, S. (2006) Interaction of muscleblind, CUG-BP1 and hnRNP H proteins in DM1-associated aberrant IR splicing. *EMBO J,* 25, 4271-83.

PELARGONIO, G., DELLO RUSSO, A., SANNA, T., DE MARTINO, G. & BELLOCCI, F. (2002) Myotonic dystrophy and the heart. *Heart,* 88, 665-70.

PHILIPS, A. V., TIMCHENKO, L. T. & COOPER, T. A. (1998) Disruption of splicing regulated by a CUG-binding protein in myotonic dystrophy. *Science,* 280, 737-41.

POZZOLI, U. & SIRONI, M. (2005) Silencers regulate both constitutive and alternative splicing events in mammals. *Cell Mol Life Sci,* 62, 1579-604.

PUSHECHNIKOV, A., LEE, M. M., CHILDS-DISNEY, J. L., SOBCZAK, K., FRENCH, J. M., THORNTON, C. A. & DISNEY, M. D. (2009) Rational design of ligands targeting triplet repeating transcripts that cause RNA dominant disease: application to myotonic muscular dystrophy

type 1 and spinocerebellar ataxia type 3. *J Am Chem Soc,* 131, 9767-79.

RANUM, L. P. & COOPER, T. A. (2006) RNA-mediated neuromuscular disorders. *Annu Rev Neurosci,* 29, 259-77.

RANUM, L. P., RASMUSSEN, P. F., BENZOW, K. A., KOOB, M. D. & DAY, J. W. (1998) Genetic mapping of a second myotonic dystrophy locus. *Nat Genet,* 19, 196-8.

REDDY, S., SMITH, D. B., RICH, M. M., LEFEROVICH, J. M., REILLY, P., DAVIS, B. M., TRAN, K., RAYBURN, H., BRONSON, R., CROS, D., BALICE-GORDON, R. J. & HOUSMAN, D. (1996) Mice lacking the myotonic dystrophy protein kinase develop a late onset progressive myopathy. *Nat Genet,* 13, 325-35.

RICKER, K., GRIMM, T., KOCH, M. C., SCHNEIDER, C., KRESS, W., REIMERS, C. D., SCHULTE-MATTLER, W., MUELLER-MYHSOK, B., TOYKA, K. V. & MUELLER, C. R. (1999) Linkage of proximal myotonic myopathy to chromosome 3q. *Neurology,* 52, 170-1.

RICKER, K., KOCH, M. C., LEHMANN-HORN, F., PONGRATZ, D., OTTO, M., HEINE, R. & MOXLEY, R. T., 3RD (1994) Proximal myotonic myopathy: a new dominant disorder with myotonia, muscle weakness, and cataracts. *Neurology,* 44, 1448-52.

ROBERTS, R., TIMCHENKO, N. A., MILLER, J. W., REDDY, S., CASKEY, C. T., SWANSON, M. S. & TIMCHENKO, L. T. (1997) Altered phosphorylation and intracellular distribution of a (CUG)n triplet repeat RNA-binding protein in patients with myotonic dystrophy and in myotonin protein kinase knockout mice. *Proc Natl Acad Sci U S A,* 94, 13221-6.

SAMBROOK, J. & RUSSELL, D. W. (2001) Molecular Cloning: A Laboratory Manual, Third Edition. Cold Spring Harbor Laboratory Press.

SAVKUR, R. S., PHILIPS, A. V. & COOPER, T. A. (2001) Aberrant regulation of insulin receptor alternative splicing is associated with insulin resistance in myotonic dystrophy. *Nat Genet,* 29, 40-7.

SAVKUR, R. S., PHILIPS, A. V., COOPER, T. A., DALTON, J. C., MOSELEY, M. L., RANUM, L. P. & DAY, J. W. (2004) Insulin receptor splicing alteration in myotonic dystrophy type 2. *Am J Hum Genet,* 74, 1309-13.

SEINO, S. & BELL, G. I. (1989) Alternative splicing of human insulin receptor messenger RNA. *Biochem Biophys Res Commun,* 159, 312-6.

SERGEANT, N., SABLONNIERE, B., SCHRAEN-MASCHKE, S., GHESTEM, A., MAURAGE, C. A., WATTEZ, A., VERMERSCH, P. & DELACOURTE, A. (2001) Dysregulation of human brain microtubule-associated tau mRNA maturation in myotonic dystrophy type 1. *Hum Mol Genet,* 10, 2143-55.

SEZNEC, H., AGBULUT, O., SERGEANT, N., SAVOURET, C., GHESTEM, A., TABTI, N., WILLER, J. C., OURTH, L., DUROS, C., BRISSON, E., FOUQUET, C., BUTLER-BROWNE, G., DELACOURTE, A., JUNIEN, C. & GOURDON, G. (2001) Mice transgenic for the human myotonic dystrophy region with expanded CTG repeats display muscular and brain abnormalities. *Hum Mol Genet,* 10, 2717-26.

SEZNEC, H., LIA-BALDINI, A. S., DUROS, C., FOUQUET, C., LACROIX, C., HOFMANN-RADVANYI, H., JUNIEN, C. & GOURDON, G. (2000) Transgenic mice carrying large human genomic sequences with expanded CTG repeat mimic closely the DM CTG repeat intergenerational and somatic instability. *Hum Mol Genet,* 9, 1185-94.

SUTKO, J. L. & AIREY, J. A. (1996) Ryanodine receptor Ca2+ release channels: does diversity in form equal diversity in function? *Physiol Rev,* 76, 1027-71.

TAKAHASHI, N., SASAGAWA, N., SUZUKI, K. & ISHIURA, S. (2000) The CUG-binding protein binds specifically to UG dinucleotide repeats in a yeast three-hybrid system. *Biochem Biophys Res Commun,* 277, 518-23.

TANEJA, K. L., MCCURRACH, M., SCHALLING, M., HOUSMAN, D. & SINGER, R. H. (1995) Foci of trinucleotide repeat transcripts in nuclei of myotonic dystrophy cells and tissues. *J Cell Biol,* 128, 995-1002.

THORNTON, C. A., GRIGGS, R. C. & MOXLEY, R. T., 3RD (1994) Myotonic dystrophy with no trinucleotide repeat expansion. *Ann Neurol,* 35, 269-72.

THORNTON, C. A., WYMER, J. P., SIMMONS, Z., MCCLAIN, C. & MOXLEY, R. T., 3RD (1997) Expansion of the myotonic dystrophy CTG repeat reduces expression of the flanking DMAHP gene. *Nat Genet,* 16, 407-9.

TIMCHENKO, L. T., MILLER, J. W., TIMCHENKO, N. A., DEVORE, D. R., DATAR, K. V., LIN, L., ROBERTS, R., CASKEY, C. T. & SWANSON, M. S. (1996a) Identification of a (CUG)n triplet repeat RNA-binding protein and its expression in myotonic dystrophy. *Nucleic Acids Res,* 24, 4407-14.

TIMCHENKO, L. T., TIMCHENKO, N. A., CASKEY, C. T. & ROBERTS, R. (1996b) Novel proteins with binding specificity for DNA CTG repeats and RNA CUG repeats: implications for myotonic dystrophy. *Hum Mol Genet,* 5, 115-21.

TIMCHENKO, N. A., PATEL, R., IAKOVA, P., CAI, Z. J., QUAN, L. & TIMCHENKO, L. T. (2004) Overexpression of CUG triplet repeat-binding protein, CUGBP1, in mice inhibits myogenesis. *J Biol Chem,* 279, 13129-39.

TISCORNIA, G. & MAHADEVAN, M. S. (2000) Myotonic dystrophy: the role of the CUG triplet repeats in splicing of a novel DMPK exon and altered cytoplasmic DMPK mRNA isoform ratios. *Mol Cell,* 5, 959-67.

TRAN, H., GOURRIER, N., LEMERCIER-NEUILLET, C., DHAENENS, C. M., VAUTRIN, A., FERNANDEZ-GOMEZ, F. J., ARANDEL, L., CARPENTIER, C., OBRIOT, H., EDDARKAOUI, S., DELATTRE, L., VAN BRUSSELS, E., HOLT, I., MORRIS, G. E., SABLONNIERE, B., BUEE, L., CHARLET-BERGUERAND, N., SCHRAEN-MASCHKE, S., FURLING, D., BEHM-ANSMANT, I., BRANLANT, C., CAILLET-BOUDIN, M. L. & SERGEANT, N. Analysis of exonic regions involved in nuclear localization, splicing activity, and dimerization of Muscleblind-like-1 isoforms. *J Biol Chem,* 286, 16435-46.

TSILFIDIS, C., MACKENZIE, A. E., METTLER, G., BARCELO, J. & KORNELUK, R. G. (1992) Correlation between CTG trinucleotide

repeat length and frequency of severe congenital myotonic dystrophy. *Nat Genet,* 1, 192-5.

UDD, B., KRAHE, R., WALLGREN-PETTERSSON, C., FALCK, B. & KALIMO, H. (1997) Proximal myotonic dystrophy--a family with autosomal dominant muscular dystrophy, cataracts, hearing loss and hypogonadism: heterogeneity of proximal myotonic syndromes? *Neuromuscul Disord,* 7, 217-28.

VICENTE, M., MONFERRER, L., POULOS, M. G., HOUSELEY, J., MONCKTON, D. G., O'DELL K, M., SWANSON, M. S. & ARTERO, R. D. (2007) Muscleblind isoforms are functionally distinct and regulate alpha-actinin splicing. *Differentiation,* 75, 427-40.

VOGT, B., CARRASCOSA, J. M., ERMEL, B., ULLRICH, A. & HARING, H. U. (1991) The two isotypes of the human insulin receptor (HIR-A and HIR-B) follow different internalization kinetics. *Biochem Biophys Res Commun,* 177, 1013-8.

WANG, G. S., KEARNEY, D. L., DE BIASI, M., TAFFET, G. & COOPER, T. A. (2007) Elevation of RNA-binding protein CUGBP1 is an early event in an inducible heart-specific mouse model of myotonic dystrophy. *J Clin Invest,* 117, 2802-11.

WANG, G. S., KUYUMCU-MARTINEZ, M. N., SARMA, S., MATHUR, N., WEHRENS, X. H. & COOPER, T. A. (2009) PKC inhibition ameliorates the cardiac phenotype in a mouse model of myotonic dystrophy type 1. *J Clin Invest,* 119, 3797-806.

WANG, Y. H., AMIRHAERI, S., KANG, S., WELLS, R. D. & GRIFFITH, J. D. (1994) Preferential nucleosome assembly at DNA triplet repeats from the myotonic dystrophy gene. *Science,* 265, 669-71.

WANG, Y. H. & GRIFFITH, J. (1995) Expanded CTG triplet blocks from the myotonic dystrophy gene create the strongest known natural nucleosome positioning elements. *Genomics,* 25, 570-3.

WARF, M. B., DIEGEL, J. V., VON HIPPEL, P. H. & BERGLUND, J. A. (2009a) The protein factors MBNL1 and U2AF65 bind alternative RNA structures to regulate splicing. *Proc Natl Acad Sci U S A,* 106, 9203-8.

WARF, M. B., NAKAMORI, M., MATTHYS, C. M., THORNTON, C. A. & BERGLUND, J. A. (2009b) Pentamidine reverses the splicing defects associated with myotonic dystrophy. *Proc Natl Acad Sci U S A,* 106, 18551-6.

WELLS, R. D. (1996) Molecular basis of genetic instability of triplet repeats. *J Biol Chem,* 271, 2875-8.

WHEELER, T. M., LUECK, J. D., SWANSON, M. S., DIRKSEN, R. T. & THORNTON, C. A. (2007) Correction of ClC-1 splicing eliminates chloride channelopathy and myotonia in mouse models of myotonic dystrophy. *J Clin Invest,* 117, 3952-7.

WHEELER, T. M., SOBCZAK, K., LUECK, J. D., OSBORNE, R. J., LIN, X., DIRKSEN, R. T. & THORNTON, C. A. (2009) Reversal of RNA dominance by displacement of protein sequestered on triplet repeat RNA. *Science,* 325, 336-9.

WINCHESTER, C. L., FERRIER, R. K., SERMONI, A., CLARK, B. J. & JOHNSON, K. J. (1999) Characterization of the expression of DMPK

and SIX5 in the human eye and implications for pathogenesis in myotonic dystrophy. *Hum Mol Genet,* 8, 481-92.

WONG, L. J., ASHIZAWA, T., MONCKTON, D. G., CASKEY, C. T. & RICHARDS, C. S. (1995) Somatic heterogeneity of the CTG repeat in myotonic dystrophy is age and size dependent. *Am J Hum Genet,* 56, 114-22.

WU, J. Y. & MANIATIS, T. (1993) Specific interactions between proteins implicated in splice site selection and regulated alternative splicing. *Cell,* 75, 1061-70.

ZHU, J., MAYEDA, A. & KRAINER, A. R. (2001) Exon identity established through differential antagonism between exonic splicing silencer-bound hnRNP A1 and enhancer-bound SR proteins. *Mol Cell,* 8, 1351-61.

APPENDIX A

Primer	Sequence (5'-3')
sinCLCN1f	GATTTATGGCCATCACAAAGAACAATT
sinCLCN1r	GCTGAAGGCTTTTGGCACTGAC
sinSERCA2f	GTTGTCCGAAAACCAGTCCTTG
pEGFP-C1F	CCTGAGCAAAGACCCCAAC
pEGFP-C1R	TTCAGGTTCAGGGGGAGGT
DsRedORFr	ATCTCGAAGTAGTGGCCGTTC
DsRedMonoF	GACCGGCCGCGGGCATGGACAACACCGAGGACG
*MIR*1-2F	TGCCATGCTTCAGGTAAAC
*MIR*1-2R	CACGTAGAAAGAAGCAAGAGC
T1F	AAAGACCCCAACGAGAAGC
T1R	GATCCTCATCCTTGCTGTCC
GdmpkF	GTTCTCCACCAGAGAATCAGC
GdmpkR	GAAGCCCTCACCTTTTCTCTC
N11	CACTGTCGGACATTCGGGAAGGTGC
133	GCTTGCACGTGTGGCTCAAGCAGCTG
IRfor	CCAAAGACAGACTCTCAGAT
IRrev	AACATCGCCAAGGGACCTGC
Serca1for	TTCGTTGCTCGGAACTACC
Serca1rev	GGTTGGGAAGGGGAATTTAC
MBNL1for	GCTGCCCAATACCAGGTCAAC
MBNL1rev	TGGTGGGAGAAATGCTGTATGC
MBNL2for	ACAAGTGACAACACCGTAACCG
MBNL2rev	TTTGGTAAAGGATGAAGAGCACC
GAPDHf	GATGACAAGCTTCCCGTTCTCAGCC
GAPDHrev	TGAAGGTCGGAGTCAACGGATTTGGT
pEGFP-C1delF	GCCCGGGACTAGTCGGATCTAGATAACTGATCATAATCAGCCATACCACATTTGTAGAGG
MBNL1-D1r	TGAAAACACTAGTACGGGTTGTAATGGGGCACCAGGCATCATGGCATTGG
MBNL1-D2r	CTCAAGTACTAGTGTTCGCATTAATTTCTGTGCAGCAGCTGCAG
MBNL1-D3r	CAGGTACACTAGTGTCATTGGTGTCAATCATTGTGCTTCAGCAGGATGAGC
MBNL1-D4r	TGGCTTGACTAGTTGCAGGGGGATGAAAGTATTTGCACTTTTCCCGAGAG
MBNL2-D1r	TTTTTAAACTAGTCGGAGGGTGAAGATACTTGCAGTTCTCTCTCGAAC
MBNL2-D2r	CCTCCAGACTAGTAGTCCTGAGAAGTTTCTGAGTTGCAGTTGAGCCCG
MBNL2-D3r	GTCACTTACTAGTATCATGGTGCTGTCTGCGGGGTGTGCAAAG
MBNL2-D4r	GCCTGCAACTAGTCAGGAGGGTGAAAATATTTGCATTTCTCCCTCATGCAACG

APPENDIX B

siRNA	Sequence (5'-3')
MBNL1	CACUGGAAGUAUGUAGAGAdTdT
MBNL2a	CACCGUAACCGUUUGUAUGdTdT
MBNL2b	GAGGAACAUGCUCACGCUCdTdT
Scrambled	GCGCGCUUUGUAGGAUUCGdTdT

APPENDIX C

Supplementary Data

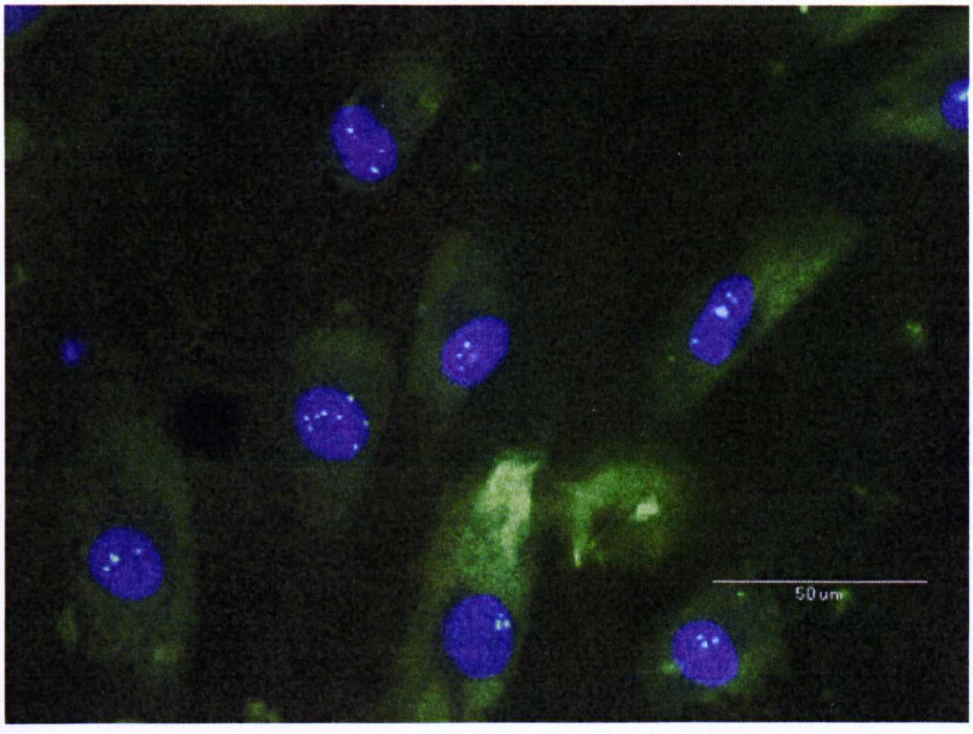

Nuclear foci screening assay for PKC inhibitor GF109203X designated as D7 showing its non-clearance effect on nuclear foci of DM1 cell